The Effect of Shot-peening on the Fatigue Limits of Four Connecting Rod Steels

by

Mohammad Mahdi Mirzazadeh

A thesis

presented to the University of Waterloo

in fulfillment of the

thesis requirement for the degree of

Master of Applied Science

in

Mechanical Engineering

Waterloo, Ontario, Canada, 2010

© Mohammad Mahdi Mirzazadeh 2010

Author's Declaration

I hereby declare that I am the sole author of this thesis. This is a true copy of the thesis, including any required final revisions, as accepted by my examiners.

I understand that my thesis may be made electronically available to the public.

Mohammad Mahdi Mirzazadeh

Abstract

This work was carried out to study the effect of shot-peening on the fatigue behaviour of carbon steels. Differently heat treated medium and high carbon steel specimens were selected. Medium carbon steels, AISI 1141 and AISI 1151, were respectively air cooled and quenched-tempered. A high carbon steel, C70S6 (AISI 1070), was air cooled. The other material was a powder metal (0.5% C) steel. Each group of steels was divided into two. One was shot-peened. The other half remained in their original conditions. All were fatigue tested under fully reversed (R=-1) tension-compression loading conditions. Microhardness tests were carried out on both the grip and gage sections of selected non shot-peened and shot-peened specimens to determine the hardness profile and effect of cycling. Shot-peening was found to be deeper on one side of each specimen. Compressive residual stress profiles and surface roughness measurements were provided. Shot-peening increased the surface roughness from 0.26±0.03μm to 3.60±0.44μm. Compressive residual stresses induced by shot-peening reached a maximum of -463.9MPa at a depth of 0.1mm.

The fatigue limit (N≈10^6 cycles) and microhardness profiles of the non shot-peened and shot-peened specimens were compared to determine the material behaviour changes after shot-peening and cycling. Also their fatigue properties were related to the manufacturing process including heat and surface treatments.

Comparing the grip and gage microhardness profiles of each steel showed that neither cyclic softening nor hardening occurred in the non shot-peened condition. Cyclic softening was apparent in the shot-peened regions of all steels except powder metal (PM) steel. The amount of softening in the shot-peened region was 55.0% on the left side and 73.0% on the right in the AISI 1141 steel , 46.0% on the left side and 55.0% on the right in the C70S6AC steel and 31.0% on the right side in AISI 1151QT steel. Softening was accompanied by a decrease in the depth of surface hardness.

It is suggested that although the beneficial effects of shot peening, compressive residual stresses and work hardening, were offset by surface roughness, crack initiation was more likely to occur below the surface. Surface roughness was not a significant factor in controlling the

fatigue lives of AISI 1141AC and C70S6 steels, since they were essentially the same for the non shot-peened and shot-peened conditions.

Shot-peening had very little effect on the push-pull fatigue limit of C70S6 steel (-2.1%), and its effect on AISI 1141AC steel was relatively small (6.0%). However, the influence of shot-peening on the AISI 1151QT and PM steels was more apparent. The fatigue limit of the PM steel increased 14.0% whereas the fatigue limit of the AISI 1151QT steel decreased 11.0% on shot peening.

Acknowledgements

I would like to sincerely thank my supervisor, Professor Alan Plumtree, for his support and guidance and for giving me this opportunity to learn.

I would also like to thank to Sooky Winkler and fellow graduate student Seyed Behzad Behravesh for their advice and support.

Finally, I would like to express my profound gratitude to my parents and my only sister for their ongoing support and encouragement throughout my education and professional career.

Table of Contents

List of Figures

xiii

List of Tables

List of Symbols

A   Almen strip type A

AC   Air-cooled

AISI   American Iron and Steel Institute

AVE   Average

FWHM   Full Width at Half Maximum

HCF   High Cycle Fatigue

HV   Vickers Pyramid Number (The unit of hardness given by the test.)

HV0.1-0.5   Both 0.1kgf and 0.5kgf loads were used to obtain the hardness values

Kgf   Kilogram-force

L   Longitudinal

LCF   Low Cycle Fatigue

L-S   Longitudinal-Short transverse

L-T   Longitudinal- Transverse

Min   minute

mm 10^{-3} Meter

MPa 10^{6} Pascal $= 1$ N/mm^{2}

N   number of cycles

N_f number of cycles to failure

PM   Powder Metallurgy

QT	Quenched-tempered
R	Stress Ratio, R=$\frac{\sigma min}{\sigma max}$
S	Short Transverse
SEM	Scanning Electron Microscope
STDEV	Standard Deviation
T	Transverse
T-S	Transverse-Short Transverse
σ_a	Stress Amplitude

Chapter 1

Introduction

Fatigue is an important parameter which should be considered for engineering components subjected to constant or variable cyclic loading. Mechanical, metallurgical and environmental factors influence the fatigue behaviour of a component [1]. The basic mechanisms leading to fatigue failure are the initiation and propagation of cracks which mostly occur on free surfaces [2]. Tensile or shear stresses cause a crack to propagate while the compressive part of the cycle closes the crack.

Surface treatment is widely used for improving the fatigue behaviour of engineering components. Shot-peening is a well-known method introduced in surface engineering to extend fatigue life of components and structures under cyclic loading. In this method hard steel balls (shots) under controlled velocity impact the surface of the component [3]. This treatment is used in the automotive industry, i.e. on gear parts, springs and connecting rods [3] and in the aerospace industry on structural components of aircraft i.e. wing panels [4] and gas turbine engines i.e. blades and disks [5]. This treatment has other applications, for instance, strengthening the component against stress corrosion and overcoming the detrimental effect of existing tensile stresses caused by manufacturing processes [6].

Shot-peening changes the fatigue behaviour of components because of three effects: a) induced compressive residual stresses on surface and sub-surface layers b) strain or work hardening on surface and sub-surface layers ,which increase the yield stress of the material, and c) an increase of surface roughness which makes high cycle fatigue properties worse due to local stress concentrations [3,7]. Their influence depends on the material, strengthening method, the geometry of the work piece and the applied stresses, which may vary from one material or component to another [3].

The objective of the present work is to investigate how shot-peening affects the fatigue lives of differently heat treated medium and high carbon steels and to gain a better understanding of shot-peening effects on these materials. The role of surface roughness is also investigated. Earlier investigations have been conducted to determine whether compressive residual stresses or

work hardening is dominant in improving the fatigue behaviour of carbon steel components [6,8,9,10,11,12,13,14,15,16]. Also the deleterious effect of surface roughening has been studied [5,7,9,10,17,18]. A number of research studies [6,8-11] indicated that the work hardening effect is dominant while some others [19,20] highlighted the induced compressive residual stress in improving fatigue behaviour of steel components.

In this study, the effect of shot-peening on the fatigue behaviour of medium and high carbon steel specimens is investigated and their fatigue properties are related to the manufacturing processes including heat treatment. Medium carbon steels, AISI 1141 and AISI 1151, were air cooled and quenched-tempered respectively. A high carbon, C70S6 (AISI 1070), and a powder metal (PM) steel were air cooled. All the steels were divided into two groups, half were shot-peened and the rest remained in the non shot-peened condition. All the steels were fatigue tested under fully reversed (R=-1) tension-compression loading conditions. Microhardness tests were carried out on both the grip and gage sections of selected non shot-peened and shot-peened specimens to determine the depth of the hardened layers and the effect of cycling on them. Initial compressive residual stress profile and surface roughness measurements were also provided for further investigation. The fatigue limits (10^6 cycles) and microhardness profiles of non shot-peened and shot-peened specimens were compared to determine the material behaviour changes after shot-peening and cycling.

The influence of shot peening may be different in steels which are used in the automobile industry than the results of the present research demonstrate the effect of shot-peening on their high cycle tension-compression fatigue behaviour and the significance of shot-peening for these specimens.

Shot-peening improves the high cycle fatigue properties of medium carbon steels used for engineering applications, especially under rotating-bending conditions. This present work deals with push-pull cyclic loading which is more critical. The effect of shot-peening on fatigue life improvement will be investigated. For this reason, differently heat treated steels, commonly used for automotive applications were selected in order to study their push-pull high cycle fatigue behaviour in the shot-peened and non shot-peened conditions.

The results of the present research will compare the effects of shot-peening on the high cycle tension-compression fatigue behavior of four steels with different processing histories, used in engineering applications, The effect of shot-peening and cycling on the hardness profile will be investigated. Also, the role of surface roughness on the fatigue lives of the four steels will be determined.

Chapter 2

Literature Review

2.1. Carbon Steels

Carbon steels are divided into: a) low carbon steels, b) medium carbon steels (carbon content 0.3% to 0.6%) c) high carbon steels (carbon content 0.6% to 1.0%) and d) ultra high carbon steels. Medium carbon steels are usually used for shafts, couplings, crankshafts, axles, gears, forgings and engine connecting rods. High carbon steels are mostly used for springs and high strength wires [21], however, these steels are used in the manufacture of engine connecting rods after the advent of crackable forging steels in the 1990s.

2.2. Heat Treatment

Steels are heat treated to produce the desired mechanical properties [22]."Normalizing" is heating the steel to the austenizing temperature and slowly cooling in air. Improving machinability, grain structure refinement, homogenization and modification of residual stresses are some of the reasons for normalizing [23]."Quenching" is rapidly cooling the steel from the austenitizing temperature to produce a non-equilibrium structure such as martensite."Tempering" is a process which follows quenching. In tempering, the steel is heated to a temperature lower than the critical temperature then cooled to obtain specific mechanical properties i.e. microstructure, hardness, strength and toughness [23].

2.3. Connecting Rods

Internal combustion engine connecting rods are high volume production components. For instance, 100 million rods are manufactured in North America annually [24]. This component must meet strict design criteria since it must have an infinite life and high performance under high rate cyclic loading conditions, therefore, the durability of these components is of critical importance and a primary design criterion is its fatigue limit [24].

The application of forging a preformed near-net shape consolidated from metal powder has been widely accepted recently. At the present time, 60% of the connecting rods in North

America are manufactured using this technique. The remaining portion of this market is produced by use of either conventional steel forging or casting processes [24].

The steel rods are conventionally produced by forging wrought steel billets at high temperature then cap ends are cut or fractured and machined separately to accommodate bearing and allow attachment to the crankshaft (Figure 2.1) [24,25].
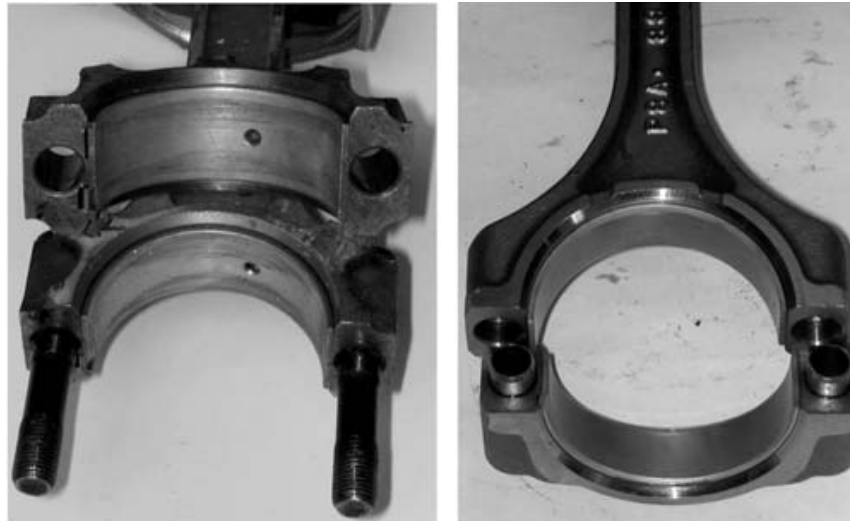
Figure 2.1.Conventional connecting rod [25]

The powder metal (PM) rods are manufactured by consolidating metal powders into a sintered preform, reheating to the forging temperature, then fully densifying by forging to the final shape, cutting of the rod cap end, and then minimal machining to achieve final dimensions. This process results in a controlled material flow which improves the mechanical properties due to a fine grain size and ultimately longer tool life. In addition, a reduction in material waste and energy savings are other advantages of this technique.

A higher carbon steel, C70S6, was introduced as a crackable forging steel in the 1990s [24,25]. The advent of crackable rods provided some advantages i.e. lower cost to separate the cap end, reducing the number of splitting steps, the surfaces of the cracked ends mated more accurately when reassembled and the tolerances of the cap end internal diameter could be closely held to a perfectly circumferential circle. The processing accuracy, product quality and bearing capability were improved and the manufacturing steps decreased up to 60% using the fracture splitting process (Figure 2.2) [24, 25].

5
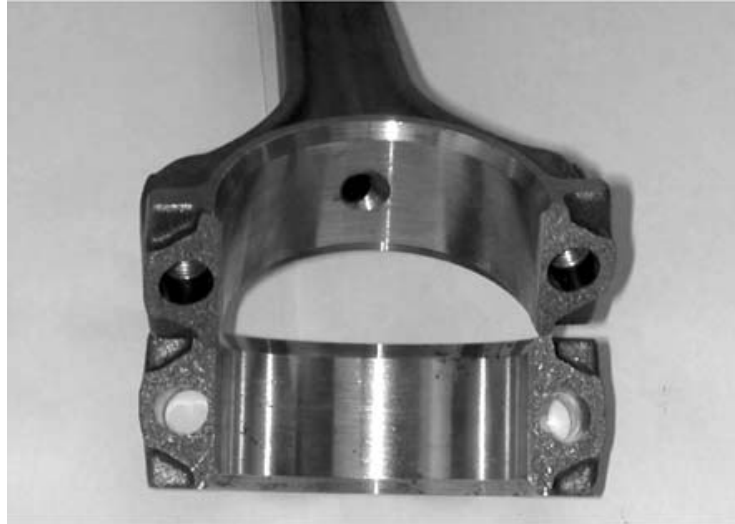
Figure 2.2.Crackable connecting rods [25]

2.4. Fatigue

Fatigue is a process which causes premature irreversible damage or failure of a component subjected to repeated loading. Fatigue generally occurs in several stages: a) cyclic slip b) fatigue crack initiation c) stage I fatigue crack growth d) stage II fatigue crack growth and e) brittle fracture or ductile rupture [2].

Figure 2.3 shows the general situation in which crack initiation (nucleation) occurs due to slip under cyclic loading. Figure 2.3a shows coarse slip under monotonic loading and Figure 2.3b shows fine slip as the result of cyclic loading. The progressive development of an extrusion-intrusion pair under cyclic loading is shown in Figure 2.3c in which vertical and sloping arrows indicate loading and deformation directions respectively.
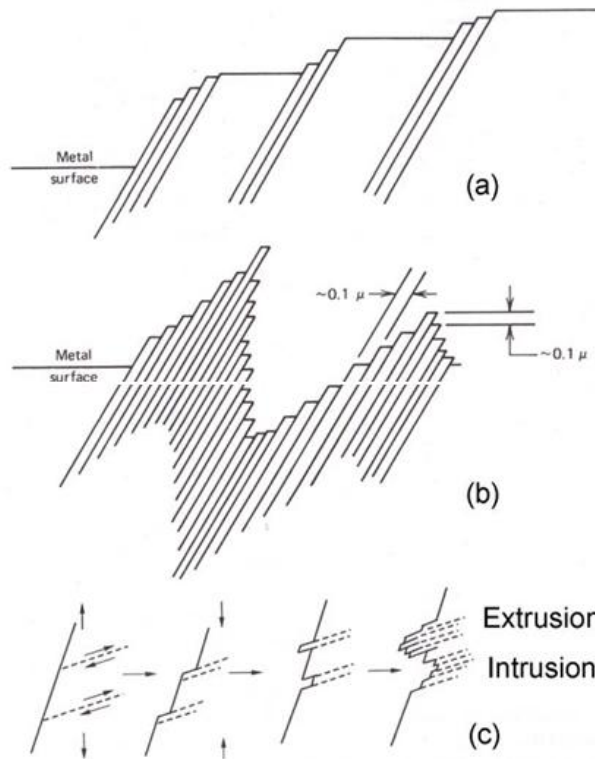
**Figure 2.3.Schematic of slip due to external loads: (a) Static (steady) stress (b) Cyclic stress
(c) Fatigue propagation in the formation of an extrusion/intrusion pair [26]**

In stage I the microcracks are nucleated at the surface and grow across several grains controlled primarily by shear stresses and strains. Therefore, the microcracks grow along the maximum shear directions, i.e. – 45º to the loading direction as shown in Figure 2.4 [26].

Once microcracks are formed in stage I and cycling continues fatigue cracks tend to coalesce and grow along the plane of maximum tensile stress which is called stage II crack growth shown in Figure 2.4. In stage II, the crack grows in a zigzag manner essentially perpendicular to the maximum tensile stress [26].
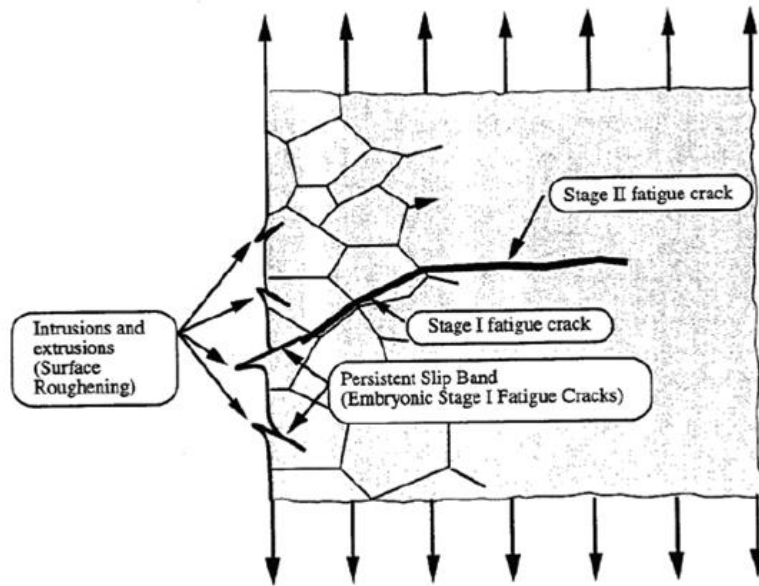
Figure 2.4.Stages I and II fatigue crack growth [2]

High cycle fatigue (HCF) describes the situation of a long fatigue life in which fatigue stresses are adequately low and the elastic strains exceed the plastic strains, so yielding effects do not dominate the behaviour. The start of the high cycle fatigue regime varies with material, but is typically between 10^2 to 10^4 cycles. Low-cycle fatigue (LCF) is characterized by high stress levels, and a short lifetime, less than 10^3 cycles, as shown in Figure 2.5. This range is rarely considered in engineering design applications. In the low-cycle range the plastic behaviour of material is important [26,27].
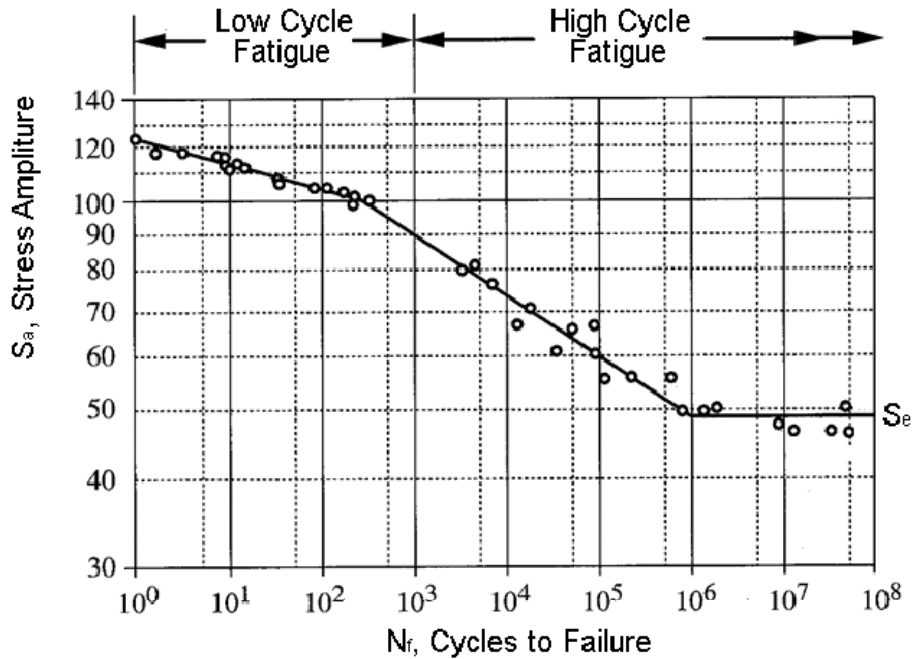
Figure 2.5.Schematic of an S-N curve [26]

The "fatigue limit" or "endurance limit" can be identified in S-N diagrams of steels in the region where the curve becomes flat, for instance, 10^6 to 10^8 cycles in Figure 2.5. The term "fatigue strength" is used to specify a stress amplitude from an S-N curve at a particular life i.e. the fatigue strength at 10^5 cycles is the stress amplitude which corresponds to $N_f=10^5$, 60MPa in Figure 2.5.

2.5. Shot Peening

"Shot peening" is a cold working process in which the surface of a component is bombarded with small metal shot under controlled velocity. A single shot plastically deforms the material making a dimple when it strikes the surface. The surrounding elastic material creates a compressive residual stress field within the cold-work hardened layers on attempting to return the yielded layers to its initial shape [28].

Shot peening effects on the surfaces and sub-surface layers can be classified into: a) mechanical b) metallurgical and c) micro-geometrical imperfections [3,7]. The mechanical effect is induced compressive residual stresses known to improve high cycle fatigue resistance. This retards crack propagation while it has little effect on crack nucleation [7]. The beneficial metallurgical effect is surface work hardening which retards crack nucleation [7]. Shot peening

9

also changes the initial surface properties and increases the surface roughness. This effect aggravates high cycle fatigue properties due to local stress concentrations which accelerate the crack nucleation phase [7]. The influence of these factors depends on the original structure, geometry of component, applied stress, strengthening method and strength or hardness of the material [3].

2.6. Work Hardening Effects

Induced compressive residual stress and work hardening are two essential factors which improve the fatigue behaviour of shot-peened parts. Some researchers [6,8-11] proposed that the influence of work hardening was greater than induced compressive residual stresses while other suggested that the greater effect was that of the compressive residual stresses [19,20].

Farrahi et al. [3] suggested that the improvement in torsion fatigue life of high carbon spring steels after shot peening was attributed to both compressive residual stress and the depth of the plastically deformed layer. The importance of these two factors depended on the material. In a study on the fatigue properties of shot-peened ductile cast iron, Yasuo et al. [29] showed that both work hardening and compressive residual stress improved rotating bending fatigue strength of ductile cast iron.

Hoffmann et al. [8] concluded that a small improvement, 14.0% for quenched and 22.0% for quenched-tempered, in bending fatigue behaviour (HCF) of smooth medium carbon steel (AISI 1045) specimens after shot peening could be more attributed to work hardening than compressive residual stresses. In another study [9] a small improvement, 10.3% for PM steels, in push-pull fatigue limit of smooth shot-peened carbon steel specimens was observed and related to work hardening since compressive residual stresses relaxed significantly after long periods of cycling.

Guechichi and Castex [10] showed respectively 9.0%, 12.0% and 22.0% enhancement in rotary bending, tension-compression and torsion fatigue limits of low-alloy medium carbon steels (35NiCrMo16 and 32CrMoVa13) after shot-peening. They also developed a model which incorporated both compressive residual stress and work hardening as beneficial effects of shot

peening. Based on the model, the effect of residual stress on the fatigue limit was negligible and any improvement of the fatigue limits was due to work hardening effect.

A.M.Eleiche et.al [6] showed an increase of the rotating-bending fatigue limit for shot-peened smooth steel specimens of high-strength martensitic steel by about 22.0%. For these specimens, they showed that after stress relieving the fatigue limit remained approximately 16.0-19.0% higher than non shot-peened conditions indicating that induced compressive residual stress was not the only reason for fatigue limit improvement, but rather the most of the shot peening strengthening effect on high cycle fatigue behaviour could be attributed to the change of surface texture introduced by the rotation of surface crystals.

Pariente and Guagliano [11] investigated the effect of shot peening on pre-cracked specimens of medium carbon steel (42CrMo4). They observed that fatigue crack propagation retarded in these specimens after shot-peening. They concluded this fatigue behaviour improvement was associated more with the surface work hardening than with the residual stress.

It is suggested that for smooth steel shot-peened specimens, the effect of residual stress on fatigue limit is of second order and fatigue limit improvement is more due to the increasing effect of work hardening [8-10].

2.7. Compressive Residual Stress

Assessment of induced residual stresses and their relaxation during cyclic loading are important aspects in design of engineering components and prediction of their life [17].

Shot peening induces compressive residual stresses at the surface. The initial residual stresses are released and redistributed during the fatigue process [10]. Stress relaxation has been investigated by many researchers [8,9,12,13,17,18].

Hoffman and Macherauch [8] demonstrated that in both smooth and notched quenched and tempered medium carbon steel (AISI 1045) specimens, compressive residual stresses decreased considerably during fully reversed bending fatigue tests. They concluded that a small increase in bending fatigue limit could be due to increased work hardening rather than small amounts of the compressive residual stresses at and below the surface. Surface stress

concentrations caused relaxation of compressive residual stress during cycling by allowing initiation and finally propagation of fatigue cracks below the surface [9].

Two stages for stress relaxation under fully reversed cyclic loading (R=-1) were identified. In the first stage, a significant relaxation of the compressive residual stresses during the first cycles ($\sim 10^3$ cycles) occurred in proportion to the magnitude of the applied load [7,10,12] and corresponded to the rearrangement of the residual stresses caused by plastic strain [10]. In the second stage, the residual stresses decreased linearly as function of Ln (N) and the change was proportional to the loading amplitude [3].

In an experimental investigation, carried out by Cao [12], similar results were obtained. In this study shot peened thin plates of medium carbon steel (AISI 4135) were fatigue tested under repeated bending at load controlled (R=0) conditions. The results showed a significant relaxation of residual stresses on the compressed surface. By a careful analysis of the change of residual stresses and FWHM profiles during the cyclic loading Cao concluded that: a) the first phase of relaxation was an effect of a balance of the residual stresses due to plastic strain redistribution in the affected layers. This step was called "quasi-static" or "elastic-shakedown". During the first cycles, relaxation was mainly due to plastic deformation followed by an elastic stabilization. b) The second phase was a slow relaxation principally due to the evolution of the mechanical properties under cyclic loading (cyclic softening or hardening of the affected layers).

Some factors such as fatigue stresses and cyclic mechanical properties of shot peened steels affect the relaxation of compressive residual stresses [7]. Torres and Voorwald [13] suggested that relaxation of compressive residual stresses was directly associated with the applied stress and the number of cycles. Guechichi and Castex [10] suggested that residual stress relaxation was associated with both the amplitude and the direction of the applied load and residual stress became stable when the superposition of the stresses remained below the cyclic yield stress. Zhuang and Halford [17] added some other influencing factors on residual stress relaxation: a) initial magnitude and gradient of the residual stress field b) degree of cold working c) fatigue stress amplitude d) mean stress ratio e) the number of cycles f) material cyclic stress-strain response and g) the degree of cyclic work hardening or softening.

2.8. Surface Roughness Effect

Shot-peening typically increases surface roughness and the surfaces of the shot-peened specimens are rougher than those of the non shot-peened ones. Roughness increase is a function of the hardness and size of shots, however, the hardness is clearly dominant [3].

In a study conducted by Plumtree [9], smooth specimens were tested under fully reversed tension-compression fatigue test (R=-1) in which the gradient of the loading stresses were shallower than any other type of fatigue tests i.e. rotating-bending tests and the gradient of compressive residual stresses became much steeper than the gradient of loading stresses, consequently, fatigue cracks initiated below the surface where loading stresses exceeded the local fatigue strength and the applied tension stresses were able to counter the compressive residual stresses.

The fractographical examinations, performed by [8,10,13,18], showed that fatigue cracks in the shot-peened specimens shifted to interior layers whereas they were located at surface for non shot-peened specimens. The mechanism of shifting fatigue cracks to interior layers minimized the detrimental effect of surface roughness on the high cycle fatigue properties since the initiation of cracks occurred in sub-surface layers in the shot-peened condition.

A study by Jiang et. al [5] on the effect of shot-peening on the bending fatigue behaviour of Ti-6Al-4V indicated that shot-peening roughened the surface but fatigue cracks, which were always initiated on the surface of as-received Ti-6Al-4V, were initiated in the sub-surface after shot-peening.

A model by Guechichi and Castex [10] determined the position of fatigue cracks for shot-peened low-alloy medium carbon steel at the depth of 0.3mm which was similar to the thickness of shot-peened layers. Wang et.al [14] performed three-point bending fatigue tests on shot-peened 20Cr, 30CrMo, 40Cr, GC4, 45 steels and Al-alloy LC9. They showed that fatigue cracks were always located at the surface for non shot-peened cases, whereas these cracks were located beneath the compressive residual stress zone in all the shot-peened specimens except medium carbon steel (AISI 1045 steel) in which crack sources were located inside the hardened layer within compressive residual stress zone.

In the micro-meso-processes theory for fatigue crack initiation and fatigue limit theory, a concept of an internal or a surface fatigue limit of material is proposed and it is confirmed that the critical stress for initiation of a fatigue crack in the interior (the internal fatigue limit of material) should be higher than at the surface (the surface fatigue limit of material) by about 40%. Transfer of the fatigue crack from surface into the interior is the beneficial mechanism caused by shot-peening and improves the fatigue limit of shot-peened specimens [18]. Landgraf and Chernenkoff [30] tested AISI 5160 steel under four point bending and found that all failures initiated subsurface, nominally where the residual stress profile became tensile.

Based on the experimental studies and the suggested models which predict the initiation of fatigue cracks in the subsurface layers, it is inferred that the surface roughening caused by shot-peening is of lesser importance than two other shot-peening effects, compressive residual stresses and work hardening, since the origin of fatigue cracks shifts into the region below the surface hardened layer.

2.9. Crack Initiation and Propagation

It is known that induced compressive residual stresses have little effect on crack nucleation, but can drastically retard crack propagation [3,7]. The metallurgical modification, observed in the majority of shot-peened materials, is favourable surface work hardening which retards crack nucleation [7].

Fracture surface observation of shot-peened specimens by Rios et al. [28] under an optical microscope and scanning electron microscope (SEM) showed that a crack usually starts growing from the edge of a specimen, initially in a quarter of a circle shape. It then assumes approximately a semi-elliptical shape, growing faster in the depth direction than on the surface, thus showing that surface compressive residual stresses delay crack growth [28].

Torres and Voorwald [13] concluded that shot peening shifted the crack sources below the surface in most of the high cycle cases due to induced compressive residual stresses that were greater than the applied stresses.

Rios et al. [28] performed pure bending fatigue tests (R=-0.8) on annealed A316 stainless steels. They showed typical initial retardation of crack growth and its subsequent acceleration in a non shot-peened condition and a significant deceleration of fatigue crack growth in a shot-peened condition as depicted in Figure 2.6.
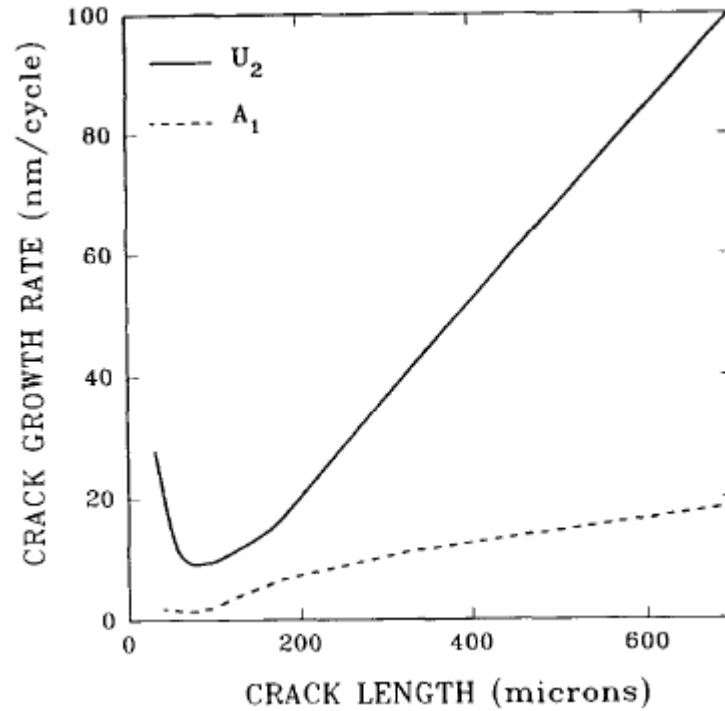
Figure 2.6.Fatigue crack propagation (U2: non shot-peened, A1: shot-peened)

One interpretation is that micro-structural barriers constrain crack tip plasticity until the stress concentration at the barrier reaches a critical value. At that point crack tip plasticity moves past the barrier, consequently, the crack growth rate begin to rise again [28].

Rios et al. also showed that shot-peening significantly affected the crack growth within the short-crack region. Crack growth in this region was dependent on the microstructure and this dependence extended for several grains. Short-crack propagation rates in the shot-peened specimens were much lower than the non shot-peened ones (Figure 2.6). In addition to the initial effect of the residual stresses, the resistance to plastic deformation at the crack tip is much higher in shot-peened condition due to the work hardening. The critical stage for crack propagation in

15

shot-peened surfaces seems not to be the overcoming of barriers, but rather the generation of sufficient crack tip plasticity to drive the crack forward [28].

Most of the studies were carried out on quenched-tempered medium carbon components to determine the effect of shot-peening on the fatigue behaviour. In this research, air cooled and quenched-tempered steels as well as a powder metallurgical steel were studied to determine and compare the effect of metallurgical structure on the high cycle fatigue properties.

In other studies [6-16], fatigue testing of shot-peened steels was carried out mostly under rotating-bending conditions but in this research fully reversed (R=-1) push-pull fatigue tests were conducted since many engineering components are subjected to these conditions. Generally, the fatigue stresses in push-pull loading result in a lower fatigue strength than bending since the stresses are uniform. This will be investigated in the present study.

Chapter 3

Experimental Design

3.1. Material

Medium carbon steels, AISI 1141 and AISI1151, have been used in the manufacture of engineering components, for example, forged steel connecting rods. Now, most North American companies use forged powder metallurgy (PM) connecting rods [31]. In 2003, 60.0% of the North American market used powder metallurgy steel rods whereas 35.0 to 40.0% were forged steel. By comparison, a crackable steel (C70) has been recently introduced and is widely used in Europe. [31].

To compare the fatigue behaviour, four groups of steels, AISI 1141, AISI 1151, powder metallurgy 0.5% C (PM) and C70S6 (AISI 1070), were chosen for investigation. The chemical compositions of these steels are shown in Table 3.1.

Table 3.1.Chemical composition (%)

Steel	Chemical Composition (%)									
	C	Mn	S	P	Si	Cu	Cr	Mo	Ni	V
AISI 1141	0.39	1.41	0.12	0.01	0.24	0.05	0.1	0.01	0.03	0.06
AISI 1151	0.48-0.55	0.7-1.00	0.08-0.13	0.04 (Max)	-	-	-	-	-	-
PM	0.5	0.31	0.12	-	-	3.06	-	-	-	-
C70S6	0.72	0.5	0.06-0.07	0.009	0.22	-	0.061	-	-	0.04

3.2. Specimens

3.2.1. Heat and surface treatments

All four steels were heat treated to give similar hardness values and good balance of strength and ductility. The AISI 1141, PM and C70S6 steels were normalized while the AISI 1151 steel was quenched and tempered. After heat treatment, half of the specimens from each group were shot peened with 100% coverage to Almen scale 14-18A using 1mm diameter steel shots.

3.2.2. Specimens shape and dimensions

The shape and size of sheet type specimens are shown in Figure 3.1. These specimens were machined from the shank of connecting rod. They were previously fatigue tested. Smaller specimens (Figure 3.2) were taken from the grip section of the sheet type specimens for tensile testing. The grip section was then used for microhardness tests. Table 3.2 gives the total number of non shot-peened and shot-peened specimens tested under tensile and fatigue conditions.
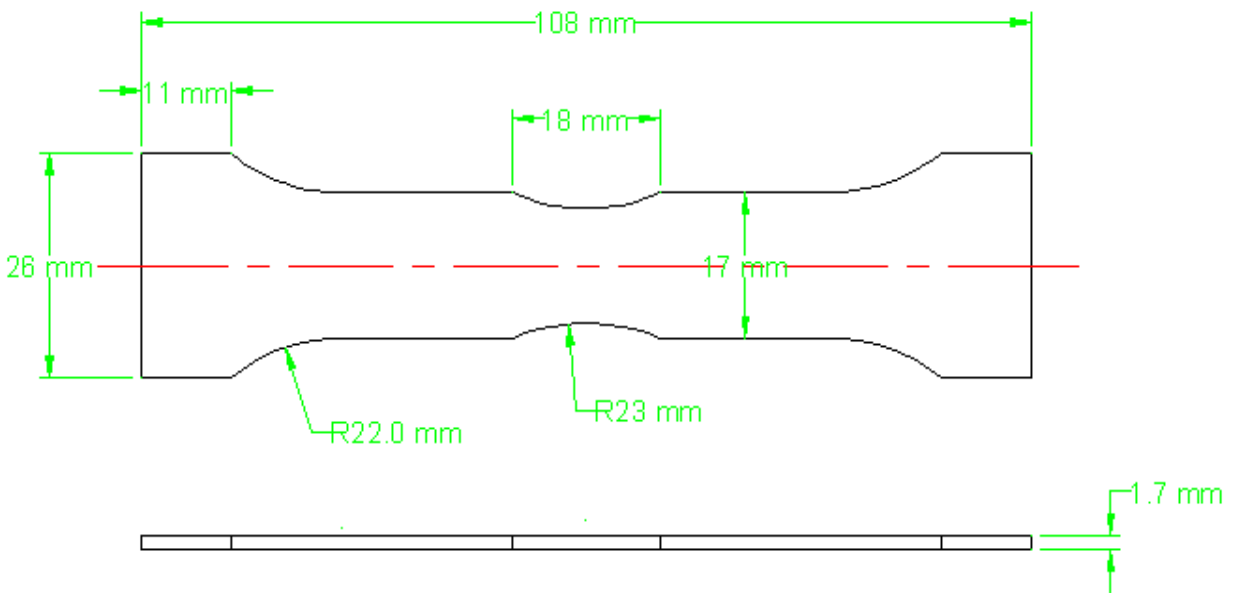
Figure 3.1.Fatigue (original) specimen dimensions
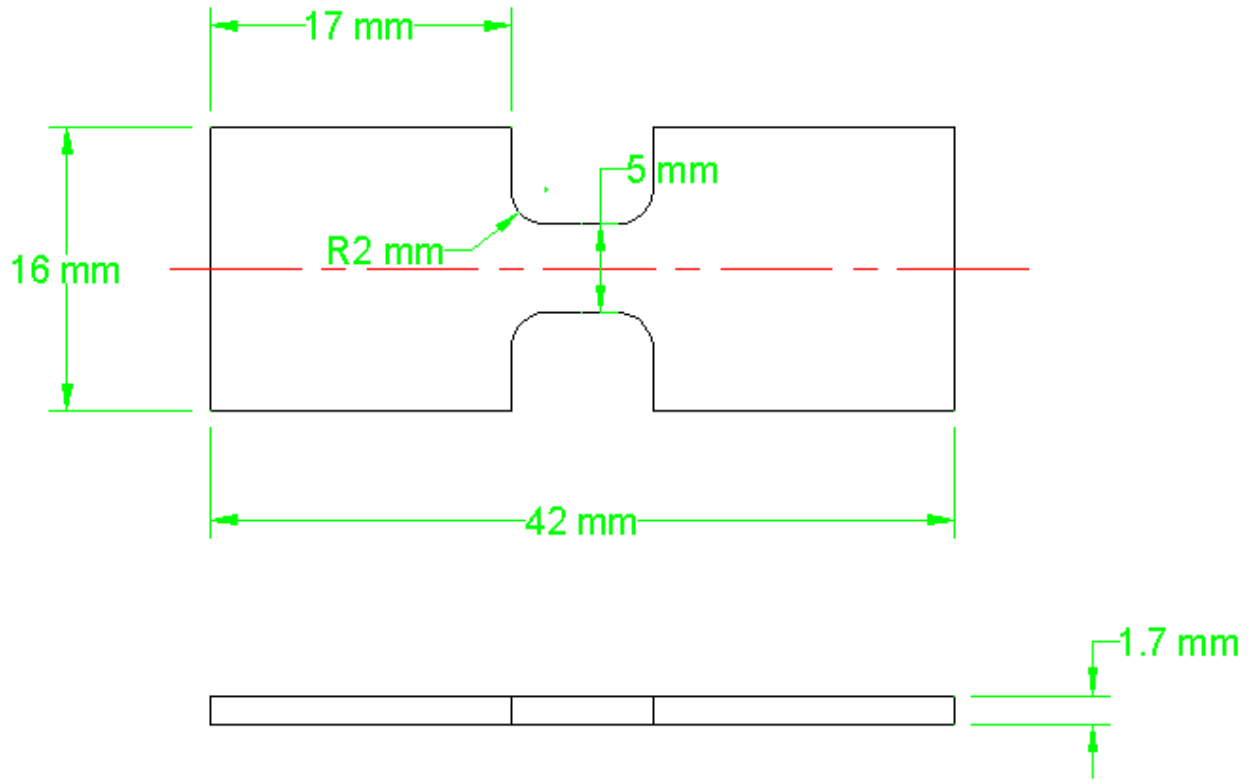
Figure 3.2.Small tensile specimen dimensions

Table 3.2. Number of specimens tested

Test	Number of Specimens	
	Non Shot-Peened	Shot-Peened
Tensile	4	4
Fatigue	36	40

3.3. Tensile Test

Tensile tests were performed with an Instron-4206 hydraulic powered 150KN tensile machine only on small specimens to compare the reported tensile strength by Galt Testing Laboratories with these test results as shown in Table 3.3. Table 4.1 and Table A1 give other tensile test data for the tested steels.

Table 3.3. Tensile test comparison

Material	Galt Testing Laboratories		MME - University of Waterloo	
	Tensile Strength (MPa)	Elongation (%)	Tensile Strength (MPa)	Elongation (%)
AISI 1141	855.0	17.0	921.2	16.2
AISI 1151	999.8	12.0	997.0	13.1
PM	889.5	15.0	956.1	16.1
AISI 1070	1006.7	13.0	980.5	14.0

3.3.1. Selection of specimens

Small specimens were prepared from each group, one shot-peened and one non shot-peened and then tensile tested.

The original specimens were numbered for fatigue testing. The same numbering was used for the tensile test. The first digit indicated the material group, where 1, 2, 3 and 4 indicated AISI 1141AC, AISI 1151QT, PM and C70S6AC respectively. The second digit expressed the specimen's condition. If non shot-peened specimen, the digit was between 1 and 9, if the specimen was shot peened it was between 10 and 19.

3.3.2. Tensile testing

Crosshead speed was 2mm/min for the first specimen (1-3) and 1mm/min for the rest.

3.4. Microhardness Tests

3.4.1. Specimens

The first series of microhardness tests were performed on the grip sections of small tensile specimens. For the remaining series of microhardness tests, the grip or gage sections of the fatigue specimens were used.

3.4.2. Specimen preparation

Careful preparation of the samples was necessary for the microhardness tests and the measurement of indentations. The practical sample preparation procedure was as follows.

3.4.2.1. Cutting

Cutting, or sectioning, was performed with a cutting-wheel. Cooling was necessary in order to avoid structural changes by heating. The specimen number was engraved on each sample immediately after cutting. The outer edge of each specimen was marked for identification purposes.

The orientations in the present tests were those which are customarily used to specify specimen and crack orientations. For these flat sections, the three standard designated directions were longitudinal (L), transverse (T), and short transverse (S). An ordered pair of these symbols, L, T and S, in which the first letter designated the direction of loading plane and the second letter (eg. L-T) designated the fracture plane (T) as shown in Figure 3.3.

The majority of the microhardness tests were performed in the L-S orientation, however, supporting tests were carried out in the T-S orientation in the grip section and in the L-T orientation in the gage section.
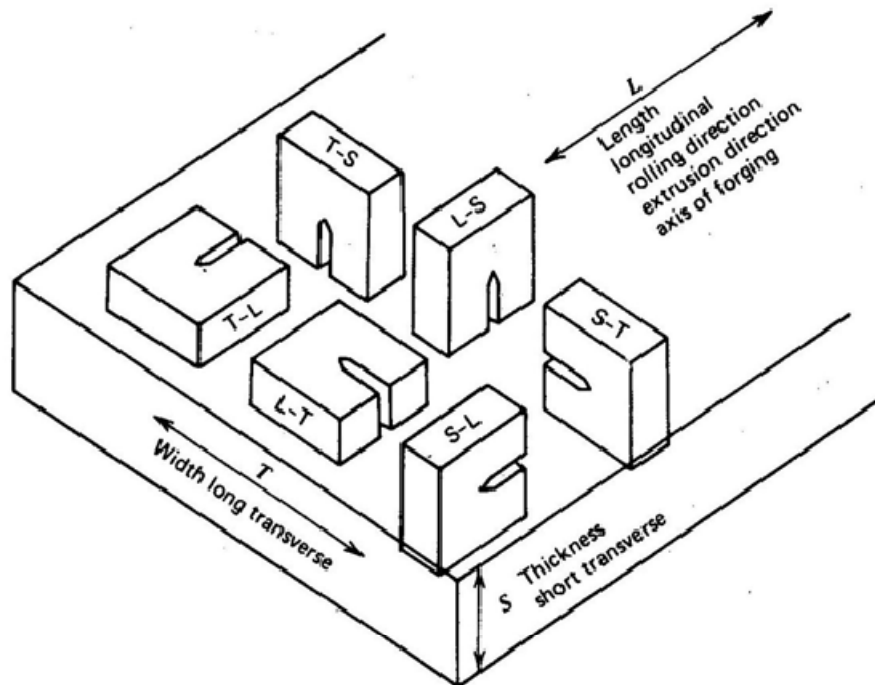
Figure 3.3.Code system for specimen orientation and crack propagation direction in plane [32]

3.4.2.1.1. Grip section (L-S and T-S)

For the first series of microhardness tests, the small specimens in L-S and T-S orientations were tested. For the rest of the tests, the original specimens in the L-S orientation were used.

3.4.2.1.2. Gage section (L-T)

Three specimens 1-16, 3-15, 4-11 were examined. Microhardness tests on the surface (L-T) parallel to the crack, at distances of 1mm to 2mm away from the crack were carried out.

3.4.2.1.3. Gage section (L-S)

The specimens were prepared to enable the user to conduct the hardness test across thickness (L-S) close to the crack site, i.e. 2mm to 8mm from the crack. For the specimens without a crack, the whole gage section was cut and the microhardness indentations were taken in the center of this section.

3.4.2.2. Mounting

After cutting, the microhardness samples were mounted using "phenolic hot mounting powder" and a Struers press. Immediately after mounting, each sample's number was engraved for identification.

3.4.2.3. Grinding

Emery paper was used to carry out the planar grinding. In the present case it has been performed in six steps with hand and spinning grinder using 240, 320, 400, 600, 1200 and 4000-grit emery papers from the roughest to the smoothest. Each step took about 10 minutes. It is important to carefully rotate the sample 90° between each step and to keep the papers wet.

3.4.2.4. Polishing

Polishing was carried out with 5μm, 1μm, 0.3μm and 0.05μm alumina powders from the roughest to the smoothest each lasting for about 5 minutes. The samples were rinsed with water

between each grade of polish and finally rinsed with alcohol to avoid stains from water on the sample surface.

3.4.3. Microhardness test

The Leco micro-indenter was used to perform the Vickers microhardness test. The loads applied were 0.1 and 0.5kgf with a standard dwell (load) time of 30 seconds for each load.

3.4.3.1. L-S and T-S

For the L-S test, both 0.1and 0.5kgf loads were used. Under 0.5kgf (HV0.5), the number of indentations was different from one specimen to another: 14 indentations in two lines or 27 indentations in three lines in a staggered pattern. On average, 7 to 9 indentations were made per line. Under 0.1kgf (HV0.1), the number of indentations was the same for all the specimens. Eighty four (84) indentations were performed in six lines. There were two series of three indentation lines each containing 42 indentations in a staggered pattern. The second series (the second 42 indentations) was carried out as a verification for the first 42 indentations. The results from both series have been included in the results.

For the T-S tests, a 0.5kgf load was applied (HV0.5). Thirteen (13) to 14 indentations were carried out in two lines of indentations, on average, 7 indentations per line. For specimen 3-5, four lines of indentations, 24 indentations in total, were made. The values of the first and second rounds are reported both separately and together in the Results section.

In general, for indentations under 0.5kgf load, the spacing was almost 250μm. Other spacings existed and have been reported on the hardness profile. The spacing between either the first or last indentation relative to the edges ranged from 40 to100μm.

Under a 0.1kgf load, the spacing between all two adjacent indentations in a line was 100μm but the spacing between the first indentation to the closest edge was different from one line to another line since the indentations were made in staggered arrangement. This spacing was 25μm for the first line while 50μm and 75μm for the second and third lines respectively.

3.4.3.2. L-T

Two lines of indentations on the surface of the gage section, parallel to the crack, 1mm and 2mm away the crack, were made. Each line included 14 to 20 indentations.

3.4.3.3. Surfaces hardness test

Since the surface hardness could not be taken for the cross section test, supplementary hardness tests were made on the surface (L-T). Hardness values at zero and 1.7mm in the L-S hardness profile were obtained by the surface tests.

For this purpose, 4 indentations (2 under 0.1kgf and 2 under 0.5kgf load) were performed on each surface. As reported in the results section, surface 1 and surface 2 correspond to zero and 1.7 mm respectively.

3.4.4. Measurements

The diagonals of the microindentations were measured using the microscope of the microhardness tester or an optical microscope and image processing and analysis software installed on lab computer namely "Image-Pro6.0". The optical microscope lenses were connected to the laboratory computer through a piece of hardware enabling the user to work with "Image-Pro6.0".

For the present tests, "Image-Pro6.0" was used to carry out the measurements. Initially, for some specimens both the microhardness tester and software were used to ensure the accuracy of the readings obtained from the software. Since the results of the software were in good agreement with microhardness tester, "Image-Pro6.0" was then used for the rest of the specimens.

To measure the diagonals under 0.5 and 0.1kgf, 50X and 100X magnification lenses were used respectively, 10X lenses were used to measure spacings which were 100 and 250μm approximately.

The diagonals of the indentations left in the surface of the material by the indenter were measured. The average measurement of diagonals was converted to a Vickers hardness number

through a hardness conversion table. It should be noted that an interpolation was used when average dimension of the diagonals did not correspond with any of the values in conversion table. Interpolation was necessary for almost all HV0.5 hardness tests whereas it was needed for only a few HV0.1 indentations.

3.5. Microstructure

Selected non shot-peened and shot-peened specimens were used for a microstructure examination. The preparation steps for etching were similar to the steps taken for a microhardness test: mounting, grinding and polishing (3.4.2.2 to 3.4.2.4). The purpose of etching is to optically enhance microstructural features such as grain size and phase features. A swab etching technique was performed using a swab cotton and Nital (%2.0) as etchant on specimen for few seconds (~5-10sec) to reveal general structure (grain and grain boundaries).

Chapter 4

Results

4.1. S-N Curves

All the non shot-peened specimens including 1-1 to 1-9, 2-1 to 2-9, 3-1 to 3-9 and 4-1 to 4-9 and all the shot-peened specimens including 1-10 to 1-19, 2-10 to 2-19, 3-10 to 3-19 and 4-10 to 4-19 were fatigue tested. Push-pull fatigue tests were conducted using a stress ratio of R=-1. The fatigue test results and the original S-N curves for all the specimens are given in Table B1 to Table B8 and Figure B1 to Figure B8 in Appendix B.

4.1.1. S-N curves non shot-peened

Figure 4.1 gives simplified S-N curves for the non shot-peened specimens. Detailed S-N curves are given in Figure B1 to B8 in Appendix B.
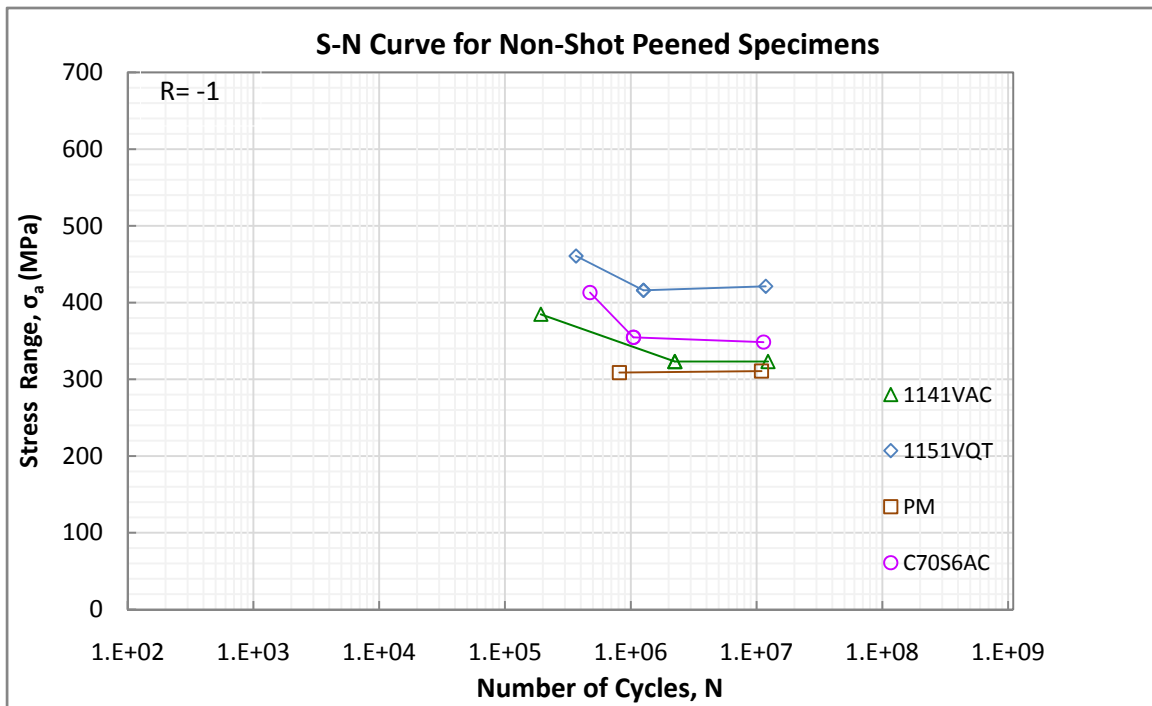
Figure 4.1.S-N curves for non shot-peened specimens

To determine the fatigue strengths at 10^6 cycles, an average and one standard deviation of stress amplitudes of those specimens, with or without cracks, which survived 10^6 cycles or higher were taken. Similarly, the stress amplitudes of the specimens with 10^7 or higher cycles

gave the fatigue strength with one standard deviation at 10^7 cycles. Detailed fatigue testing data for non shot-peened and shot-peened specimens are given in Table B1 to B8 in Appendix B.

At N=10^6 and 10^7, the fatigue strengths of the non shot-peened AISI 1151QT specimens were 418.3±18.6MPa and 427.3±7.6MPa and for PM were 310.0±13.8MPa and 311.0±19.5MPa respectively. Fatigue strengths of two other non shot-peened ones, AISI 1141AC and C70S6AC, at N=10^6 were 323.2±7.3MPa and 349.8±5.2MPa and at N=10^7 were 324.3±5.1MPa and 348.8±5.5MPa respectively.

4.1.2. S-N curves shot-peened

The S-N curves for the shot-peened specimens are shown in Figure 4.2.
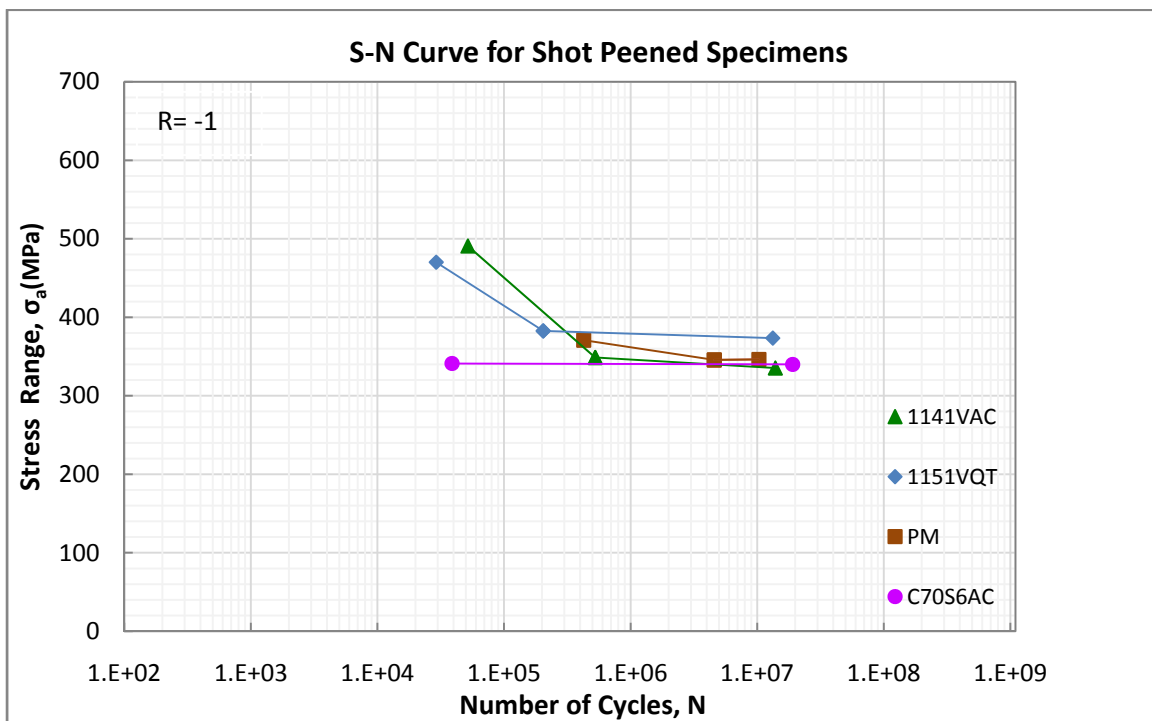
Figure 4.2.S-N curves for shot-peened specimens

The shot-peened specimens fatigue strengths were 372.3±31.3MPa and 375.9±32.7MPa for AISI 1151QT and 353.5±19.4MPa and 343.2±22.4MPa for PM at N=10^6 and 10^7 respectively. For the C70S6AC (crackable) steel, the fatigue strengths were 342.6±8.4MPa and 341.3±7.4MPa and for the AISI 1141AC steel, fatigue strengths were 342.7±14.9MPa and 331.6±2.6MPa at 10^6 and 10^7 cycles respectively.

4.2. Tensile Test

As mentioned in the Experimental Design section, small (sub-size) specimens were cut from the grip section of fatigue (original) specimens for tensile testing. Both non shot-peened and shot-peened specimens were tensile tested. The test data is given in Table 4.1. Engineering and true stress-strain curves for the specimens are shown in Figure 4.3 to Figure 4.10.

Table 4.1.Tensile test results

Specimen		Length Elongation (%)	Tensile Strength σ_{UTS} (MPa)
Non Shot-peened	1-3	16.2	921.2
	2-2	13.1	997.0
	3-5	16.1	956.1
	4-5	14.0	980.5
Shot-peened	1-12	17.1	912.2
	2-10	16.2	958.5
	3-19	9.5	962.8
	4-10	13.1	983.1

Specimen 2-2 (AISI 1151QT non shot-peened) had the highest tensile strength among the non shot-peened specimens whereas specimen 4-10 (crackable) was the greatest among the shot-peened specimens. The results of the non shot-peened specimens were in good agreement with the results from Galt Testing Laboratories carried out on other non shot-peened specimens from the same group (Table A1).
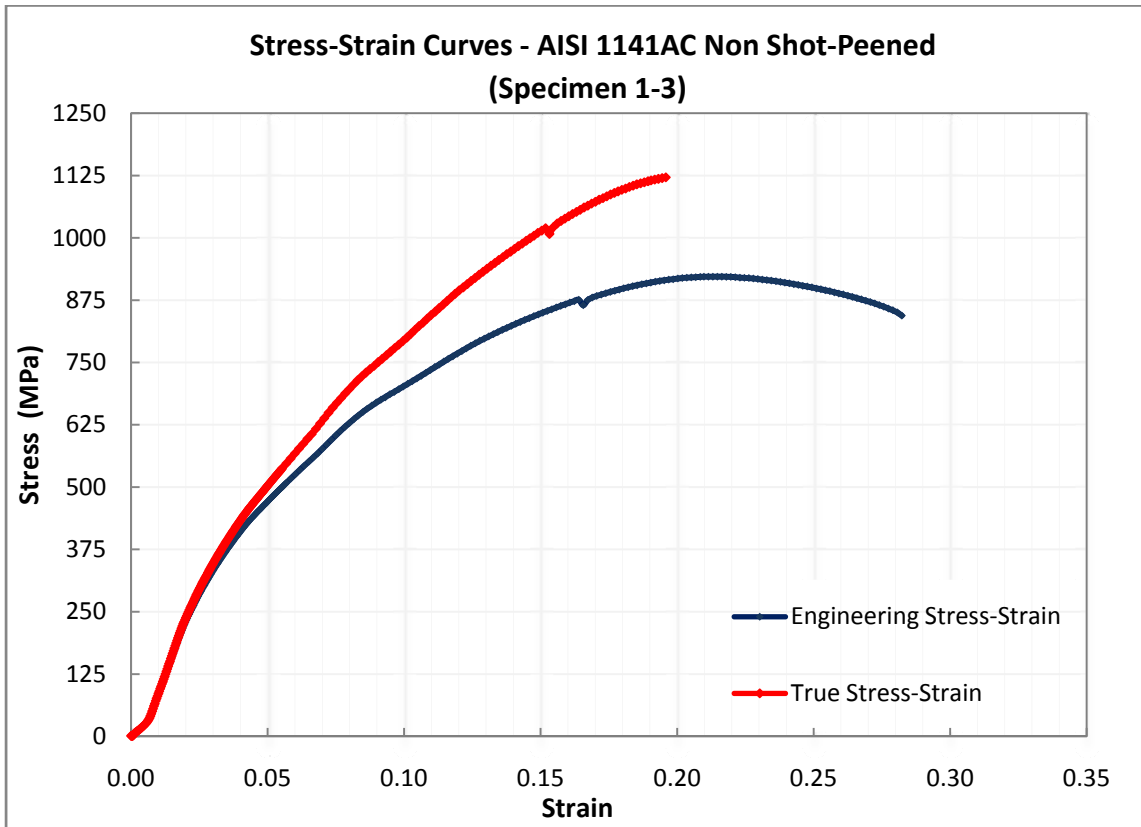
Figure 4.3.Engineering and true stress-strain curve for non shot-peened AISI 1141AC
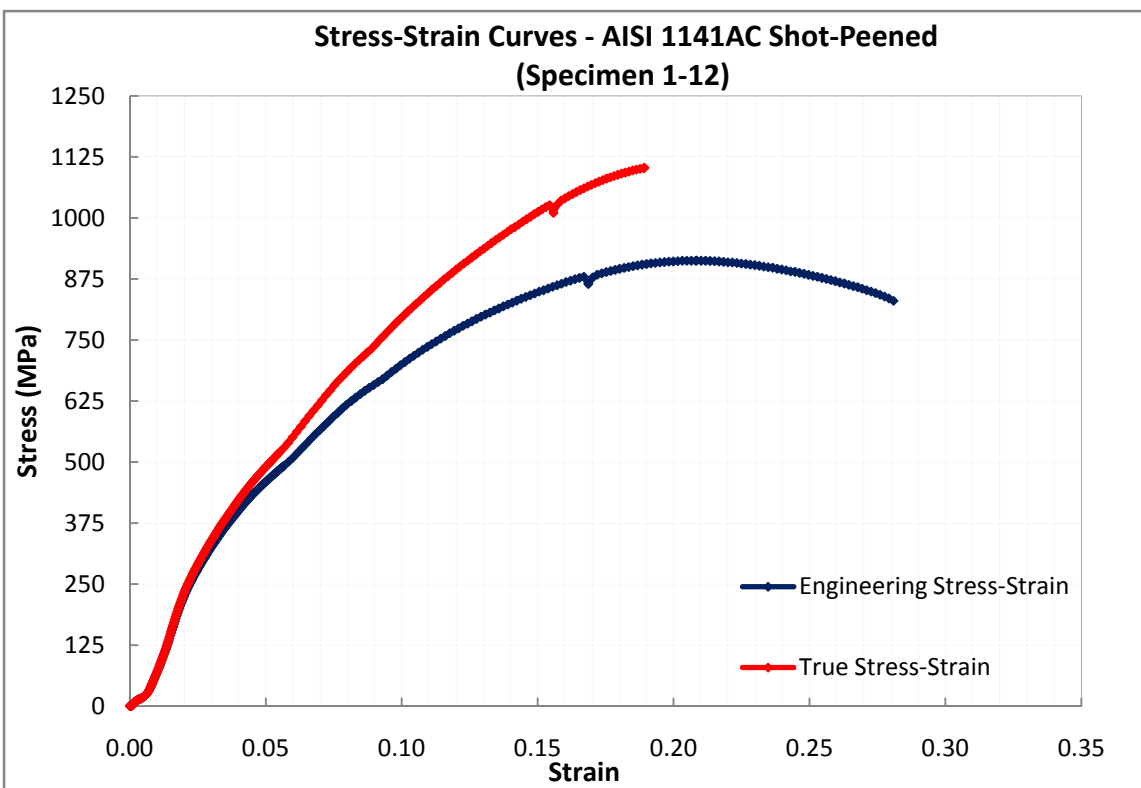
Figure 4.4.Engineering and true stress-strain curve for shot-peened AISI 1141AC
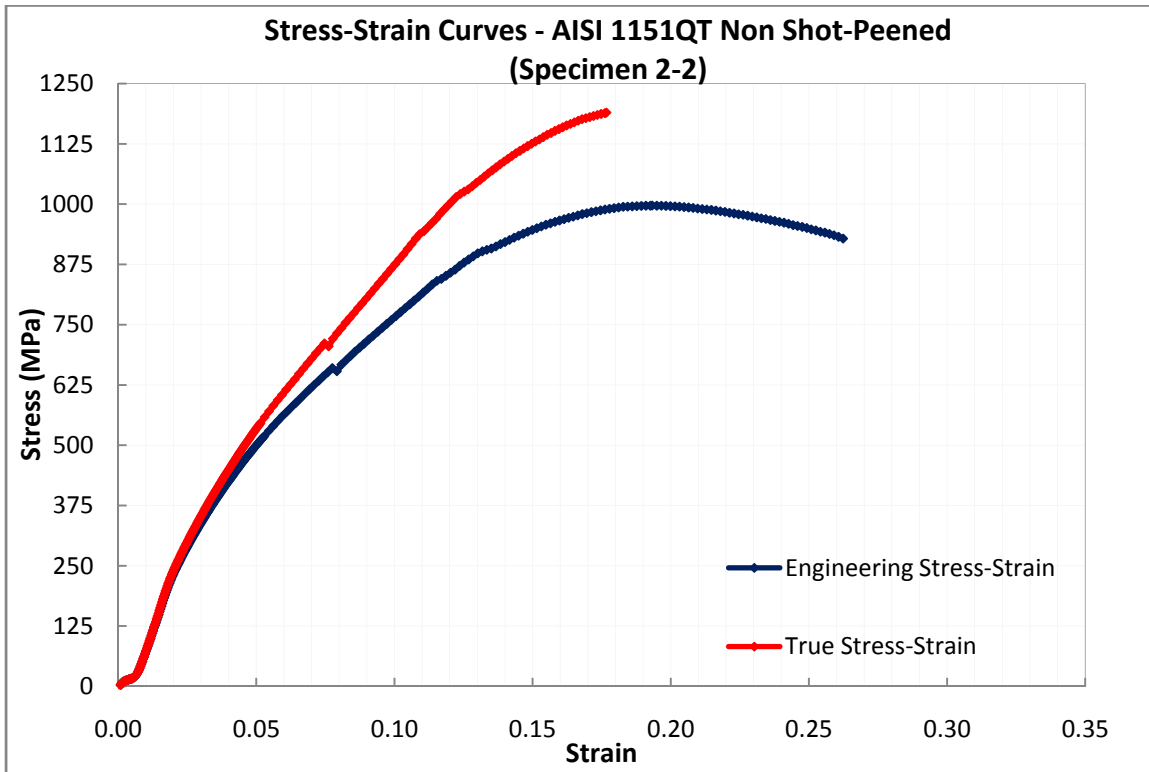
Figure 4.5. Engineering and true stress-strain curve for non shot-peened AISI 1151QT

Figure 4.6. Engineering and true stress-strain curve for shot-peened AISI 1151QT
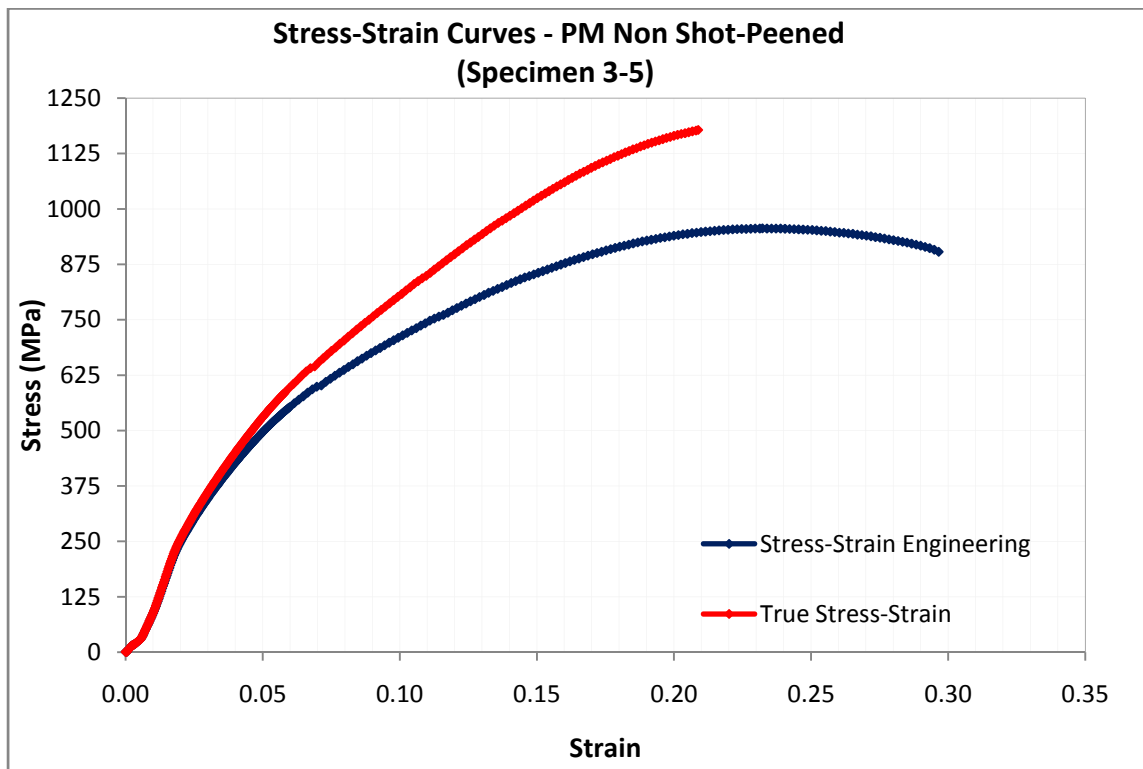
Figure 4.7.Engineering and true stress-strain curve for non shot-peened PM
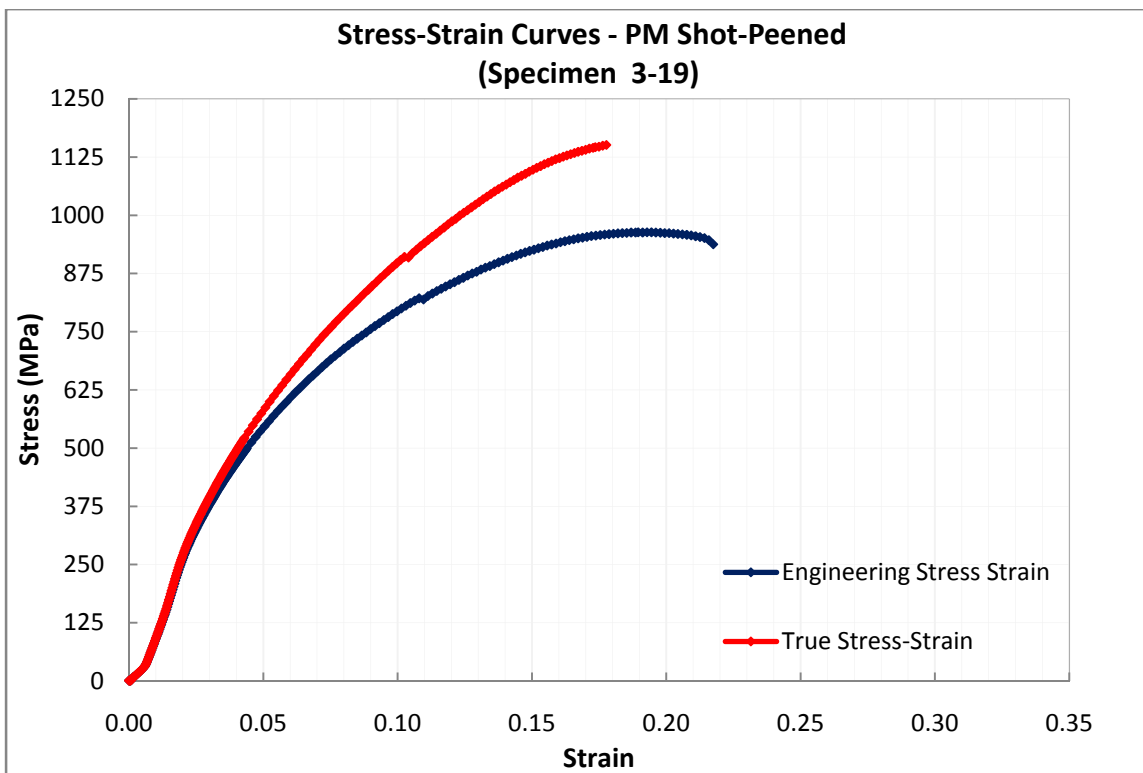
Figure 4.8.Engineering and true stress-strain curve for shot-peened PM
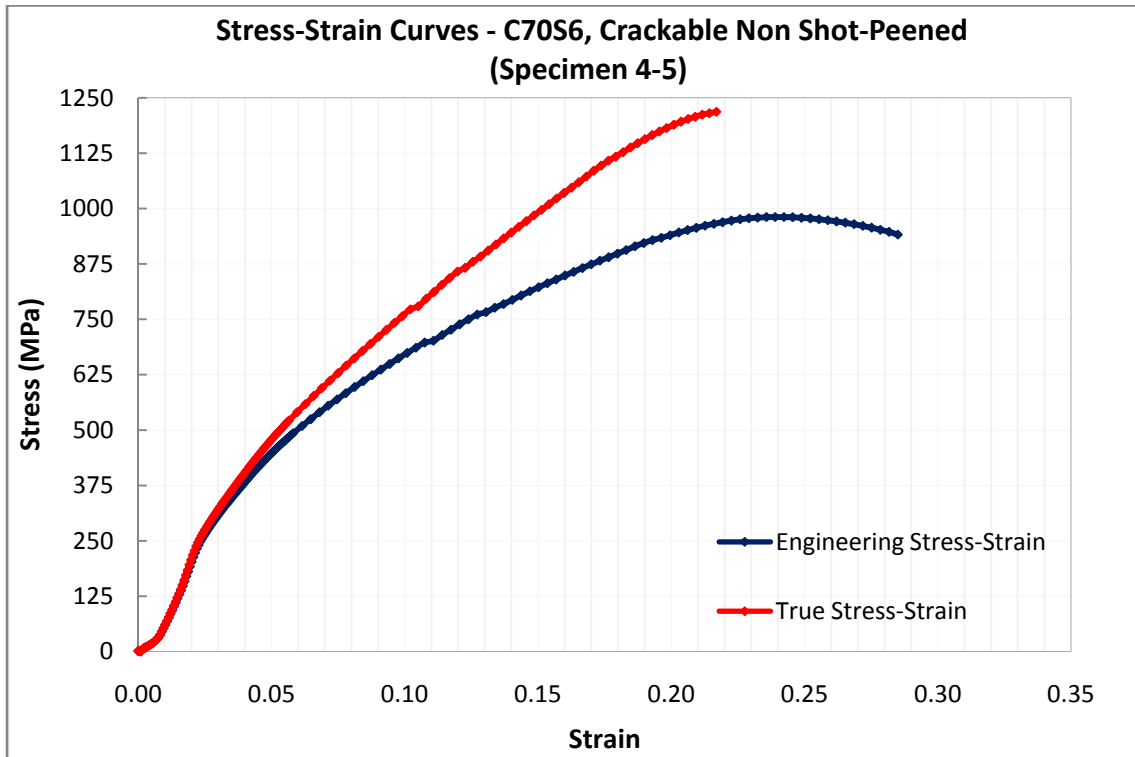
Figure 4.9.Engineering and true stress-strain curve for non shot-peened C70S6AC
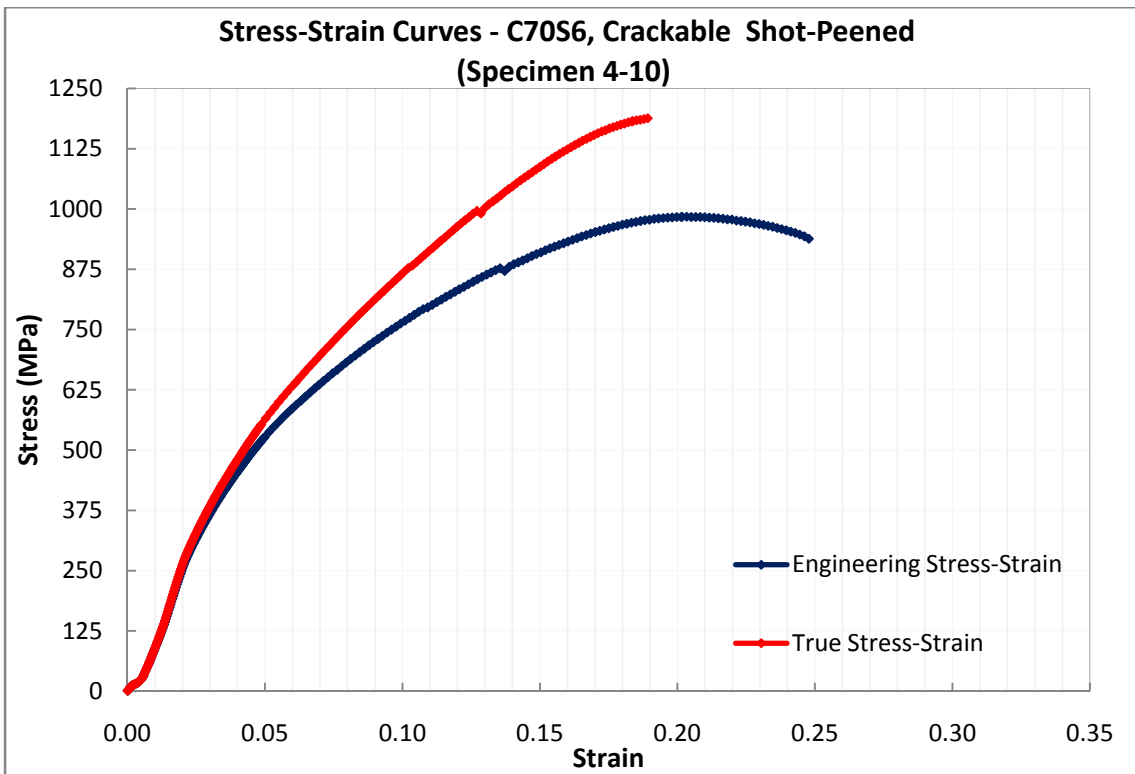
Figure 4.10.Engineering and true stress-strain curve for shot-peened C70S6AC

4.3. Microhardness

The average and standard deviations of the Vickers microhardness values plus fatigue test data for the non shot-peened specimens are shown in Table 4.2 to Table 4.5. The following curves give the microhardness values for the grip and gage sections in the L-S and T-S directions.

4.3.1. AISI 1141 Air cooled

4.3.1.1. AISI 1141AC non shot-peened specimens

Table 4.2 shows the L-S and T-S average microhardness values of the individual non shot-peened specimens.

Table 4.2.AISI 1141AC grip and gage section average hardness

SPECIMEN	σ_a (MPa)	R ($\sigma_{min}/\sigma_{max}$)	N (CYCLES TO FRACTURE)	GRIP SECTION HARDNESS (HV 0.5)		GAGE SECTION HARDNESS (HV 0.5)
				L-S	T-S	L-S
1-3	349.9	-1	587,800	277.2±8.1	287.9±8.5	281.5±7.5
1-7	319.6		10,073,900	291.0±5.3	NA	285.6±10.9

Microhardness Vickers tests were carried out on the grip section of specimen 1-3 in L-S and T-S directions (Figure 4.11) and specimen 1-7 in L-S direction (Figure 4.12). The test was also performed on the gage section of specimens 1-3 and 1-7 only in L-S direction as shown in Figure 4.14 and Figure 4.15. HV0.5 is indicative of Vickers hardness test using 0.5kgf load.
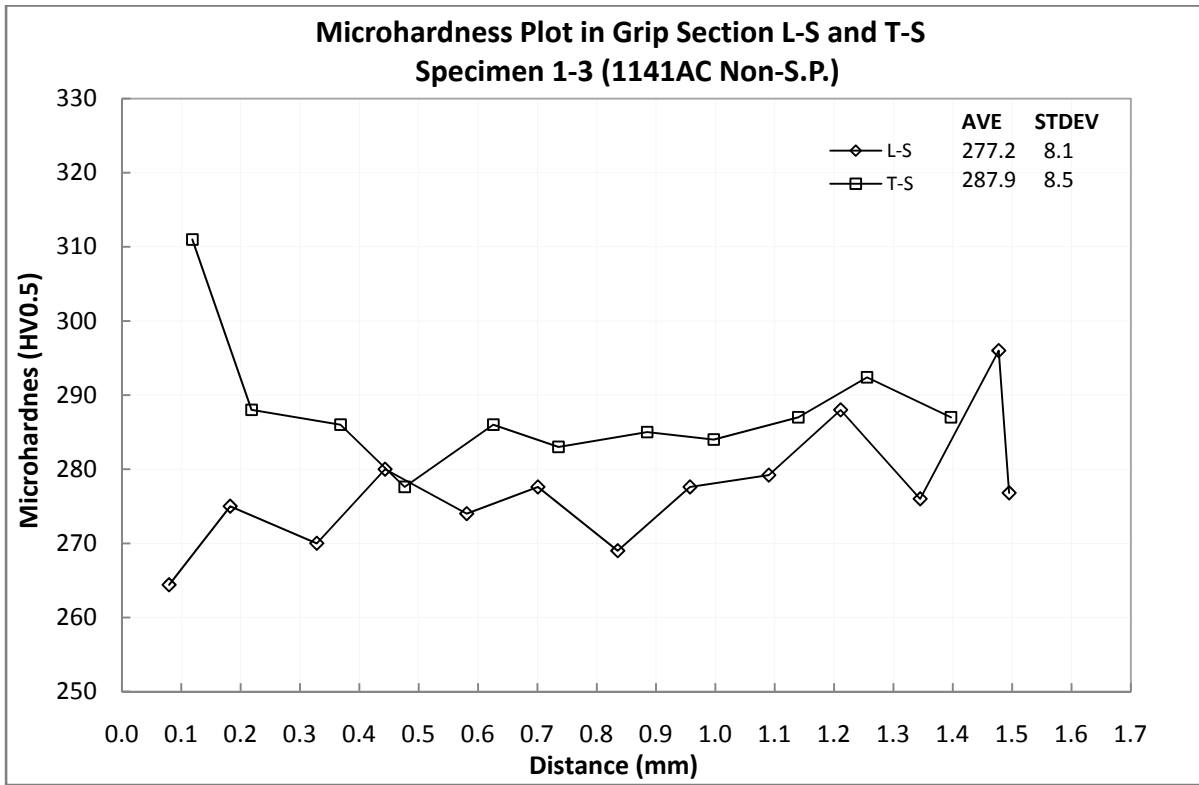
Figure 4.11.Specimen 1-3 microhardness plot in grip L-S and T-S
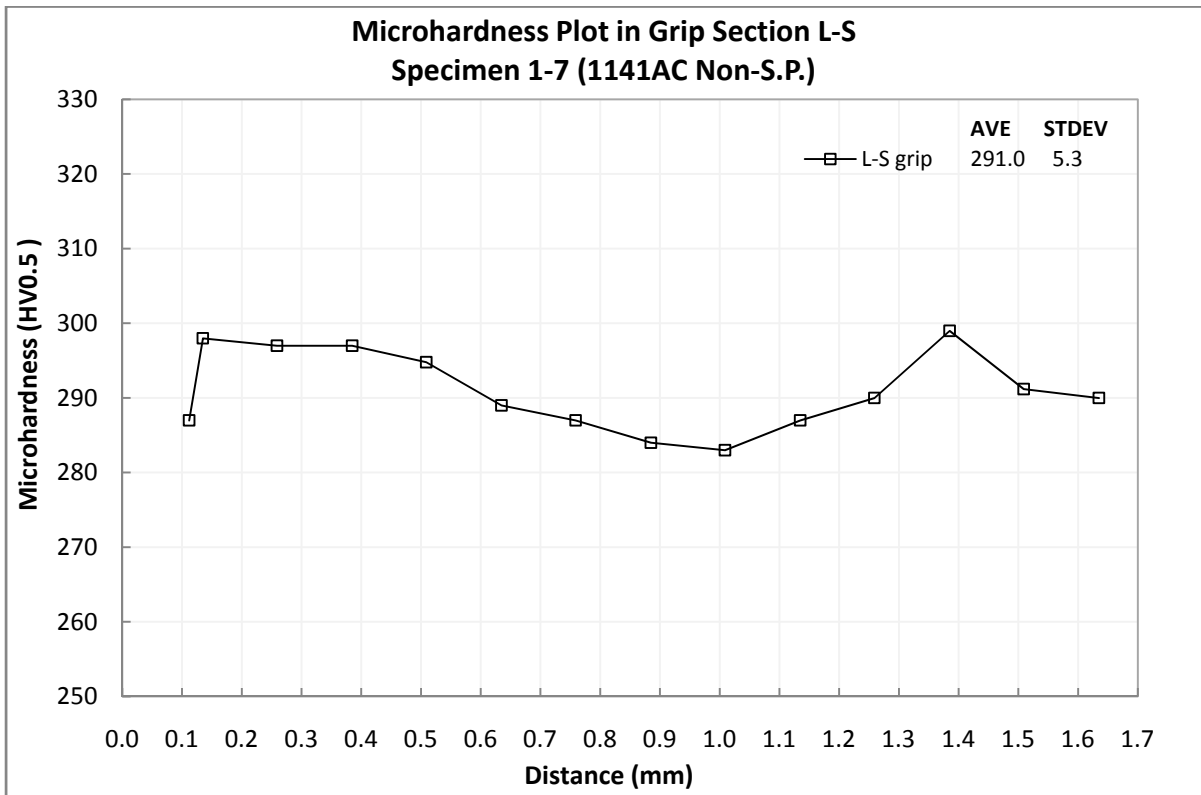
Figure 4.12.Specimen 1-7 microhardness plot in grip L-S
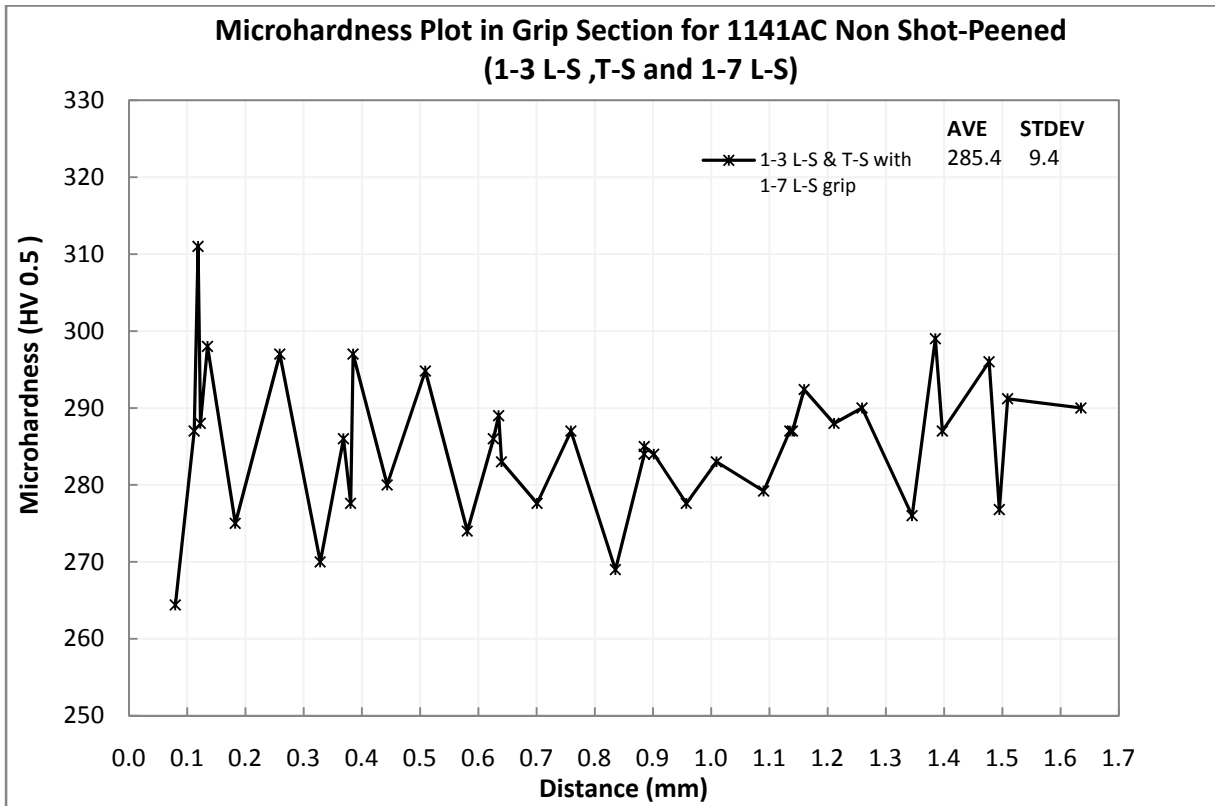
Figure 4.13.AISI 1141AC non shot-peened grip section microhardness plot

The results of specimens 1-3 and 1-7 were combined into a single plot, Figure 4.13, to generate an average hardness representative of the non shot-peened AISI 1141AC set. This average hardness in the grip section of AISI 1141AC was 285.4±9.4 HV0.5.

Figure 4.14 and Figure 4.15 show microhardness profiles (HV0.5) in the gage sections of specimen 1-3 and 1-7 respectively. The average hardness values in the gage section of these two specimens, 281.5±7.5HV0.5 for specimen 1-3 and 285.6±10.9HV0.5 for specimen 1-7, were very similar.
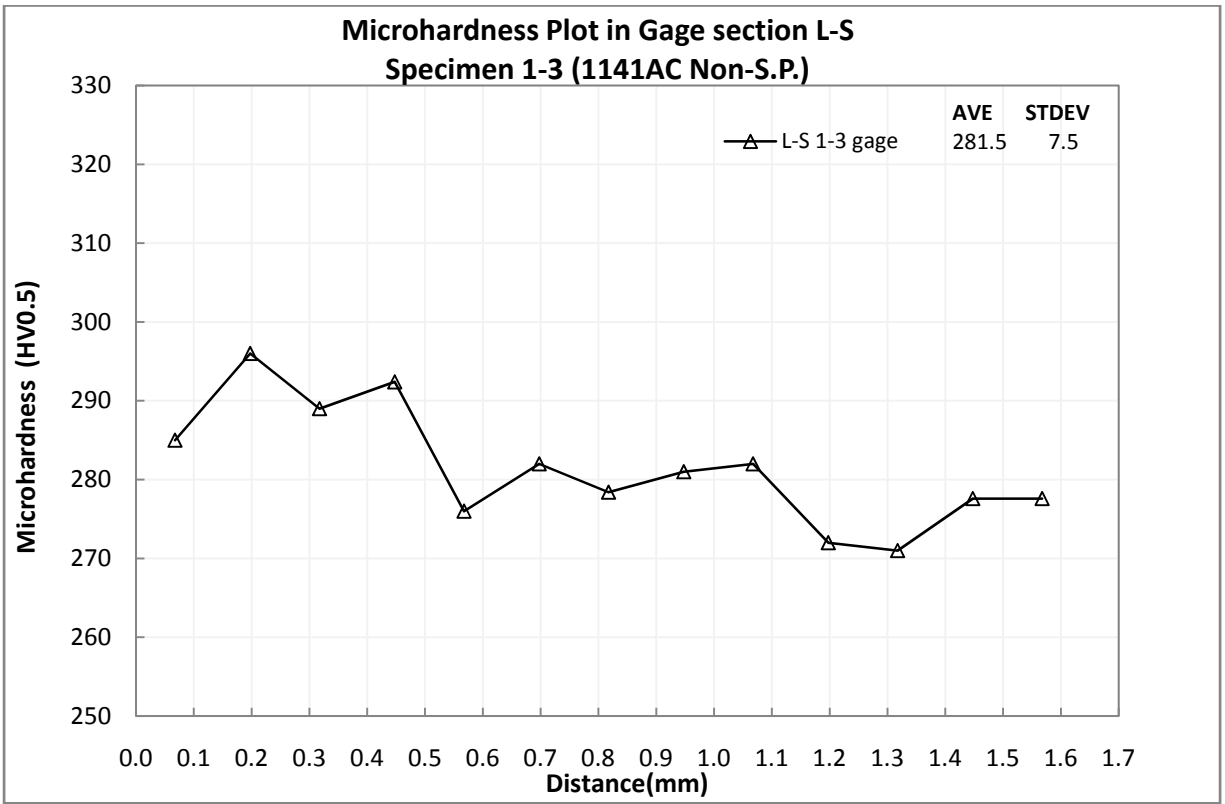
Figure 4.14.Specimen 1-3 microhardness plot in gage L-S
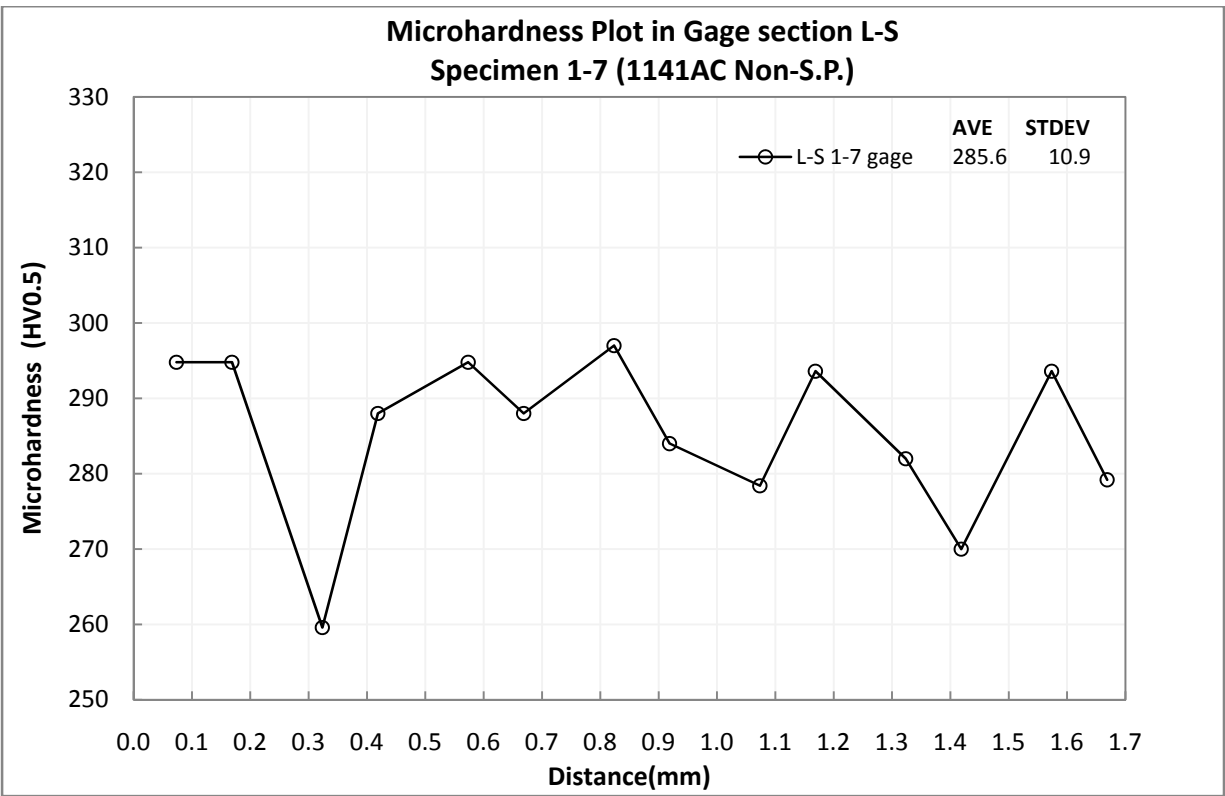
Figure 4.15.Specimen 1-7 microhardness plot in gage L-S

These results were combined into a single plot, Figure 4.16, to generate an average hardness representative of the non shot-peened AISI 1141AC in the gage section. This average hardness in the gage section of AISI 1141AC was 283.6 ± 9.5 HV0.5 after 5.8×10^5 cycles at $\sigma_a = 349.9$ MPa.
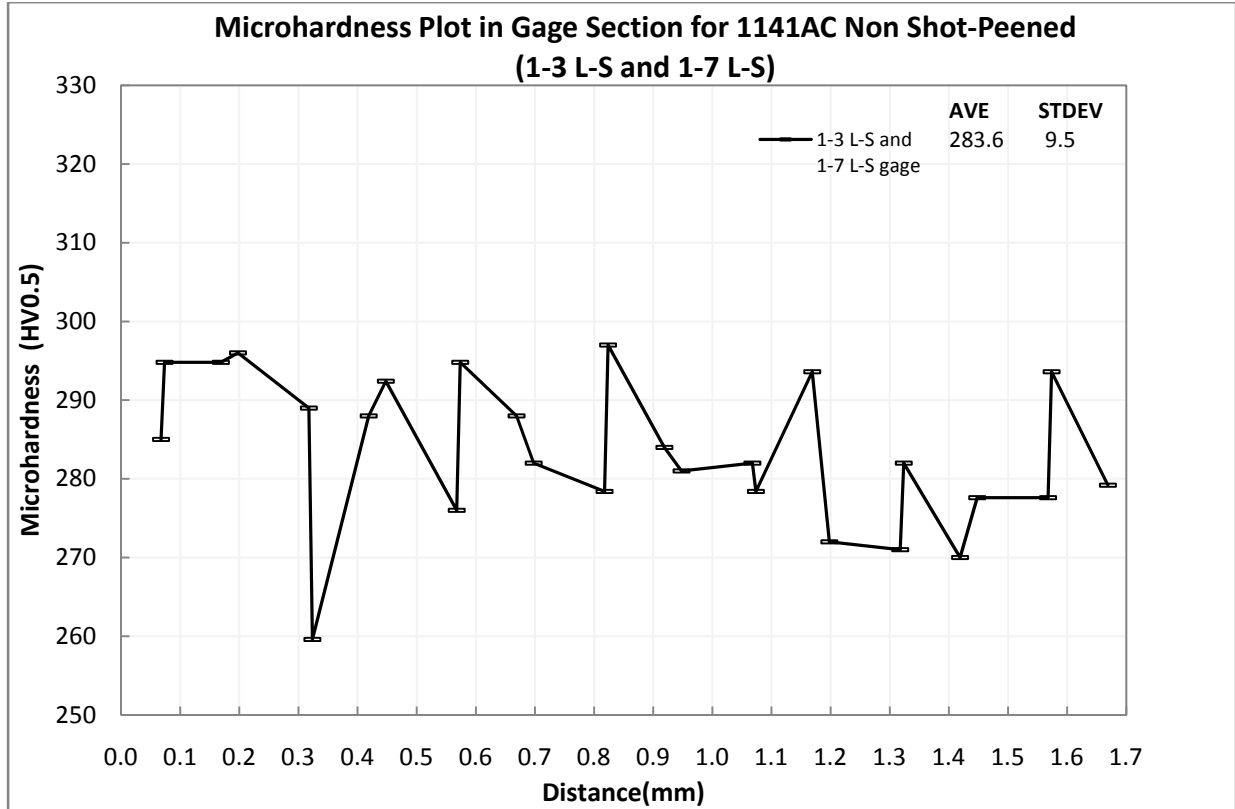
Figure 4.16. AISI 1141AC non shot-peened gage section microhardness plot

4.3.1.2. AISI 1141AC shot-peened specimens

Several microhardness profiles were taken on each specimen and an example of the results is shown in Appendix B. The profile was then arranged according to blocks of 0.1mm.

Specimen 1-16 was tested as representative of AISI 1141AC shot-peened group. Microhardness Vickers tests were carried out in the grip section in L-S direction and the gage section in L-S and L-T directions.
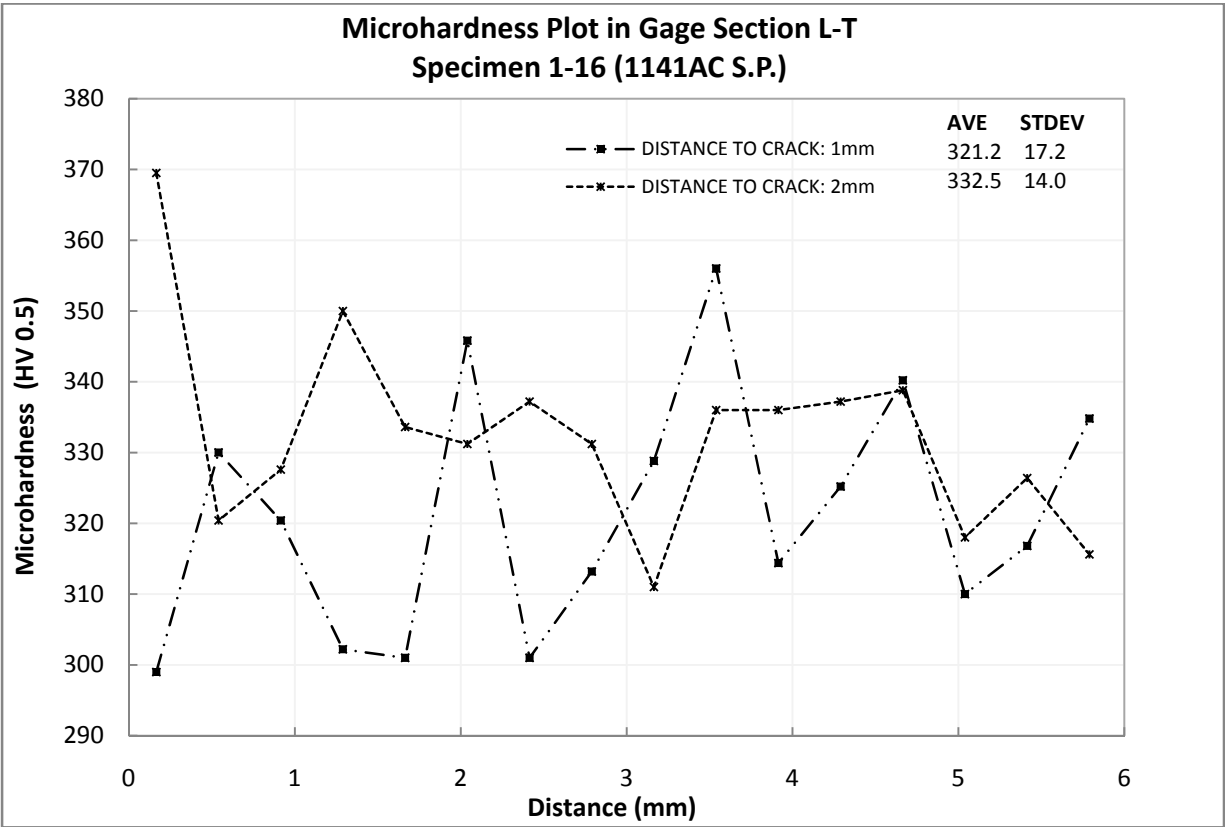
Figure 4.17.Specimen 1-16 L-T microhardness plot in gage section

The crack site was in the middle of the gage section in the L-T direction. Two L-T microhardness tests were performed parallel to the crack but 1mm and 2mm away from the crack. The L-T average hardness values for 1mm and 2mm away from the crack after 9.2×10^5 cycles at σ_a= 349.7MPa were 321.2±17.2 HV0.5 and 332.5±14.0 HV0.5 respectively (Figure 4.17). High variations were seen in this orientation.
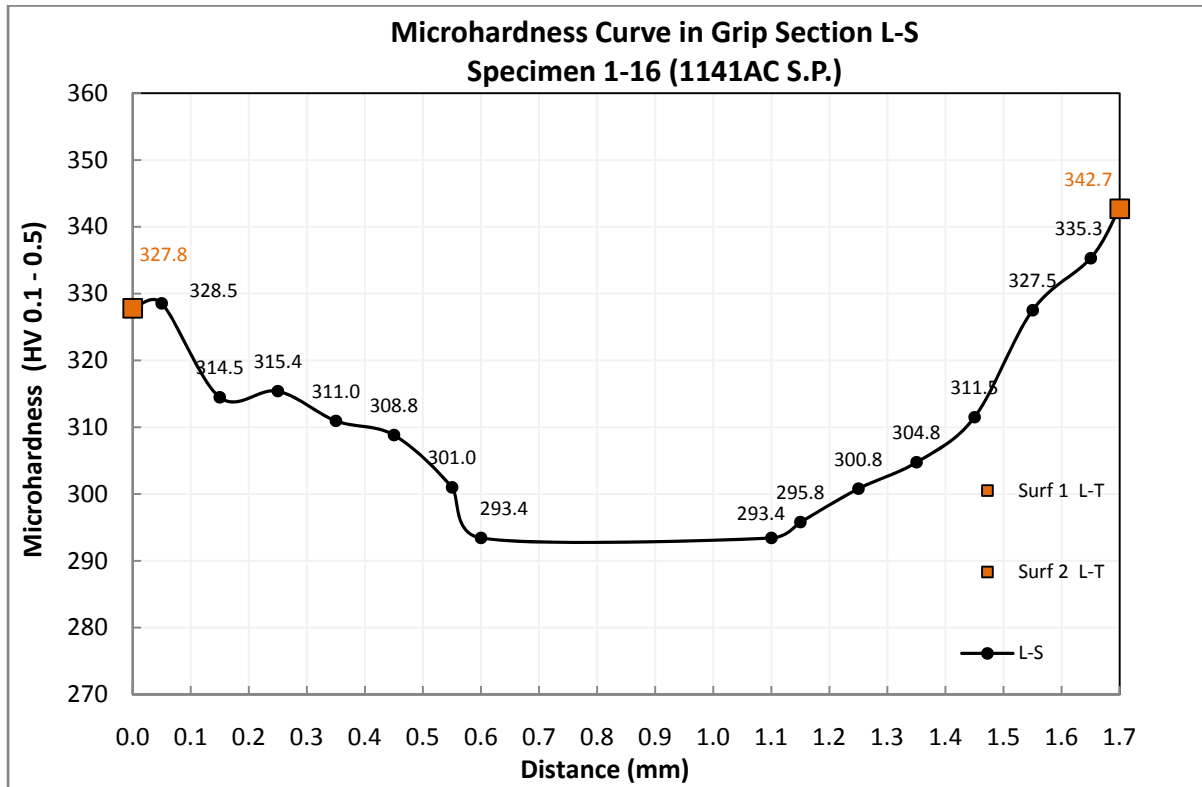
Figure 4.18.Specimen 1-16 grip section L-S microhardness profile

The hardness curves of specimen 1-16 in the grip section in the L-S direction, obtained from 0.1 and 0.5kgf (HV0.1 and HV0.5) tests, are included in a single diagram (Figure 4.18). This figure is divided into 0.1mm blocks except center region (0.6mm-1.1mm) which considered as a single block. The average and standard deviations were calculated for each 0.1mm block covering all tests data in that block. For the center, 0.6mm to 0.11mm, the average and standard deviations were calculated individually.

The L-S direction in both grip and gage sections of specimen 1-16 were divided into two regions namely: a) shot-peened and b) non shot-peened (the center).

In Figure 4.18 and Figure 4.19 the center line indicates the average hardness in the center or non shot-peened region resulting from all the tests data from 0.6 to 1.1mm and the side curved lines are trend lines showing change of hardness from one block to another.

Grip section (Figure 4.18):

a) The shot peened region in the grip section was 0.0 (surface1) to 0.6mm and 1.1 to 1.7mm (surface2). From 0.0 to 0.4mm, the hardness was from 310.0 to 328.5 HV0.1-0.5. After reaching its highest value, 328.5, at 0.05mm it reduced to 314.5 at 0.15mm and remained relatively unchanged up to 0.3mm. It again decreased to 311.0 at 0.35mm without any significant change up to 0.45mm. The hardness reduced to 301.0 at 0.55mm. From 0.1 to 0.5mm, the hardness variations were small.

On the right side of the center, the hardness increased from 295.8 to 311.5 HV0.1-0.5 between 1.15 to 1.45mm. A greater increase was seen between 1.45 to 1.55mm where hardness increased to 327.5. The maximum hardness in the L-S orientation was 335.3 at 1.65mm. The hardness variations in the right side were higher than the left. The L-S hardness drastically changed between 0.0 to 0.2mm and 1.45 to 1.55mm.

b) The center, non shot-peened region, was from 0.6 to 1.1mm with a hardness of 293.4±14.9 HV0.1-0.5. This hardness value in the center of 1-16 grip section was similar to that of the non shot-peened specimens (Figure 4.11 and Figure 4.12) considering standard deviations.

Surface 1 (left) and surface 2 (right) L-T hardness values, 327.8 and 342.7 HV0.1-0.5, completed L-S hardness curve. It should be noted that a reference surface have been designated for all specimens including 1-16. The zero level in both grip and gage curves corresponds to the reference surface or surface 1.
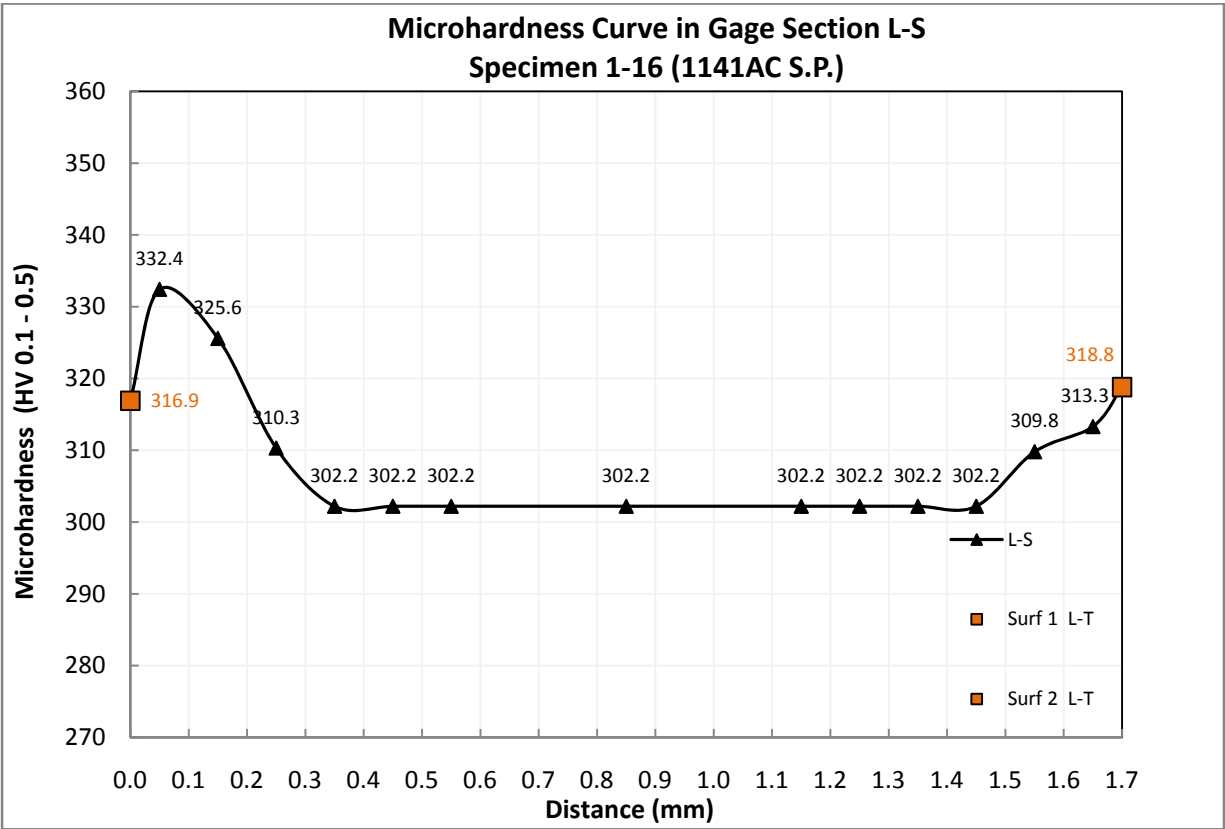
Figure 4.19.Specimen 1-16 gage section L-S microhardness profile

Gage section (Figure 4.19):

The gage section hardness results were processed in the same manner, as shown in Figure 4.19. The original curves for all specimens are shown in Figure B1to Figure B8 in Appendix B.

a) The shot-peened region in the gage section was between 0.0 (surface1) to 0.3mm in the left side and 1.4 to 1.7mm (surface2) in the right side. The hardness reached a maximum of 332.4HV0.1-0.5 at 0.05mm then decreased to 302.2 at 0.35mm. The rate of change between 0.05 to 0.35mm was similar. The hardness variations between 1.4 and 1.5mm were greater than 1.5 to 1.6mm but lower than the left side. Hardness variations in the left shot peened region were higher than the right.

b) The non shot-peened region or the center in the gage section was wider than the grip section. It started from 0.35mm and ended at 1.45mm. The hardness in this region was 302.2 ± 15.1 HV0.1-0.5 after 9.2×10^5 cycles at $\sigma_a= 349.7$MPa.

The hardness values 316.9 and 318.8 HV0.1-0.5 respectively on surface 1 and 2 were similar,

Comparing the hardness in the grip and gage centers, a very small increase of hardness was apparent in the gage section especially when their standard deviations were considered. In general, the rate of hardness change in the shot-peened regions of the grip section was higher than in the gage section.

Comparing the hardness averages in the L-T orientation in the grip (335.3 HV0.1-0.5) and gage (322.4 HV0.1-0.5) of shot-peened AISI 1141AC with the averages in the L-S orientation in the grip (285.4±9.4 HV0.5) and gage (283.6±9.5 HV0.5) sections of the non shot-peened ones showed 17.5 and 13.7% of increase in the grip and gage hardness values respectively. The L-T direction in shot-peened condition represented a fully shot-peened surface whereas the L-S direction in non shot-peened condition represented the initial condition of the steel.

4.3.2. AISI 1151 quenched and tempered

4.3.2.1. AISI 1151QT non shot-peened specimens

Table 4.3 shows the L-S and T-S average hardness values of the individual non shot-peened specimens.

Table 4.3.AISI 1151QT grip and gage section average hardness

SPECIMEN	σ_a (MPa)	R ($\sigma_{min}/\sigma_{max}$)	N (CYCLES TO FRACTURE)	GRIP SECTION HARDNESS (HV 0.5)		GAGE SECTION HARDNESS (HV 0.5)
				L-S	T-S	L-S
2-2	440.8	-1	653,600	315.5±6.8	310.7±2.9	314.0±4.5
2-7	432.7		10,878,000	308.9±4.4	NA	321.5±3.7

Figure 4.20 shows microhardness profile in the grip section of specimen 2-2 in the L-S and T-S directions. The average hardness was 315.5±6.8 HV0.5 and 310.7±2.9 HV0.5 in the grip section in L-S and T-S directions respectively.
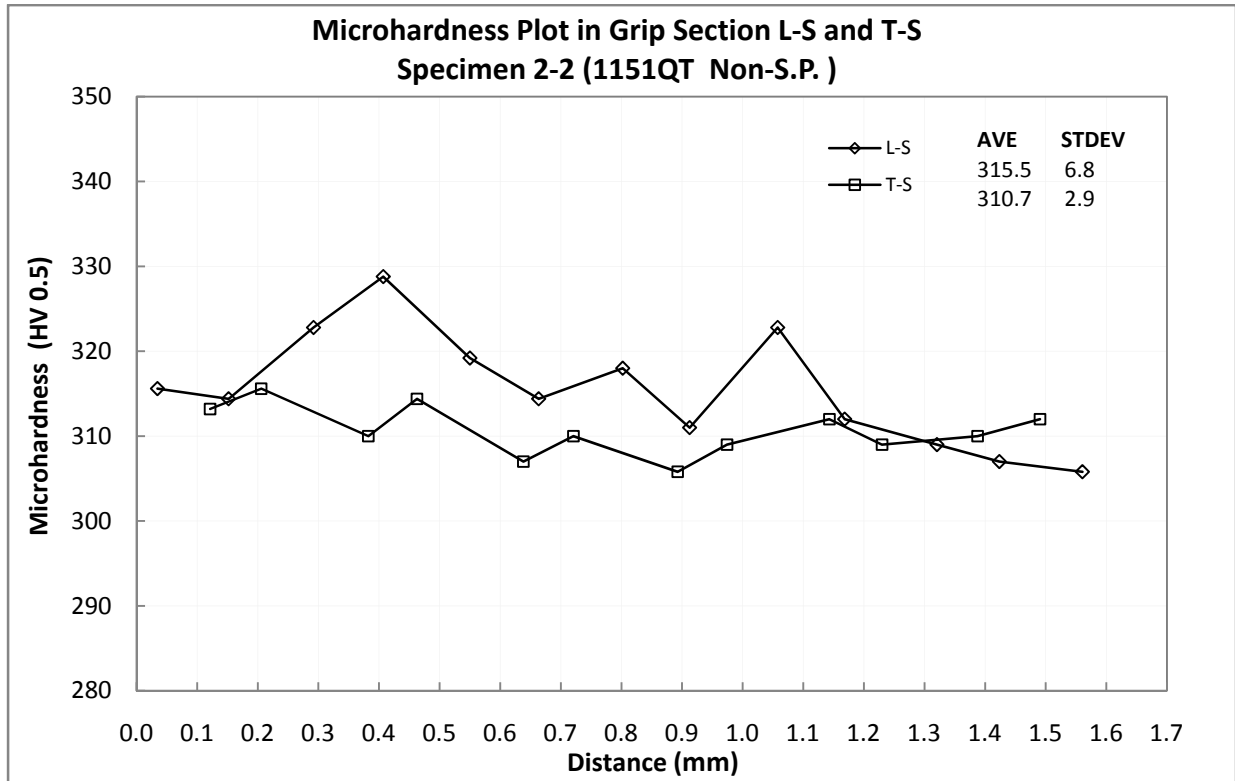
Figure 4.20.Specimen 2-2 microhardness plot in grip L-S and T-S

The L-S hardness profile of specimen 2-7 in the grip section is depicted in Figure 4.21. The average hardness in the grip section for this specimen was 308.9±4.4 HV0.5. These hardness profiles were combined into a single plot, Figure 4.22, to produce an average hardness for the non shot-peened AISI 1151QT group. The average hardness in the grip section of this combination was 311.6±5.6 HV0.5 (Figure 4.22).
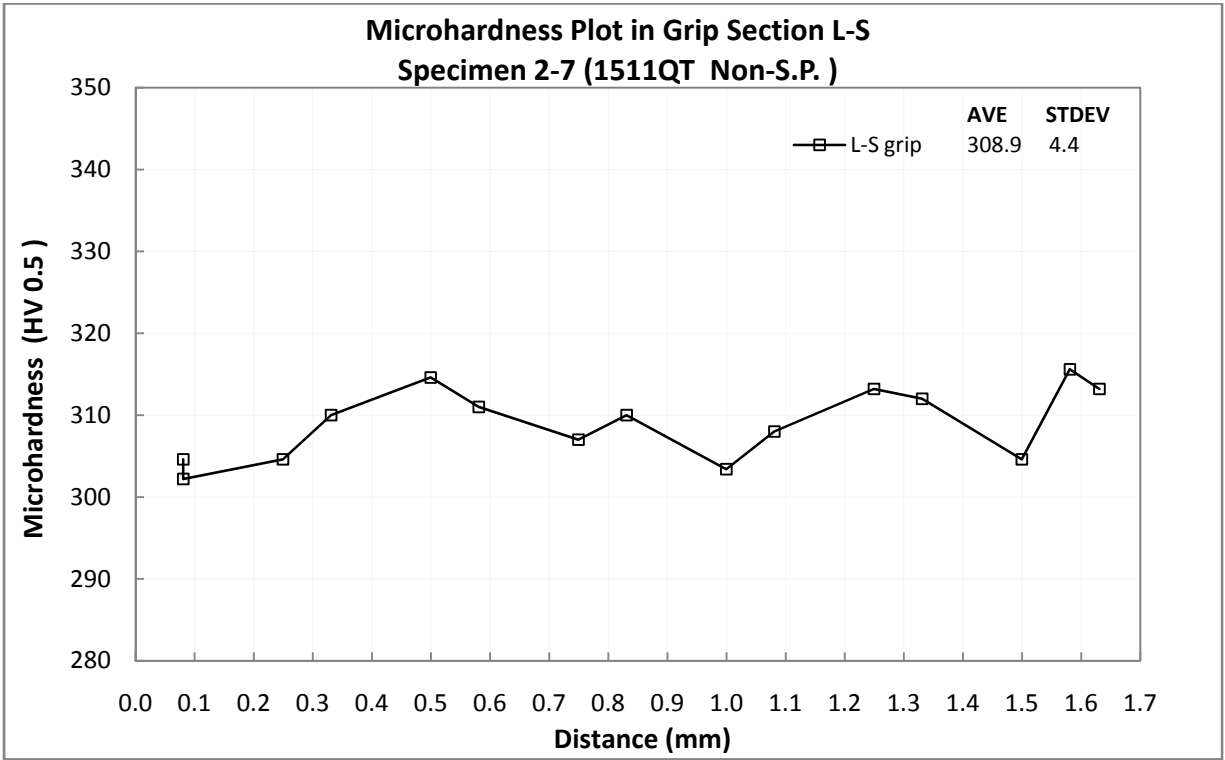
Figure 4.21.Specimen 2-7 microhardness plot in grip L-S
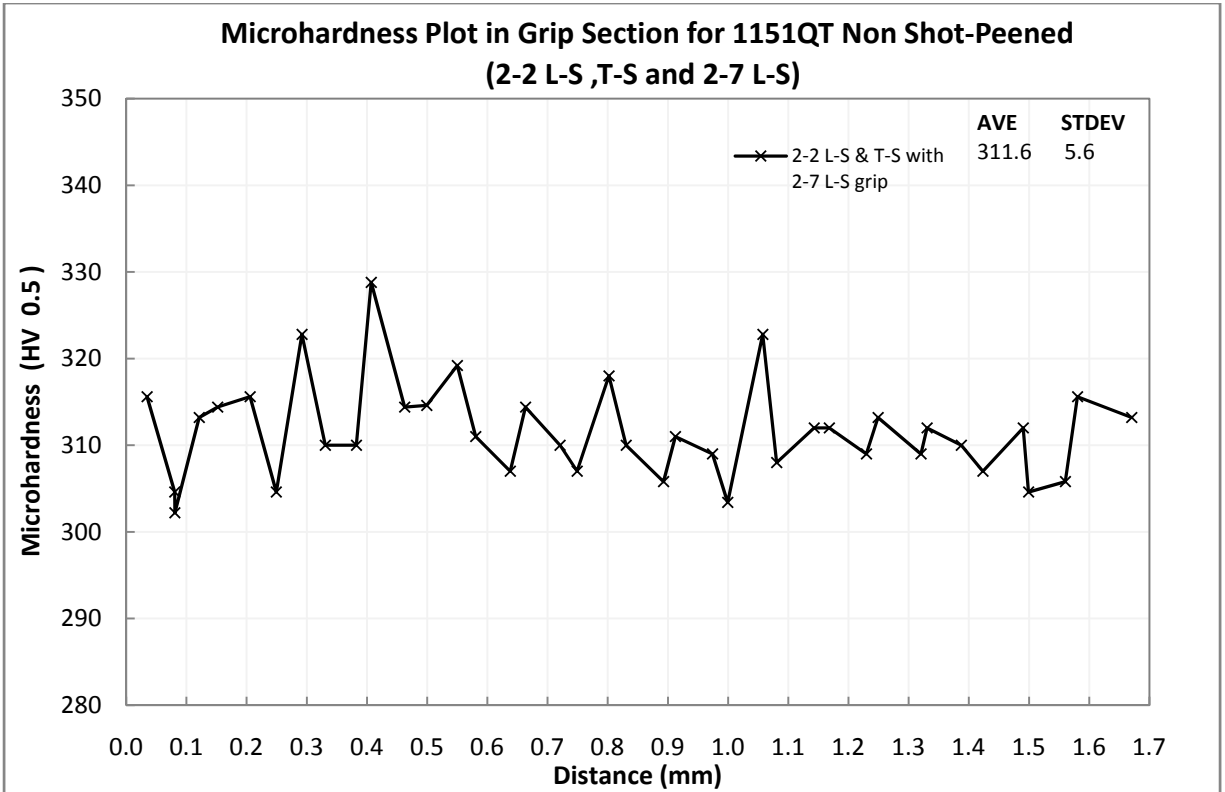
Figure 4.22.AISI 1151QT non shot-peened grip section microhardness plot L-S

Figure 4.23 and Figure 4.24 show microhardness profile in the gage section of specimen 2-2 and 2-7 in the L-S direction. For specimen 2-2, the average hardness was 314.0±4.5 HV0.5 and for specimen 2-7, the average hardness was 321.5±3.7 HV0.5.
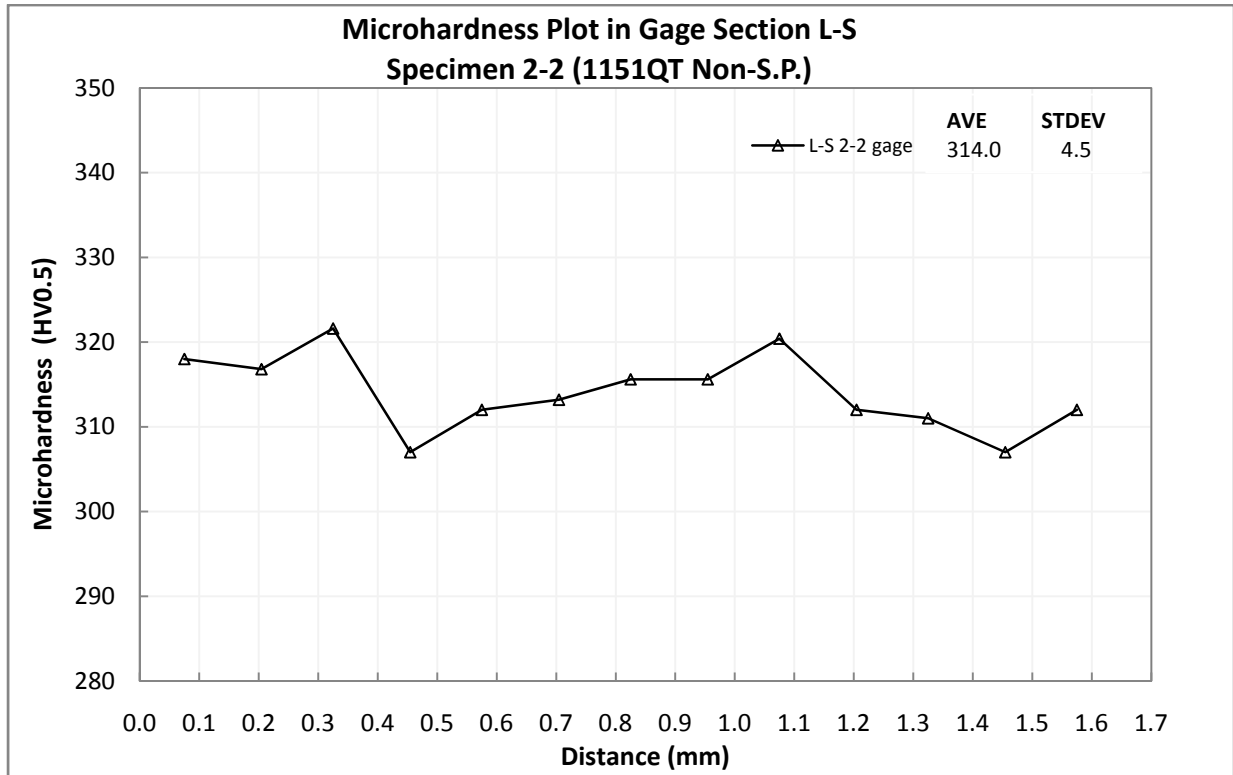
Figure 4.23.Specimen 2-2 microhardness plot in gage L-S

The hardness profiles of specimen 2-2 and 2-7 were combined into a single plot to generate an average representing the L-S gage section hardness in the non shot-peened AISI 1151QT. The plot is shown in Figure 4.25 indicating 317.8±5.6 as the average hardness for the non shot-peened AISI 1151QT after 6.5×10^5 cycles at σ_a=440.8MPa.
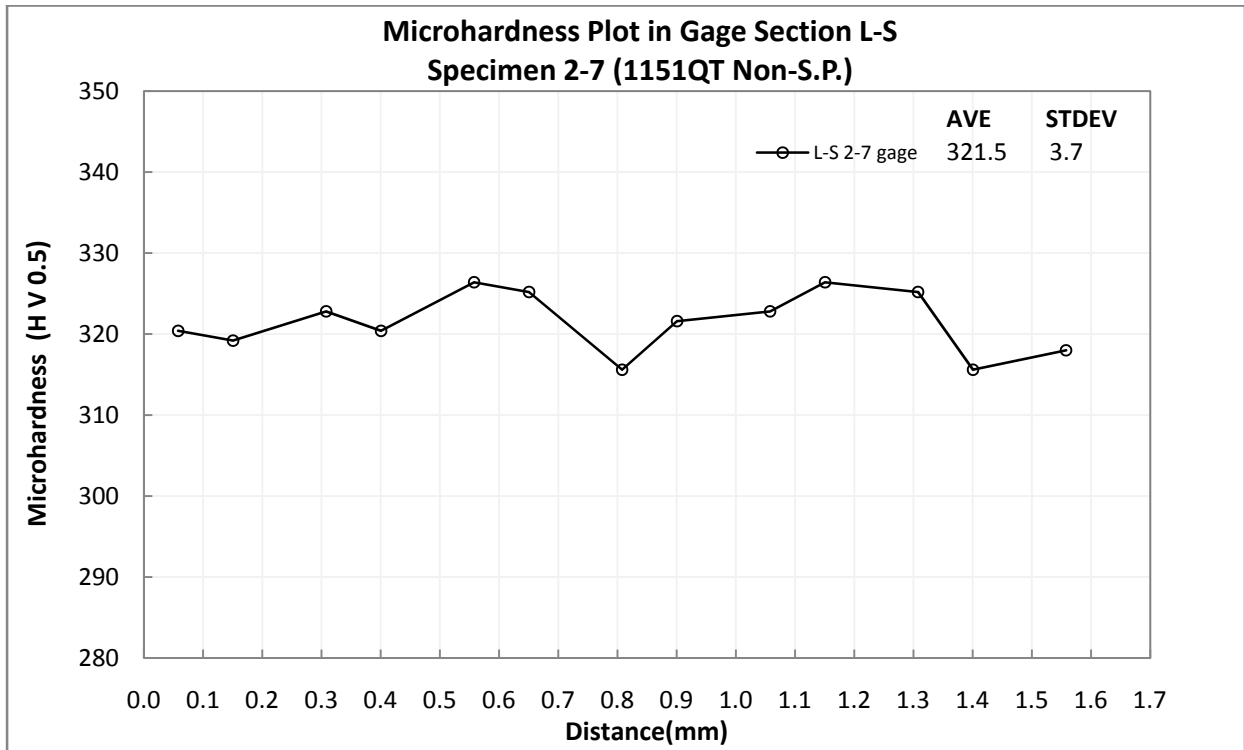
Figure 4.24.Specimen 2-7 microhardness plot in gage L-S
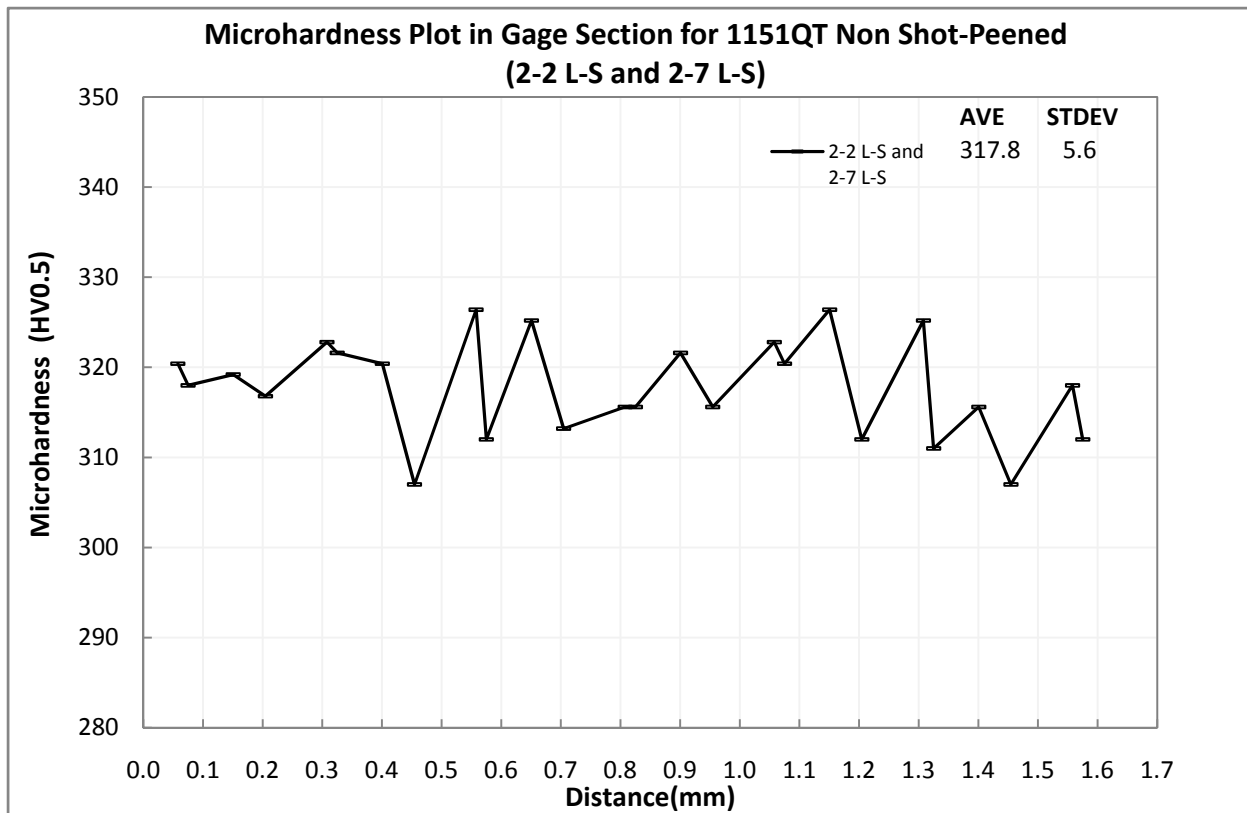
Figure 4.25.AISI 1151QT non shot-peened gage section microhardness plot L-S

4.3.2.2. AISI 1151QT shot-peened specimens

Figure 4.26 and Figure 4.27 show respectively the grip and gage sections hardness curves for specimen 2-18 in the L-S direction. All the hardness values, HV0.1 and HV0.5, in a given 0.1mm block were initially combined together to give an average and standard deviation. The original center region in both grip and gage sections was from 0.6 to 1.1mm, it is apparent that this region was broadened due to similar hardness values of adjacent blocks.

The zero level in both the grip and gage curves correspond to the reference surface (surface1) of specimen 2-18.

The grip and gage sections were divided into two regions namely: a) shot-peened and b) non shot-peened (the center).
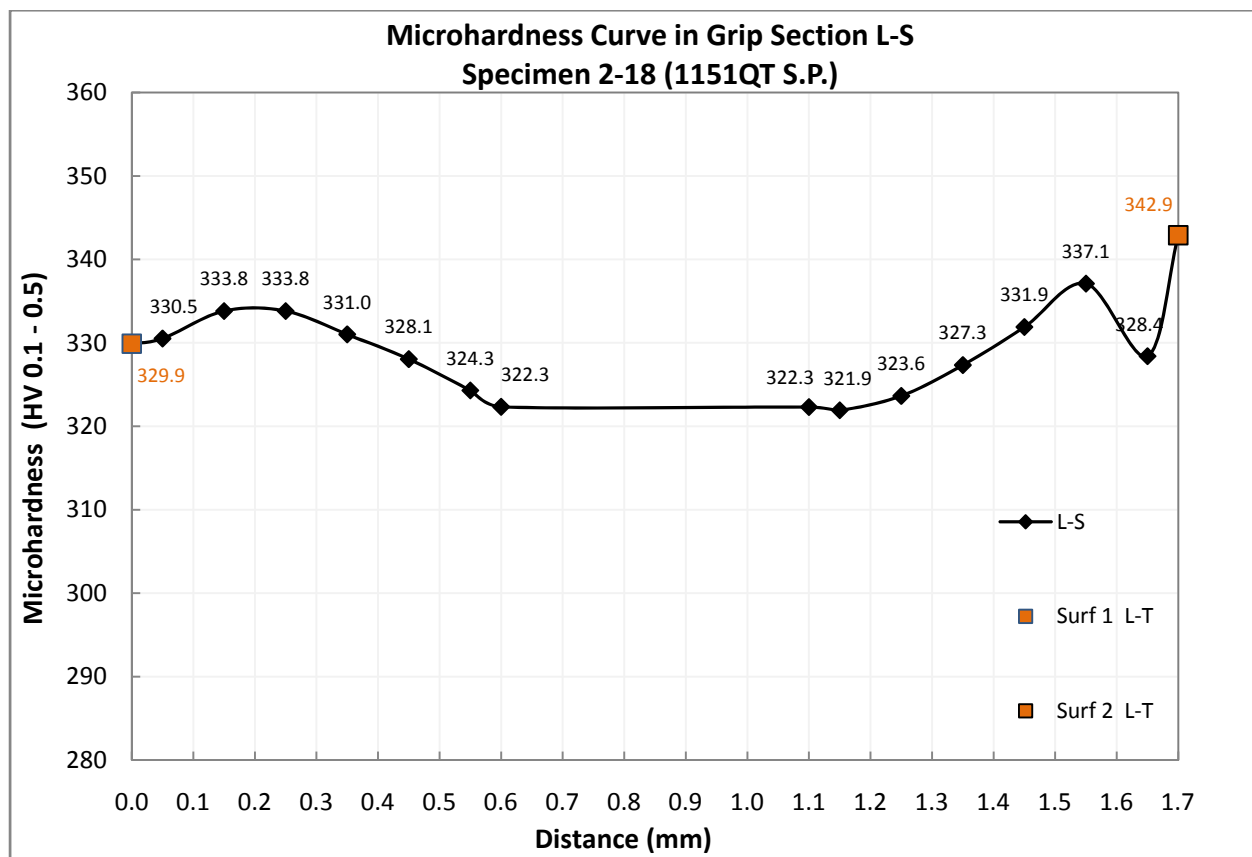
Figure 4.26.Specimen 2-18 grip section L-S microhardness profile

Grip section (Figure 4.26):

a) The shot-peened region was from 0.0 (surface1) to 0.6mm and from 1.2 to 1.7mm (surface2). The hardness values were between 330.0 and 333.8 HV0.1-0.5 from 0.0 to 0.4mm and reached the highest value, 333.8 in the left region between 0.15 to 0.25mm. It decreased from 333.8 to 322.3 from 0.2 to 0.6mm with a similar reduction rate. The hardness remained unchanged, 322.3-323.6, from 1.1 to 1.25mm. The hardness reached its maximum of 337.1 between 1.5 to 1.6mm then decreased to 328.4 at 1.65mm.

b) The center, non shot-peened region, ranged from 0.6 to 1.3mm with a hardness of 321.9-324.3 HV0.1-0.5 in this region.

Surface 1 and 2 L-T hardness values, 329.9 and 342.9 HV0.1-0.5, completed the L-S curve.
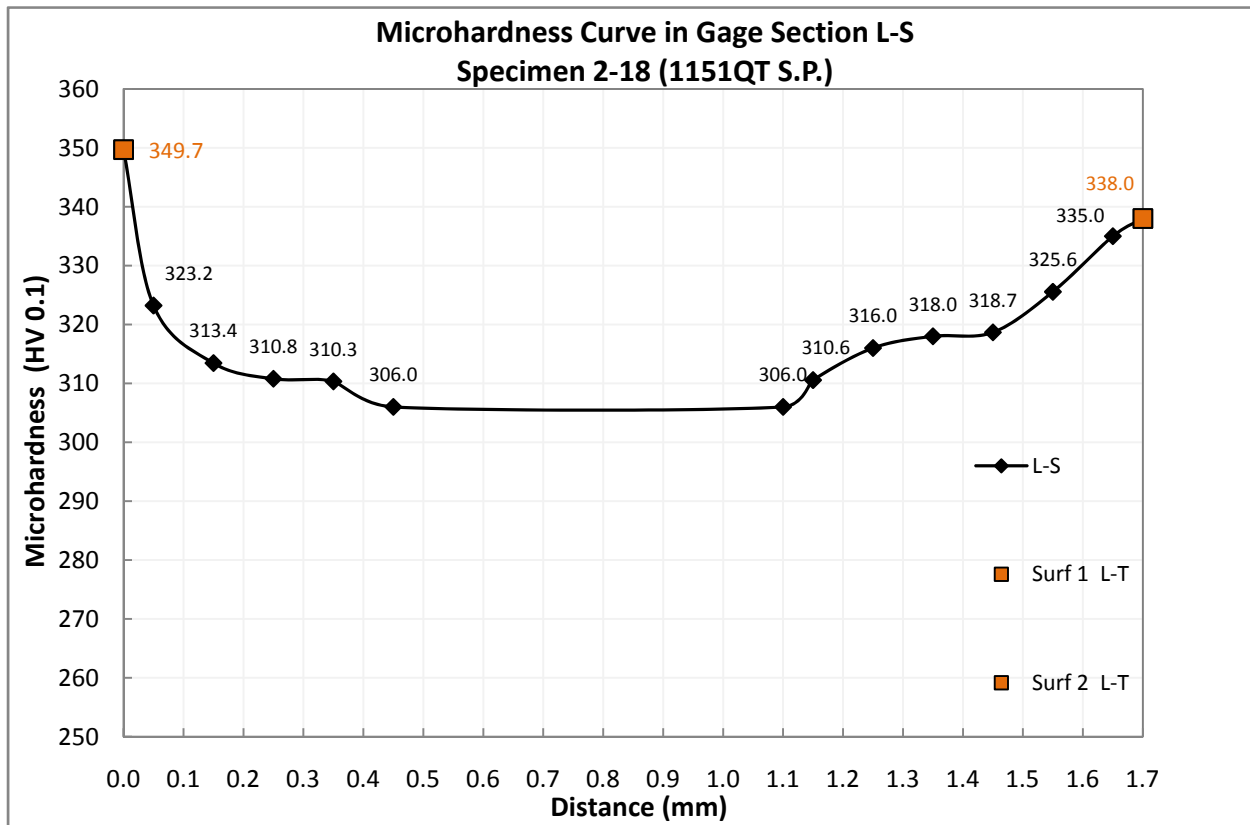
Figure 4.27.Specimen 2-18 L-S gage section microhardness profile

Gage section (Figure 4.27):

a) The shot-peened region was from 0.0 (surface1) to 0.4mm and from 1.1 to 1.7mm (surface2). The hardness value at 0.05mm, 323.2 HV0.1-0.5, was the highest on the left side. On the right side, the hardness at 1.15mm was 310.6 increasing to 316.0 at 1.25mm then remained unchanged, 316.0-318.7, from 1.25 to 1.45mm. The hardness increased to 325.6 at 1.55mm then 335.0 at 1.65mm.

b) The center was originally from 0.6 to 1.1mm, but due to similar value of hardness, 306.0, the center extended from 0.6 to 0.45mm on the left side.

Comparing the grip (Figure 4.26) and gage sections (Figure 4.27) of the shot-peened specimens, the hardness was higher in the grip than the gage section, indicating that in general, cyclic softening had taken place after 2.9×10^4 cycles at 461.1MPa.

Comparing the hardness averages of AISI 1151QT in the L-T orientation in the grip (336.4 HV0.1-0.5) and gage (343.9 HV0.1-0.5) in shot-peened condition with L-S orientation in the grip (311.6 HV0.5) and gage (317.8 HV0.5) of the non shot-peened ones showed a 8.0 and 8.2% hardness increase in the grip and gage sections respectively. The L-T direction in shot-peened condition represented a fully shot-peened surface whereas the L-S direction in non shot-peened condition represented the non shot-peened condition of the steel.

4.3.3. Powder metallurgy (PM)

4.3.3.1. Powder metallurgy (PM) non shot-peened specimens

Table 4.4 shows the L-S and T-S average hardness values of the individual non shot-peened PM specimens.

Table 4.4.PM grip and gage section average hardness

SPECIMEN	σ_a (MPa)	R ($\sigma_{min}/\sigma_{max}$)	N (CYCLES TO FRACTURE)	GRIP SECTION HARDNESS (HV 0.5)		GAGE SECTION HARDNESS (HV 0.5)
				L-S	T-S	L-S
3-2	304.4	-1	811,700	307.1±26.5	NA	296.0±18.1
3-5	305.7		10,007,900	293.9±24.6 302.9±25.1	313.7±32.2 300.5±28.4	304.8±25.1

Microhardness tests were performed in the grip section in the L-S and T-S directions of specimen 3-5. The hardness curve is shown in Figure 4.28. Due to large variations in the first microhardness test results, as seen in Figure 4.28, a second microhardness test was carried out. Both tests conditions were similar and performed using the same load (0.5kgf). Figure 4.29 shows the results of the second test.

The average hardness values resulting from the first test in L-S and T-S directions were 293.9±24.6 HV0.5 and 313.7±32.2 HV0.5 respectively (Figure 4.28). The averages of the second test in L-S and T-S directions were 302.9±25.1 HV0.5 and 300.5±28.4 HV0.5, (Figure 4.29), which were in good agreement with the first test results considering the standard deviations. Compared to other steels, the standard deviations were higher.
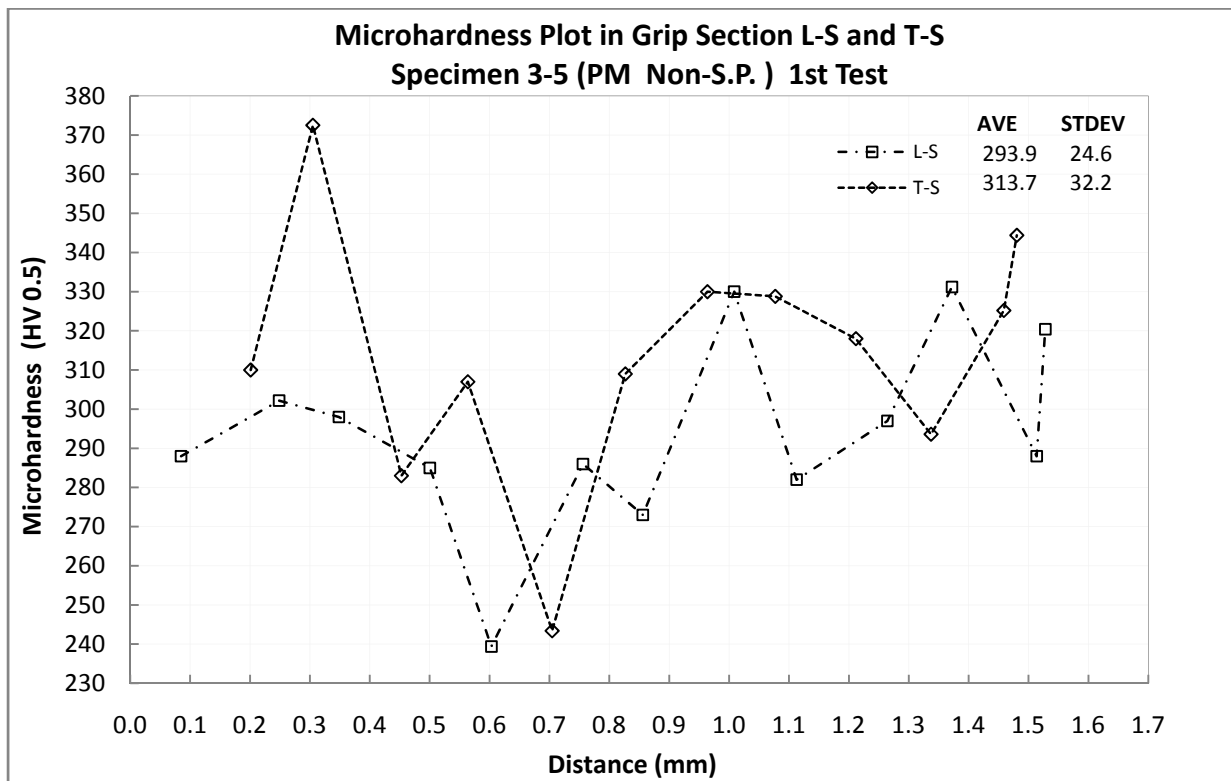
Figure 4.28.Specimen 3-5 microhardness plot in grip L-S and T-S (first test)
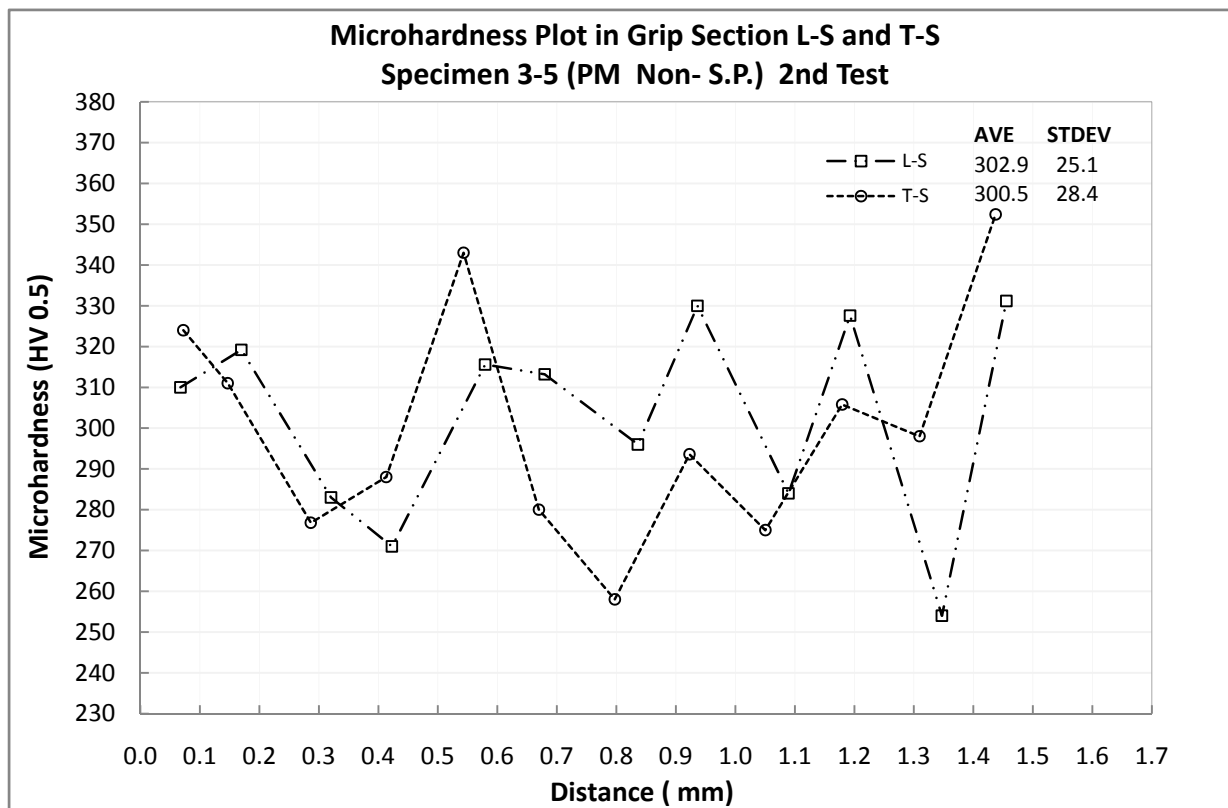
Figure 4.29.Specimen 3-5 microhardness plot in grip L-S and T-S (second test)
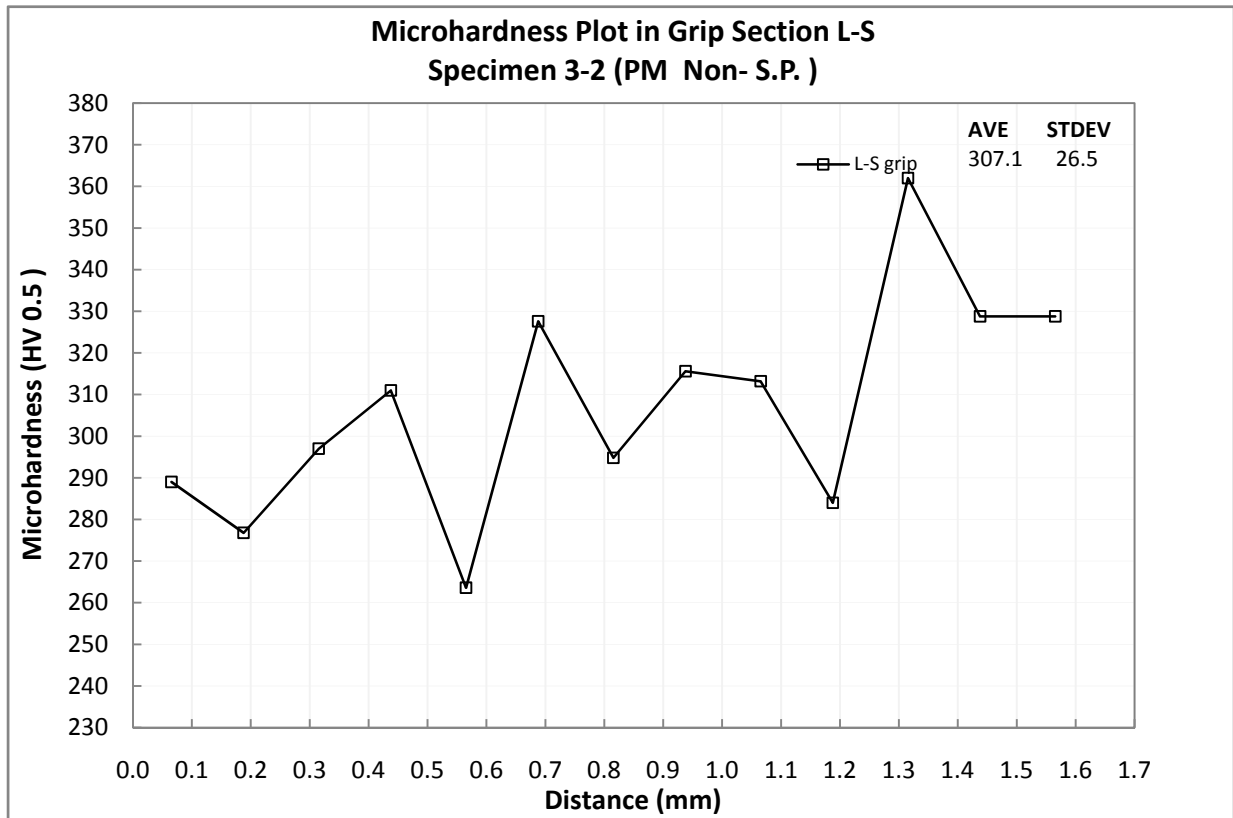
Figure 4.30.Specimen 3-2 microhardness plot in grip L-S

The average hardness in the grip section in the L-S direction for specimen 3-2 was 307.1±26.5 HV0.5. The standard deviation of this result was similar to specimen 3-5 results. To produce a value as the average hardness of the non shot-peened PM specimens in the grip section, the results of two separate hardness tests on specimen 3-5 in the L-S and T-S directions (Figure 4.28 and Figure 4.29) were combined with the hardness results of 3-2 in the L-S direction (Figure 4.30). The combinations of these test results are shown in Figure 4.31, representing the average hardness profile in the grip section of the non shot-peened PM (303.5±27.3 HV0.5).
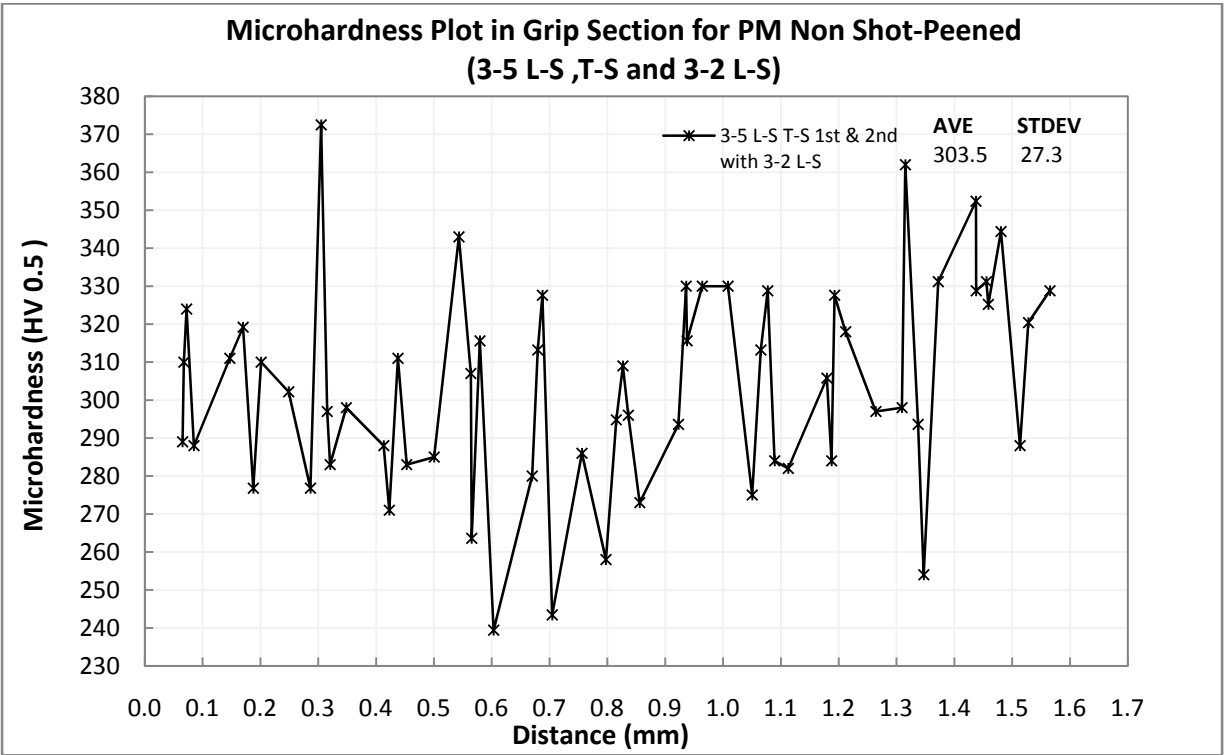
Figure 4.31.Powder Metallurgy (PM) non shot-peened grip section microhardness plot L-S
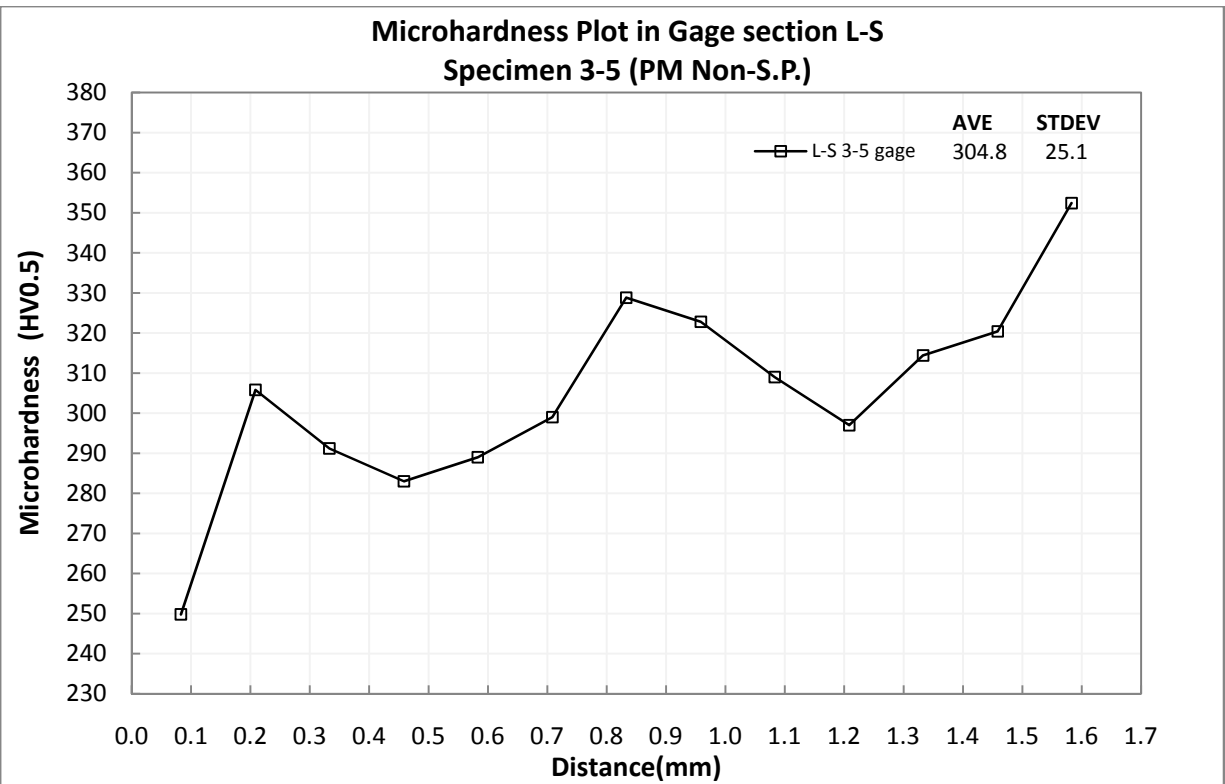
Figure 4.32.Specimen 3-5 microhardness plot in gage L-S
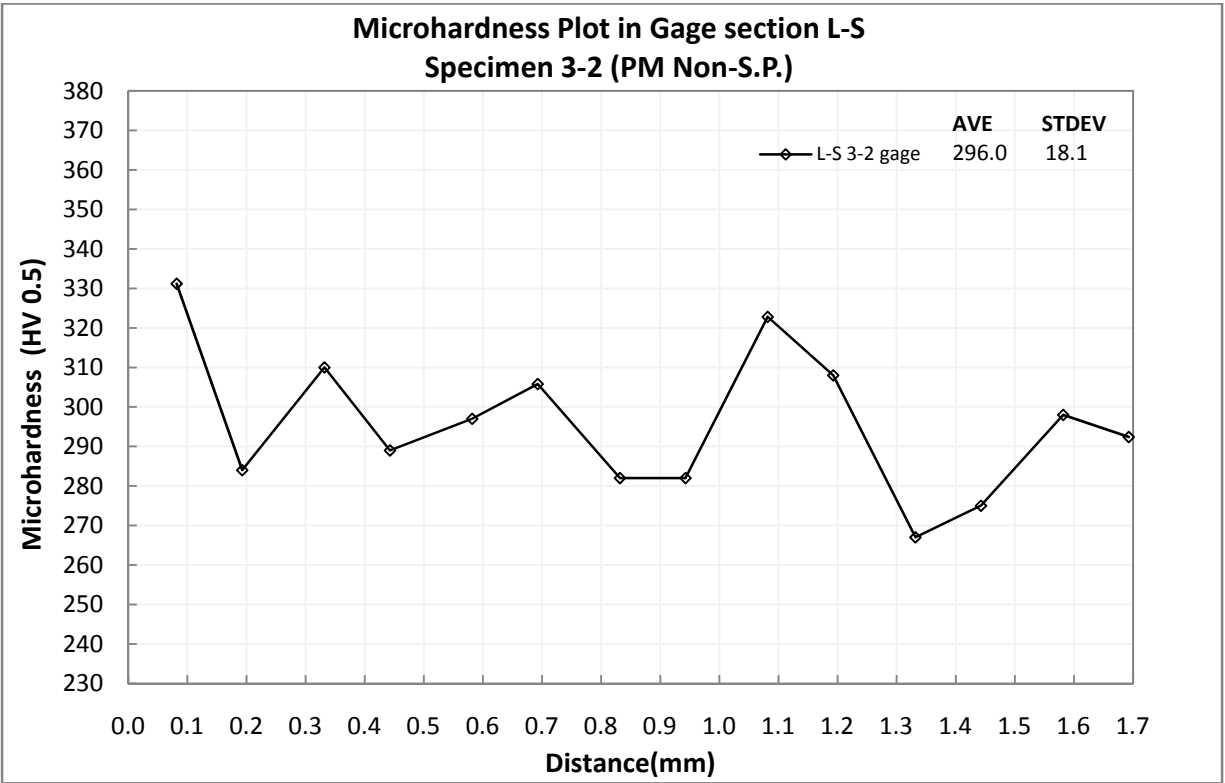
Figure 4.33.Specimen 3-2 microhardness plot in gage L-S
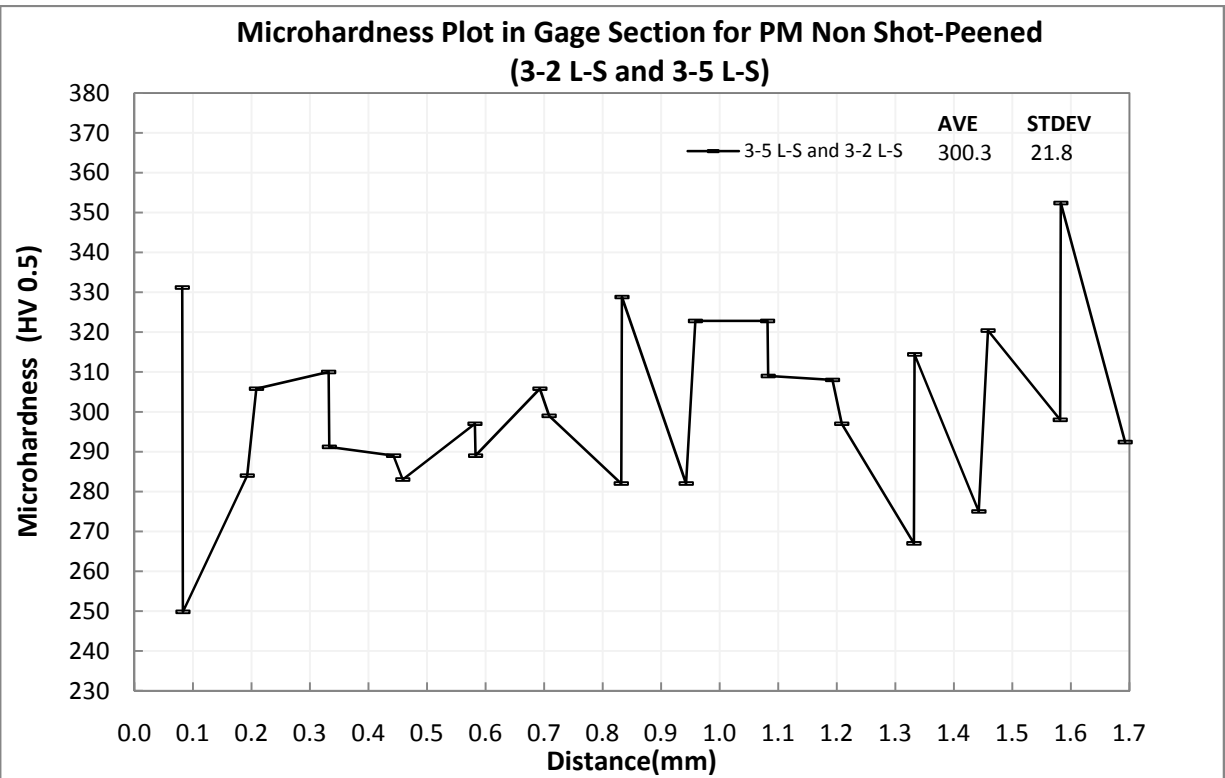
Figure 4.34.Metallurgy (PM) non shot-peened gage section microhardness plot L-S

To determine an average hardness for the gage section of the non shot-peened PM specimens the results of two separate microhardness tests in the L-S direction of specimens 3-5

54

and 3-2 (Figure 4.32 and Figure 4.33) were combined. Figure 4.34 shows the resulting gage curve from the combination of specimens 3-2 and 3-5 in the L-S direction. The average hardness in the gage section of the non shot-peened PM specimens was 300.3±21.8 HV0.5 after 8×10^5 cycles at σ_a=304.3MPa.

4.3.3.2. Powder metallurgy (PM) shot-peened specimens

As shown in Figure 4.35, the specimen 3-15 average hardness on surface (L-T) 1mm and 2mm away from the crack site were 376.7±22.2 HV0.5 and 391.2±21.9 HV0.5 respectively after 1.8×10^6 cycles at σ_a= 368.5MPa.
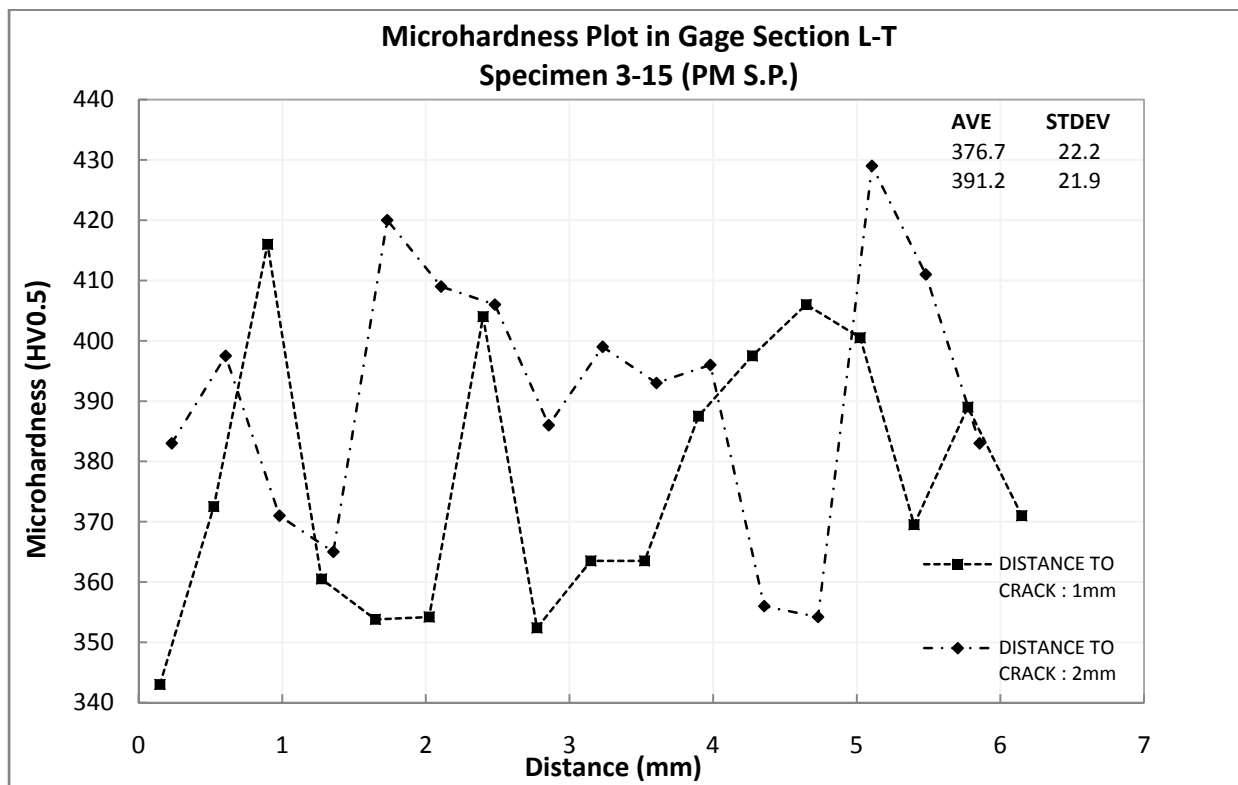
Figure 4.35.Specimen 3-15 L-T microhardness plot in gage section
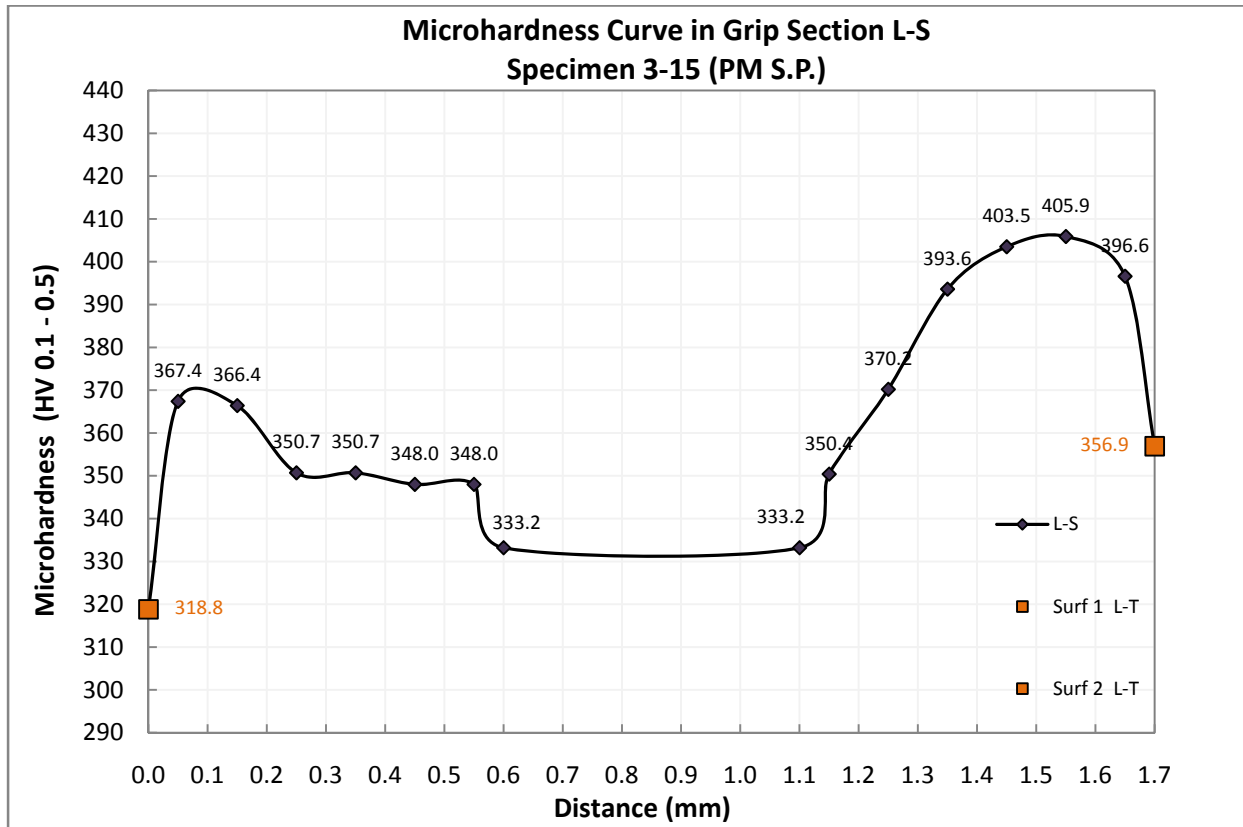
Figure 4.36.Specimen 3-15 grip section microhardness profile

All the hardness results of specimen 3-15 in the grip section were combined, as shown in Figure 4.36. The L-S direction in both grip and gage sections of specimen 3-15 were divided into two regions namely: a) shot-peened and b) non shot-peened (the center).

Grip section (Figure 4.36):

a) The shot-peened region ranged from 0.0 to 0.6mm on the left side and from 1.1 to 1.7mm on the right. On the left side, the hardness reached the highest value, 367.4 HV0.1-0.5, at 0.05mm and decreased from 366.4 to 350.7 at 0.25mm. From 0.25 to 0.55mm, the hardness remained unchanged, 348.0 to 350.7 then decreased to 333.2 at 0.6mm.

The hardness increased from 350.4 to 403.5 between 1.15 to 1.45mm. The hardness reached the maximum, 405.9, at 1.55mm then decreased to 396.6 HV0.1-0.5. The hardness change rate from 1.4 to 1.65mm was small when compared to 1.1 to 1.45mm. Relatively, on the right side, hardness variations were more significant than the left side.

b) The center, non shot-peened region, was from 0.6 to 1.1mm. The hardness was 333.2±11.2 in this region.

Surface 1 and 2 (L-T) hardness values completed the microhardness profile at 0.0 and 1.7mm with the hardness values of 318.8 and 356.9 HV0.1-0.5 respectively.
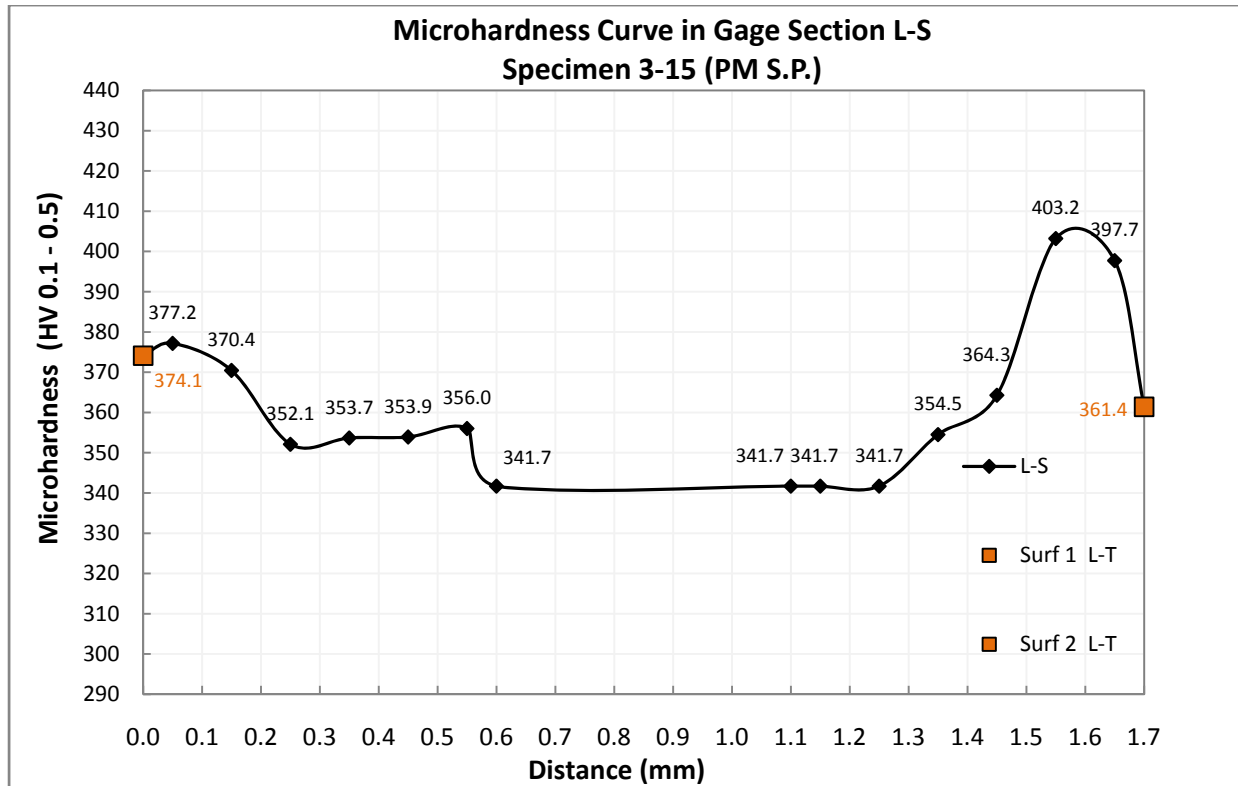
Figure 4.37.Specimen 3-15 gage section microhardness profile

Gage section (Figure 4.37):

a) In the gage section of specimen 3-15, the shot-peened region was from 0.0 (surface1) to 0.6mm and from 1.25 to 1.7mm (surface2). The highest value of the hardness in the left side was 377.2 HV0.1-0.5 at 0.05mm. The hardness was between 360.0 to 377.2 from 0.0 to 0.2mm. The highest change of hardness was seen between 0.15 and 0.25mm in which the hardness decreased from 370.4 to 352.1. From 0.2 to 0.55mm, no change was seen and the hardness value was between 352.1 to 356.0.

On the right side, from 1.3 to 1.45mm, hardness change rate was insignificant, 354.5-364.3 HV0.1-0.5, when compared to 1.45-1.6mm where hardness drastically increased to reach

the maximum value, 403.2, then decreased to 397.7. The hardness variations were higher in the right side than the left side in the gage section.

b) The hardness value in the center was 341.7±5.1. This region, originally from 0.6 to 1.1mm, extended to 1.3mm on the right side.

Comparing the hardness values after 1.8×10^6 cycles at 368.5MPa in the grip and gage centers, respectively 333.2±35.5 and 341.7±27.9HV0.1-0.5, a very small increase of hardness was apparent in the gage section especially when their standard deviations were considered.

Surface 1 and 2 (L-T) hardness completed the microhardness profile at 0.0 and 1.7mm with the hardness values of 374.1 and 361.4 HV0.1-0.5 respectively.

Comparing the average hardness values in the grip and gage sections of the non shot-peened PM specimens (303.5 and 300.3 HV0.5) with the average grip and gage hardness values of specimen 3-15 in L-T direction, showed 11.3% and 25.2% increase of hardness in the grip and gage sections respectively. The L-S direction represented a non shot-peened surface whereas the L-T was a fully shot-peened surface.

4.3.4. C70S6 (Crackable) air cooled

4.3.4.1. C70S6AC non shot-peened specimens

Table 4.5 shows the L-S and T-S average hardness values of the individual non shot-peened C70S6AC specimens.

Table 4.5.C70S6AC (Crackable) grip and gage section average hardness

SPECIMEN	σ_a (MPa)	R ($\sigma_{min}/\sigma_{max}$)	N (CYCLES TO FRACTURE)	GRIP SECTION HARDNESS (HV 0.5)		GAGE SECTION HARDNESS (HV 0.5)
				L-S	T-S	L-S
4-3	341.8	-1	10,618,300	309.8±11.3	NA	298.4±14.3
4-5	355.0		739,800	299.3±7.9	295.1±8.6	312.7±10.4

The microhardness profiles of specimen 4-5 in the grip section in the L-S and T-S directions are shown in Figure 4.38. Average hardness was 299.3±7.9 and 295.1±8.6 HV0.5 in the grip section in the L-S and T-S directions respectively.
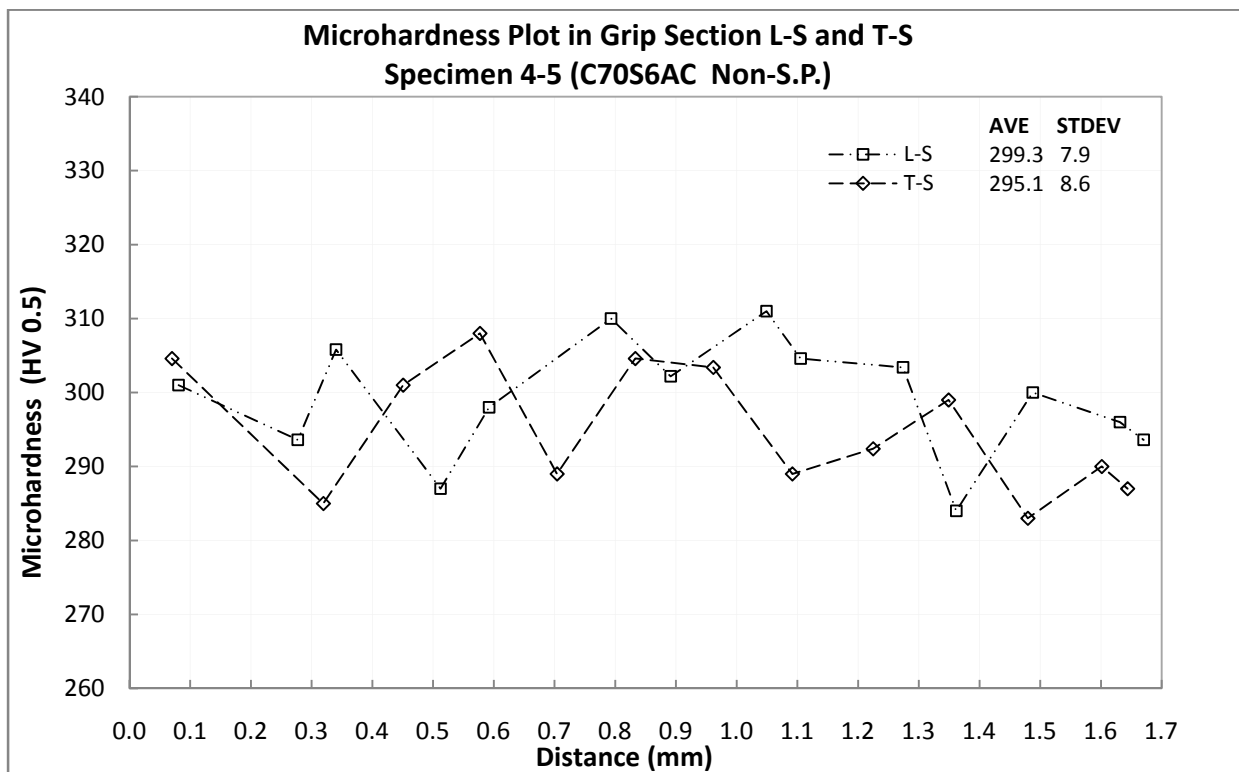
Figure 4.38.Specimen 4-5 microhardness plot in grip L-S and T-S

Both the L-S and T-S hardness variations were similar, ±7.9 for L-S and ±8.6 for T-S, in the grip section of specimen 4-5 (Figure 4.38).

Figure 4.39 gives specimen 4-3 hardness profile for the grip section in the L-S direction. The average hardness was 309.8±11.3 HV0.5.
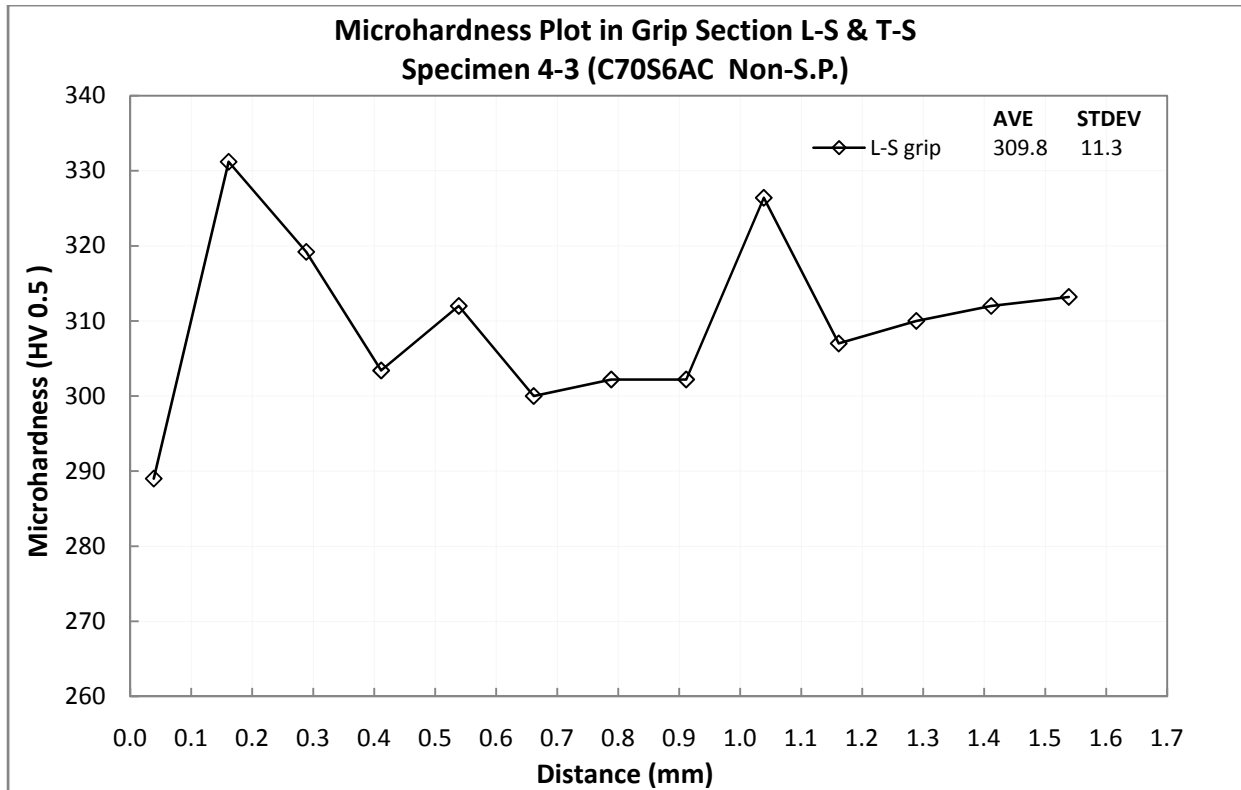
Figure 4.39.Specimen 4-3 microhardness plot in grip L-S

The microhardness results for the grip section of specimens 4-5 and 4-3 were combined and shown in Figure 4.40. The average hardness was 301.4±11.0 HV0.5.
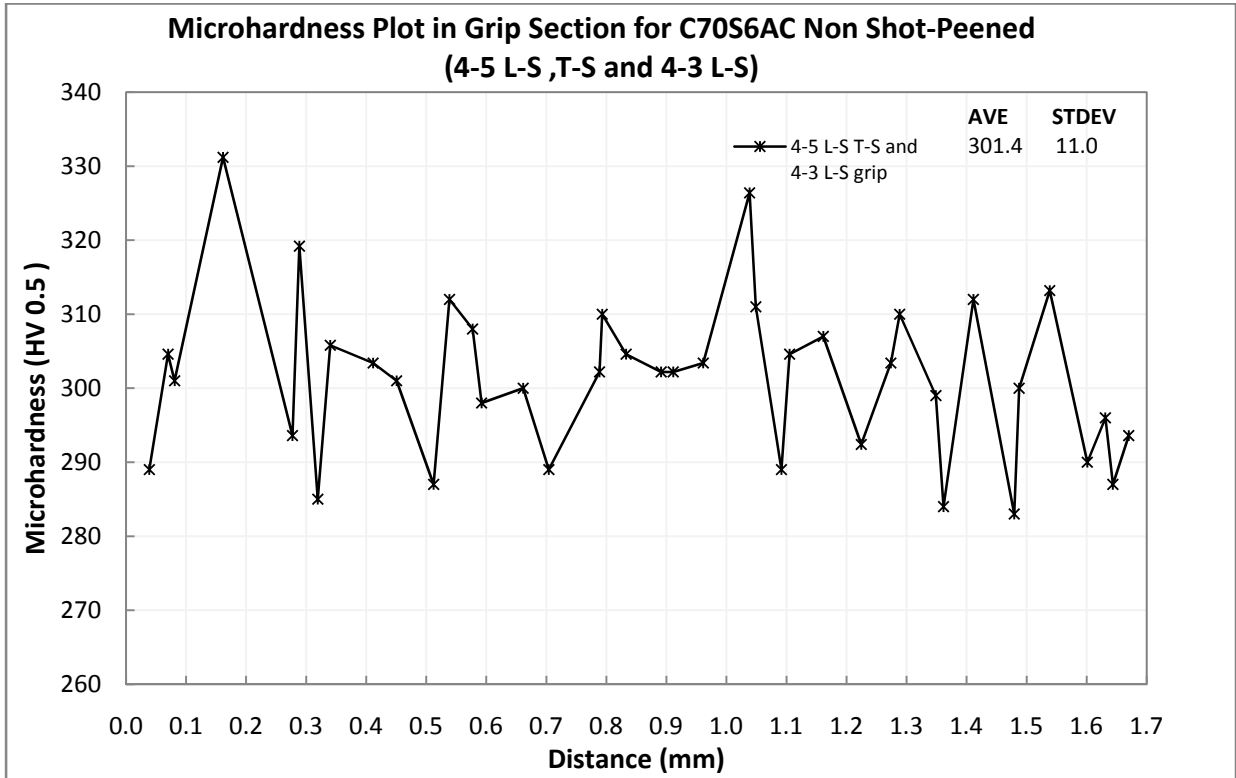
Figure 4.40.C70S6AC (Crackable) non shot-peened L-S grip section hardness
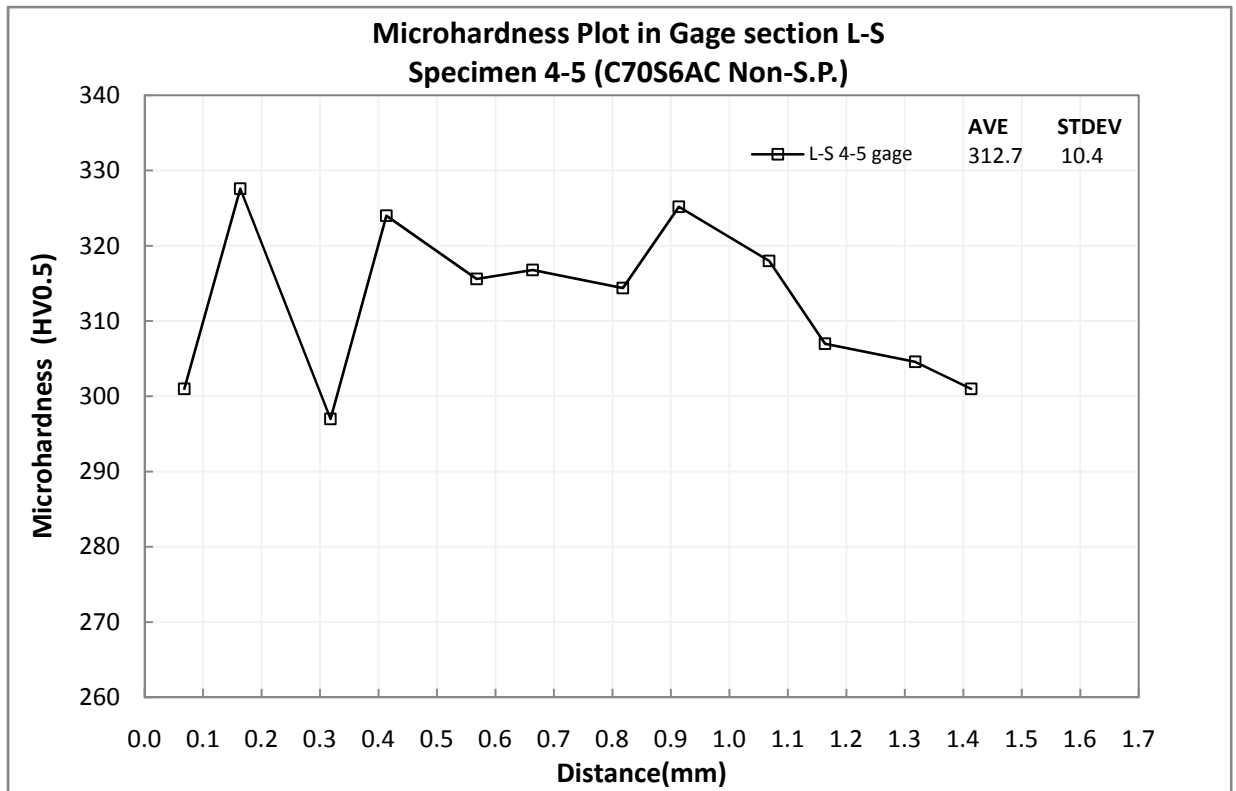
Figure 4.41.Specimen 4-5 microhardness plot in gage L-S
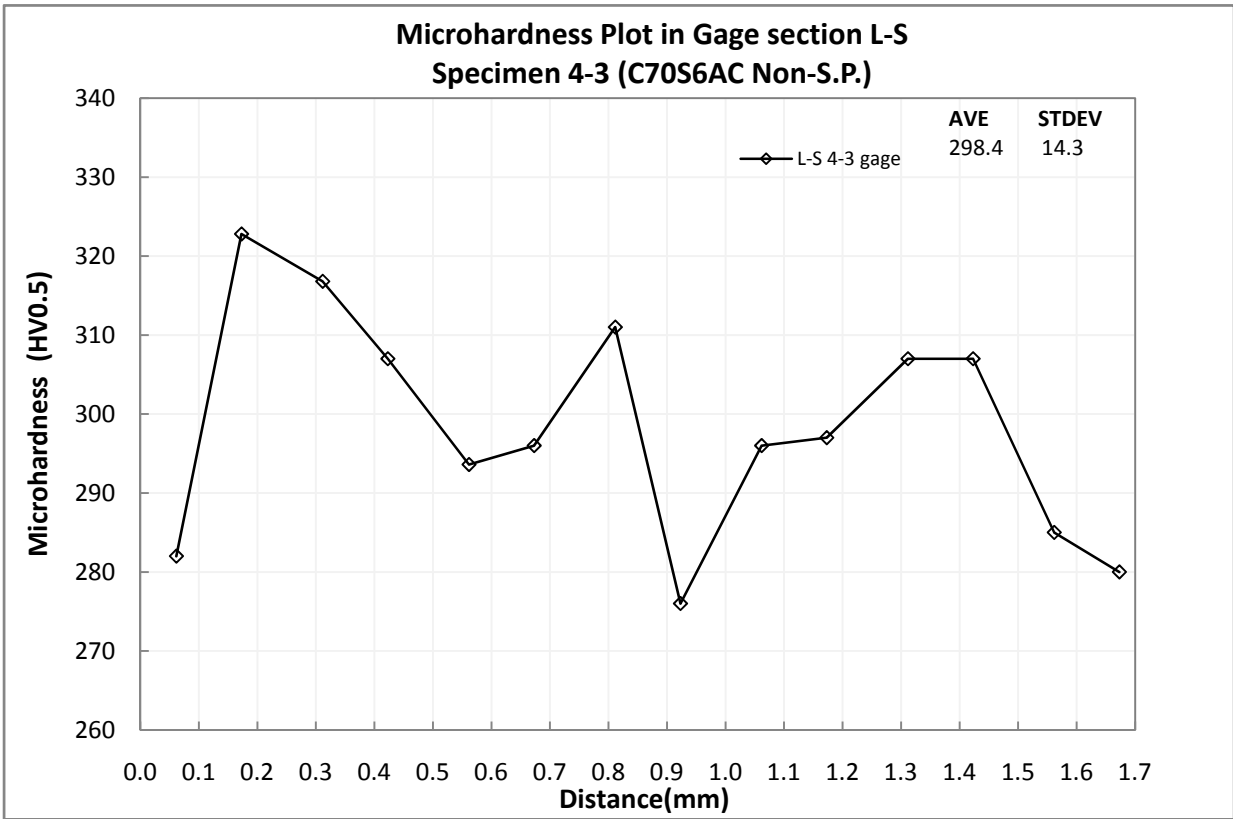
Figure 4.42.Specimen 4-3 microhardness plot in gage L-S
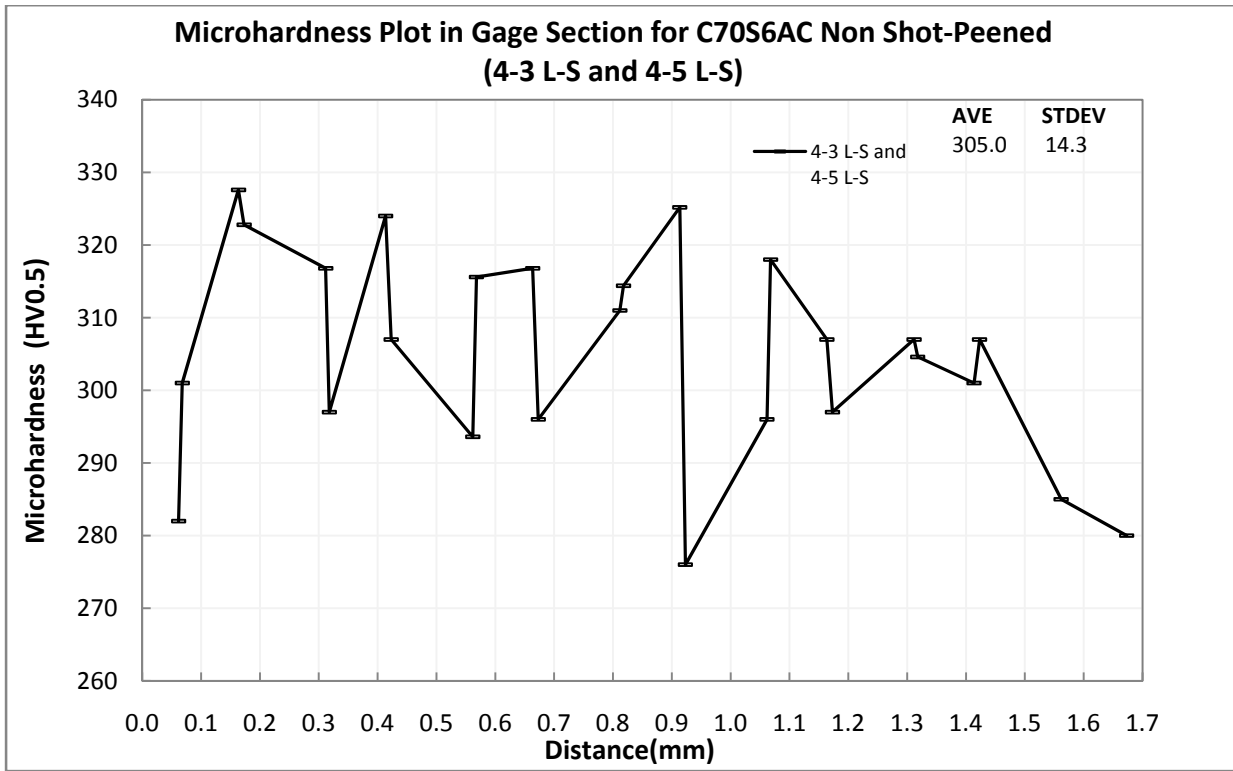
Figure 4.43.C70S6AC (Crackable) non shot-peened L-S gage section hardness

The microhardness profiles in the gage section of specimen 4-5 and 4-3 are depicted in Figure 4.41 and Figure 4.42 respectively. Average hardness for specimen 4-5 in the gage section in the L-S direction was 312.7±10.4 HV0.5 after 7.3×10^5 at σ_a=355.0MPa and 298.4±14.3 HV0.5 for specimen 4-3 after 10^7 cycles at σ_a=341.8MPa.

The gage section microhardness profiles of specimens 4-5 and 4-3 were combined to find an average hardness value and the resulting curve is shown in Figure 4.43. The average hardness value for the gage section was 305.0±14.3 HV0.5.

4.3.4.2. C70S6AC shot-peened specimens
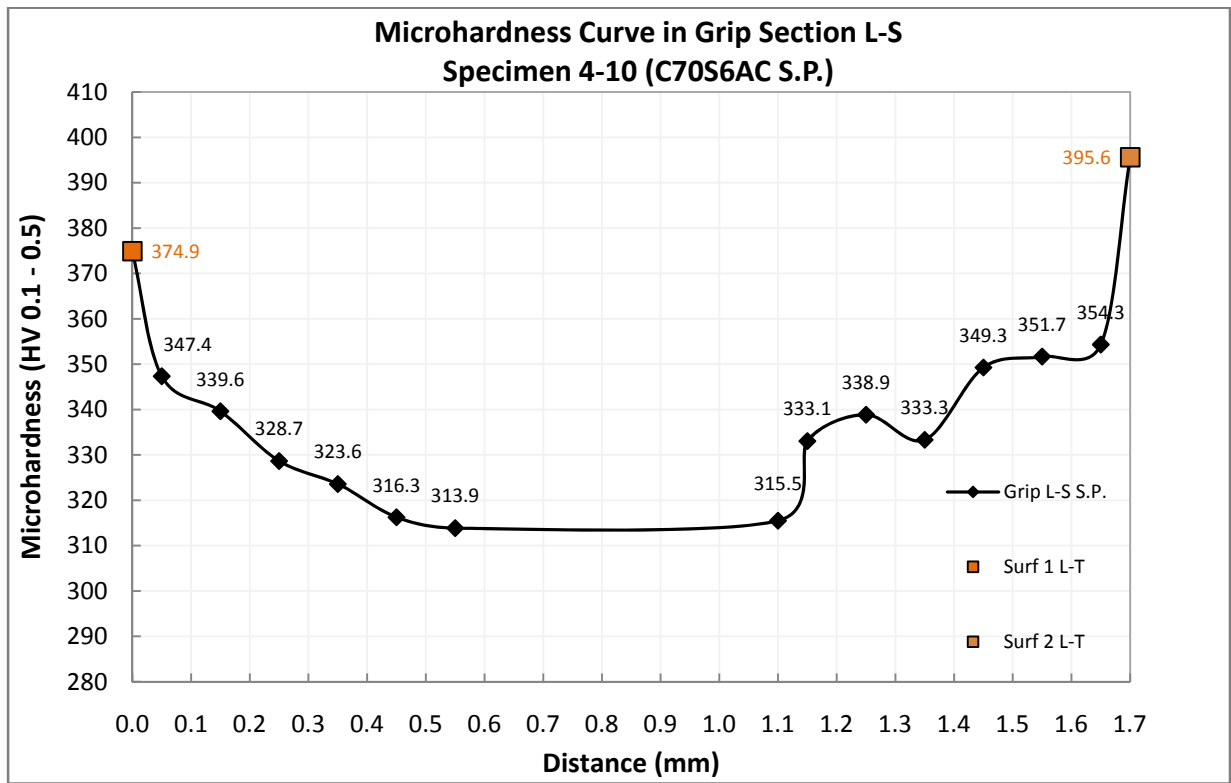
Figure 4.44.Specimen 4-10 grip section hardness profile

All the hardness results of specimen 4-10 in the grip section were combined as shown in Figure 4.44. The L-S direction in both the grip and gage sections of specimen 4-10 were divided into two regions namely: a) shot-peened and b) non shot-peened (the center).

Grip section (Figure 4.44):

a) The shot-peened region in the grip section was from 0.0 (surface1) to 0.5mm and from 1.1 to 1.7mm (surface2). The hardness rate of change on the left side was similar from 0.1 to 0.5mm. The highest hardness value in this side was 347.4 HV0.1-0.5 at 0.05mm decreasing continuously to 316.3 from 0.05 to 0.45mm. On the right side, from 1.15 to 1.4mm, the hardness values were similar. From 1.35 to 1.5mm the hardness increased significantly from 333.3 to 349.3. From 1.5 to 1.7mm, the change of hardness was insignificant, 351.7-354.3. The maximum of the L-S hardness value in the shot-peened region was 354.3 at 1.65mm.

b) Non shot-peened region was from 0.5 to 1.1mm in the center with the hardness value of 313.9±15.5 HV 0.1- 0.5.

Surfaces 1 and 2 (L-T) with the hardness values of 374.9 and 395.6 HV0.1-0.5 completed the L-S hardness curve of the grip section.
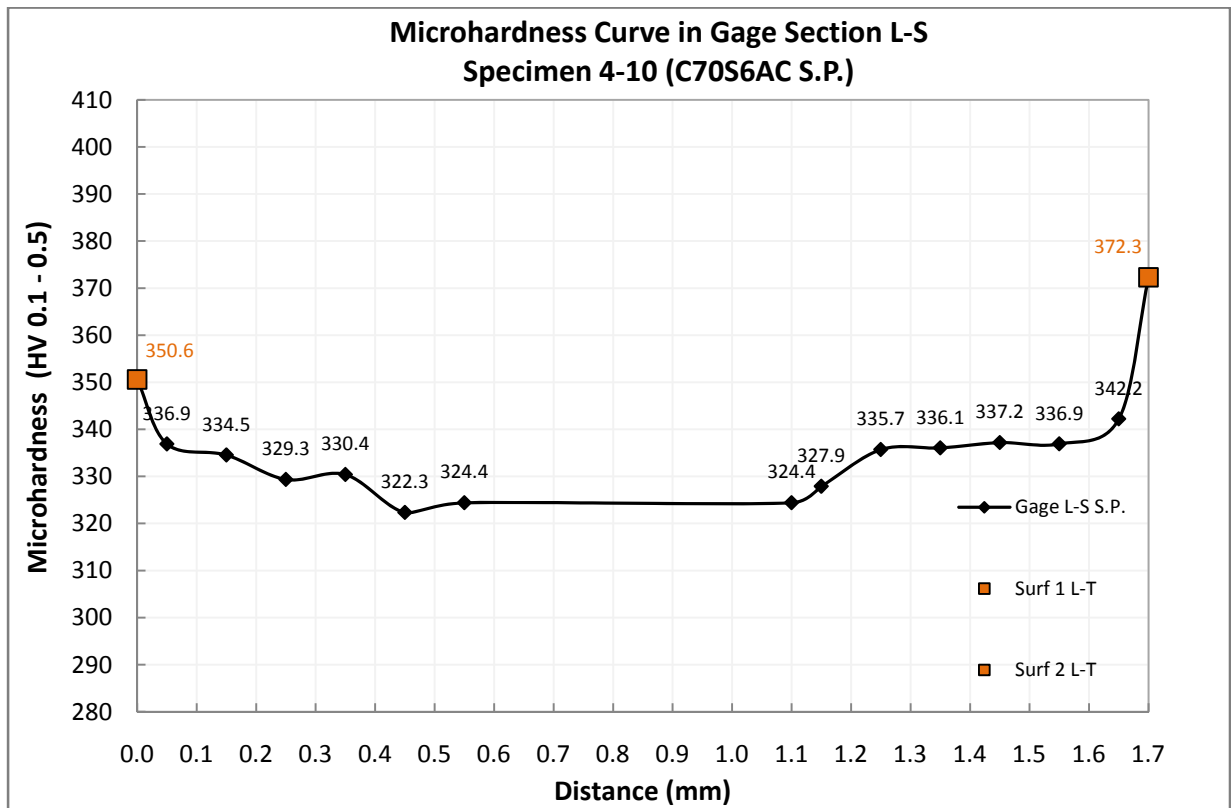
Figure 4.45.Specimen 4-10 gage section hardness profile

Gage section (Figure 4.45):

a) The shot-peened region ranged from 0.0 (surface1) to 0.5mm on the left side and from 1.1 to 1.7mm (surface2) on the right side. The hardness almost remained unchanged from 0.0 to 0.35mm on the left and from 1.25 to 1.6mm on the right side.

b) The center was expanded to 0.4mm and 1.15mm on the left and right side respectively. In general, the hardness variations in the grip section were higher than the gage section.

Surface 1 and 2 L-T hardness values were 350.6 and 372.3 HV0.1-0.5 respectively.

Comparing the average hardness values in the grip and gage sections of the non shot-peened PM specimens (301.4 and 305.0 HV0.5) with the average hardness values of the grip and gage sections of specimen 3-15 in L-T direction (385.3 and 361.5 HV0.1-0.5), showed 27.8% and 18.50% increase of hardness in the grip and gage sections respectively. The L-S direction represented a non shot-peened surface whereas the L-T was a fully shot-peened surface.

4.4. Microstructure

4.4.1. AISI 1141AC
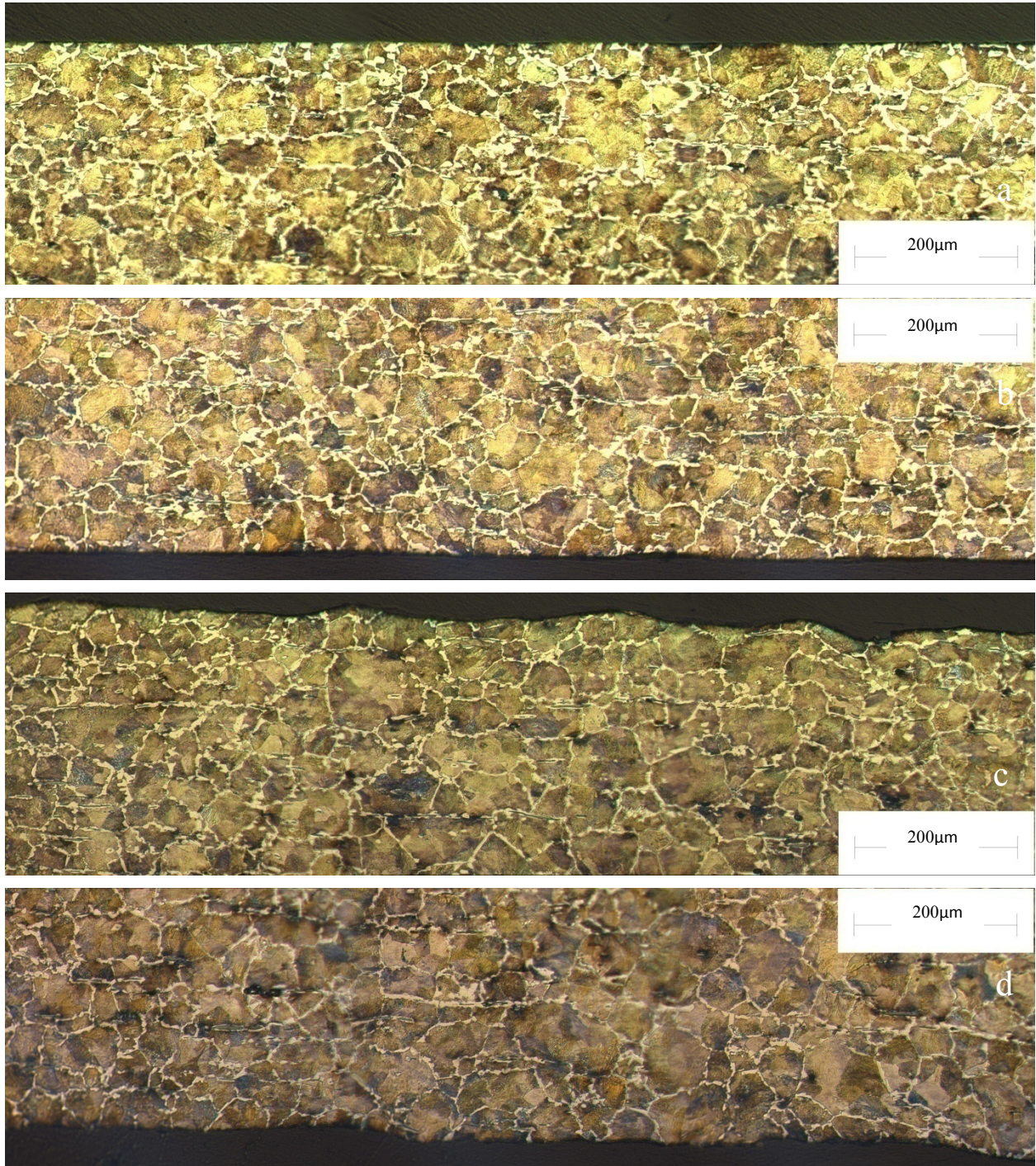
Figure 4.46.AISI 1141 AC microstructure (etched in 2.0% Nital) a,b) non shot-peened top and bottom c,d) shot-peened top and bottom

The microstructure of the AISI 1141AC steel in the non shot-peened and shot-peened condition is shown in Figure 4.46 a,b and c,d respectively indicating the microstructure of hypoeutectoid steel in which the islands of pearlite are surrounded by the primary ferrite (white).

4.4.2. AISI 1151QT

Figure 4.47 a,b and c,d respectively show the microstructure of the quenched-tempered AISI 1151 steel in the non shot-peened and shot-peened condition. The AISI 1151 microstructure is that of tempered martensite showing fine carbide in a ferrite matrix.

4.4.3. PM

The microstructure of powder metallurgy (PM) steel in non shot-peened and shot-peened condition is shown in Figure 4.48a,b and c,d respectively. These figures show some islands of pearlite are surrounded by primary ferrite.

4.4.4. C70S6AC

The microstructure of C70S6AC steel in the non shot-peened and shot-peened condition is shown in Figure 4.49a,b and c,d respectively indicating the microstructure of a hypoeutectoid steel in which pearlite is surrounded by primary ferrite.
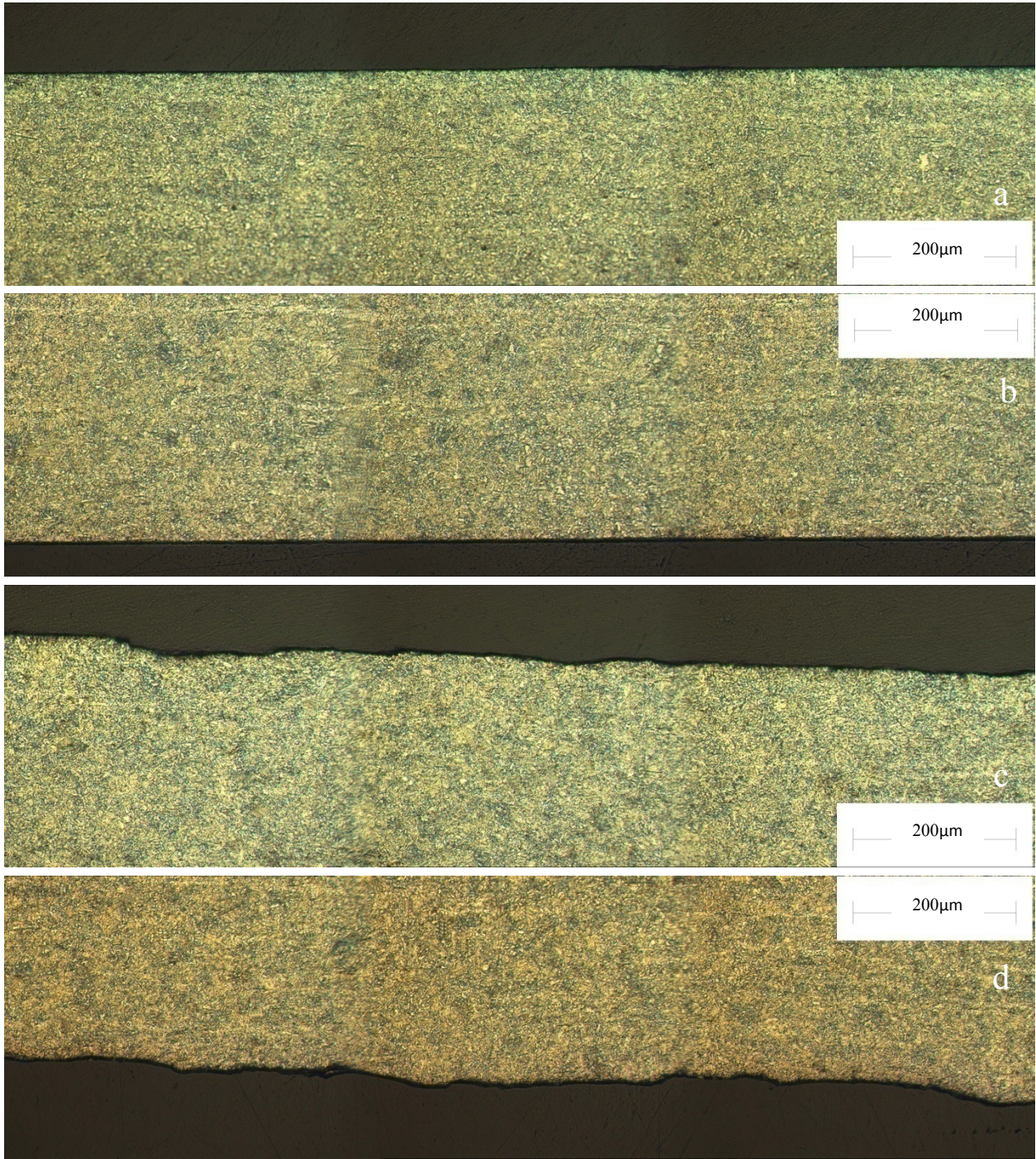
Figure 4.47.AISI 1151 QT microstructure (etched in 2.0% Nital) a,b) non shot-peened top and bottom c,d) shot-peened top and bottom
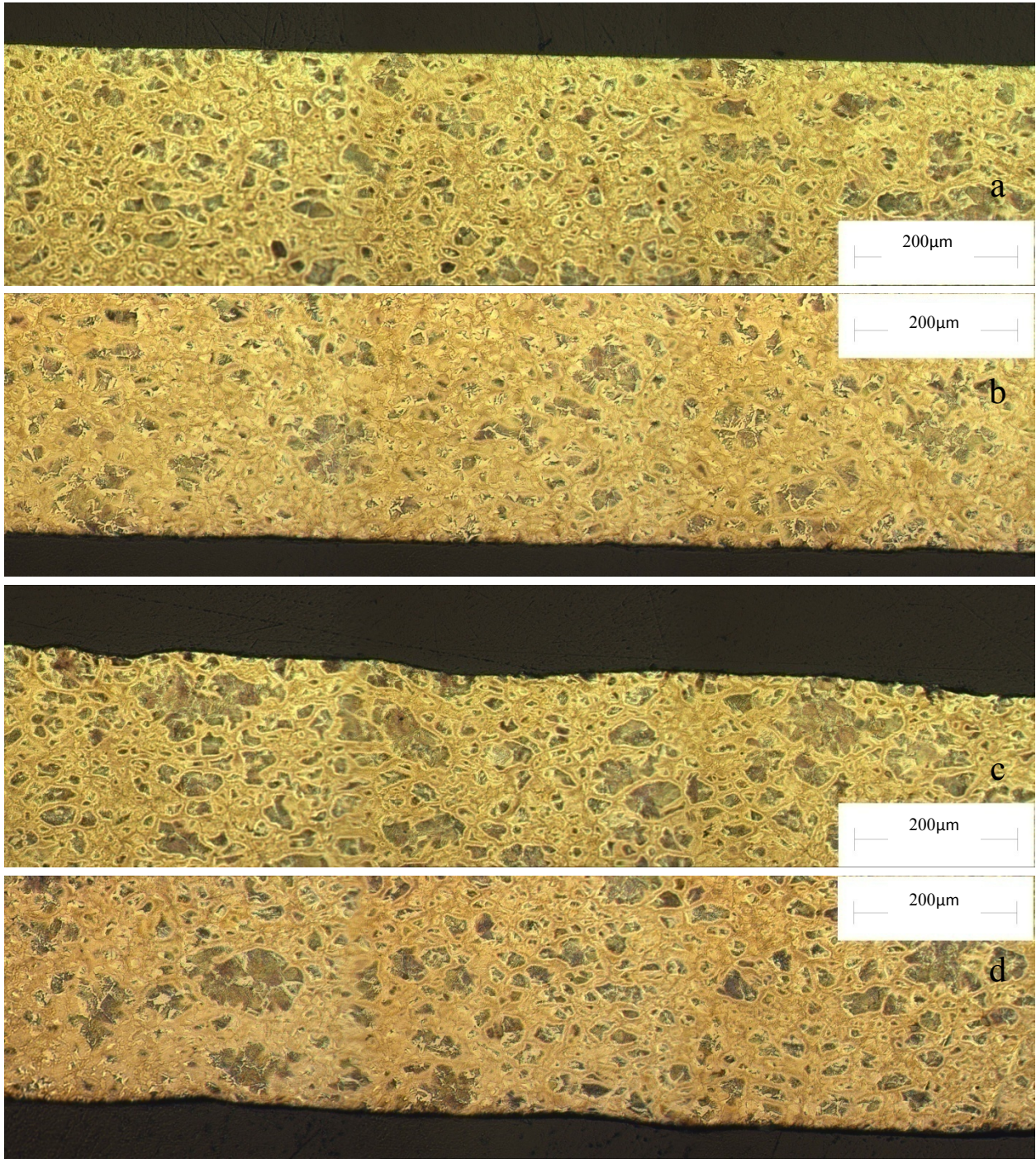
Figure 4.48.PM microstructure (etched in 2.0% Nital) a,b) non shot-peened top and bottom c,d) shot-peened top and bottom
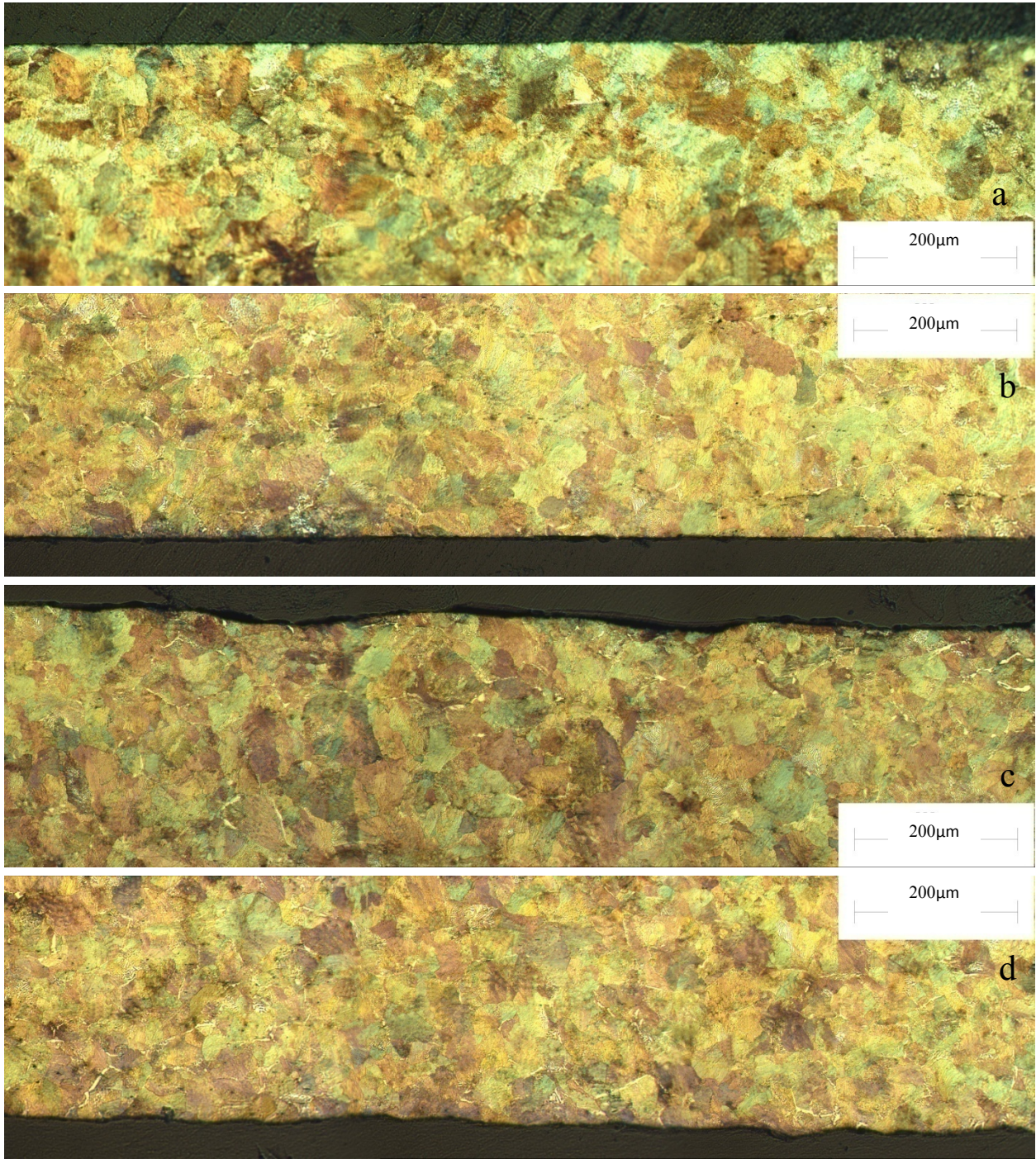
**Figure 4.49.C70S6AC microstructure (etched in 2.0% Nital)   a,b) non shot-peened top and bottom
c,d) shot-peened top and bottom**
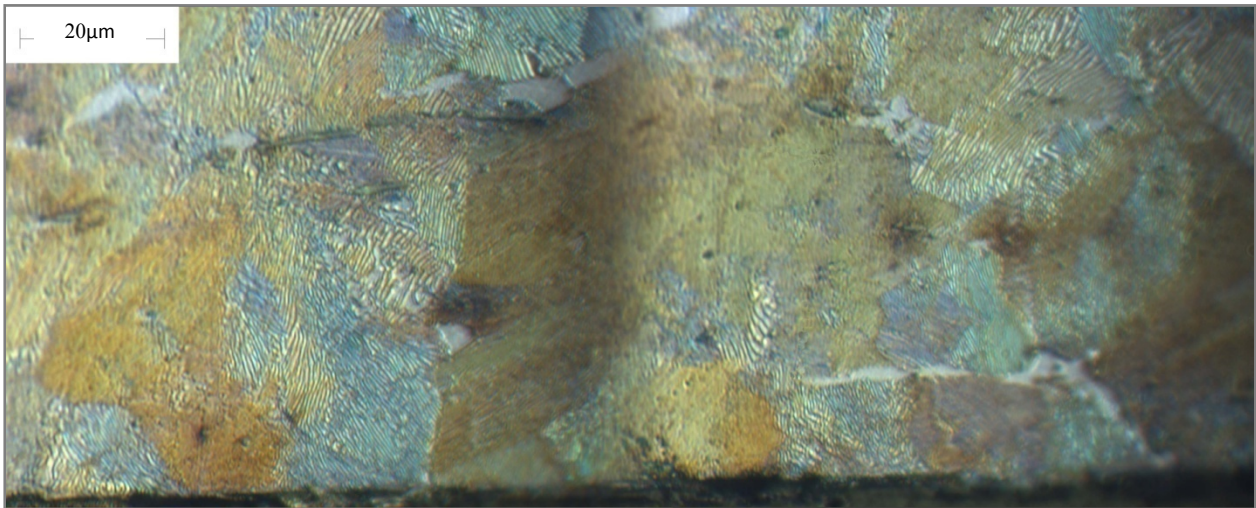
Figure 4.50.C70S6AC microstructure

Figure 4.50 shows islands of pearlite in air cooled C70S6 at higher magnification.

4.4.5. Indentations

The indentations caused by microhardness Vickers test are shown in Figure 4.51. The distance between the two indentations on the left (1 and 2) to the edge were 0.05 and 0.3mm and on the right (3 and 4) to the edge were 0.16 and 0.41mm respectively. These indentations correspond to the marked point on microhardness curve shown in Figure 4.52.
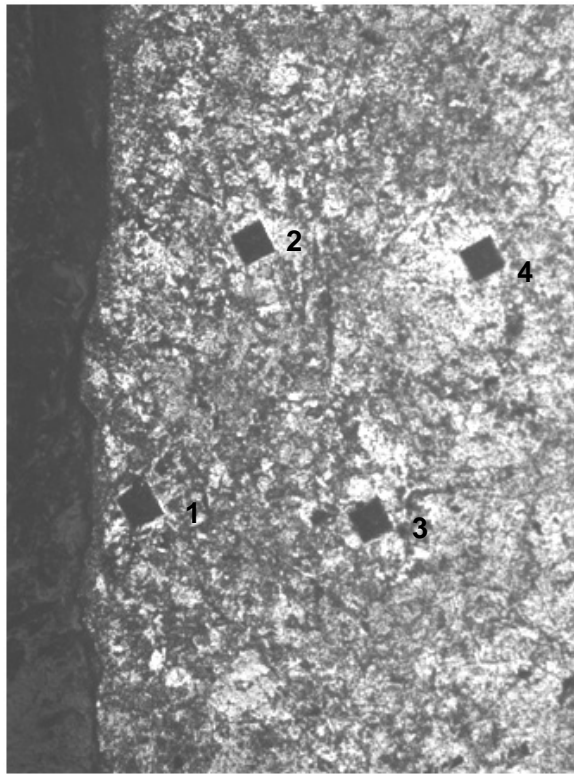
Figure 4.51. Indentations - Microhardness Vickers Test

As depicted on the microhardness curve (Figure 4.52) the closer the indentation to the edge (the surface), the higher the hardness value was, however, no deformation was apparent.
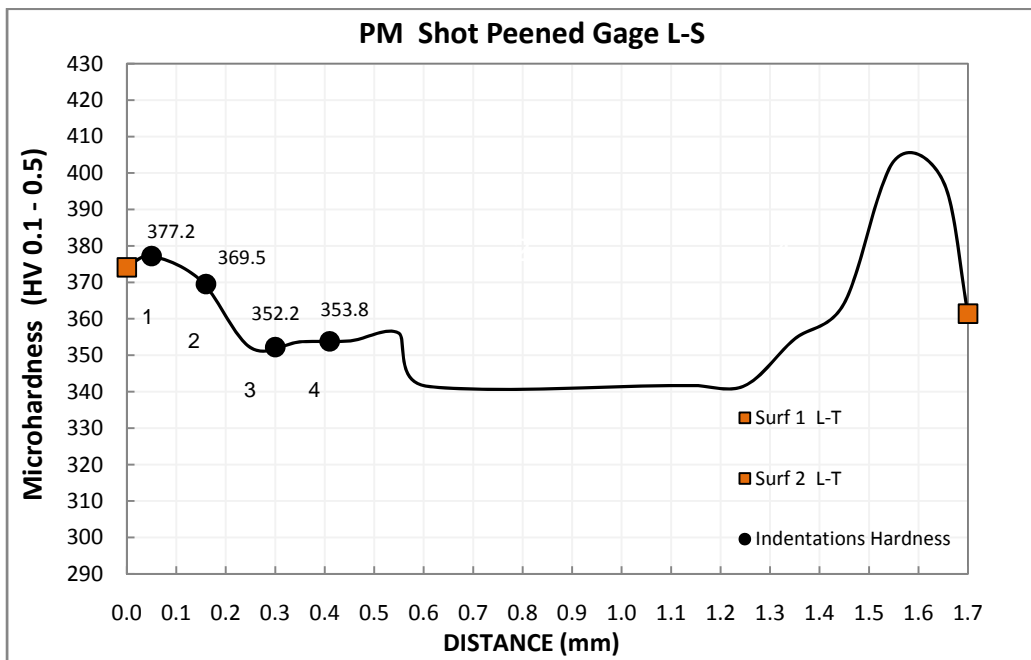
Figure 4.52.Indentations on microhardness curve

4.5. Surface Roughness

Figure 4.53a, b to Figure 4.56 a, b show top and bottom surfaces of non shot-peened AISI 1141AC, AISI 1151QT, PM and C70S6AC specimens respectively. The increase of surface roughness after shot-peening was apparent as top and bottom surfaces of shot-peened specimens are shown in Figure 4.53c, d to Figure 4.56c, d.

The surface roughness of different non-shot peened steels was similar (0.26±0.03μm), likewise after shot-peening all the specimens had a similar surface roughness of (3.60±0.44μm) [9].
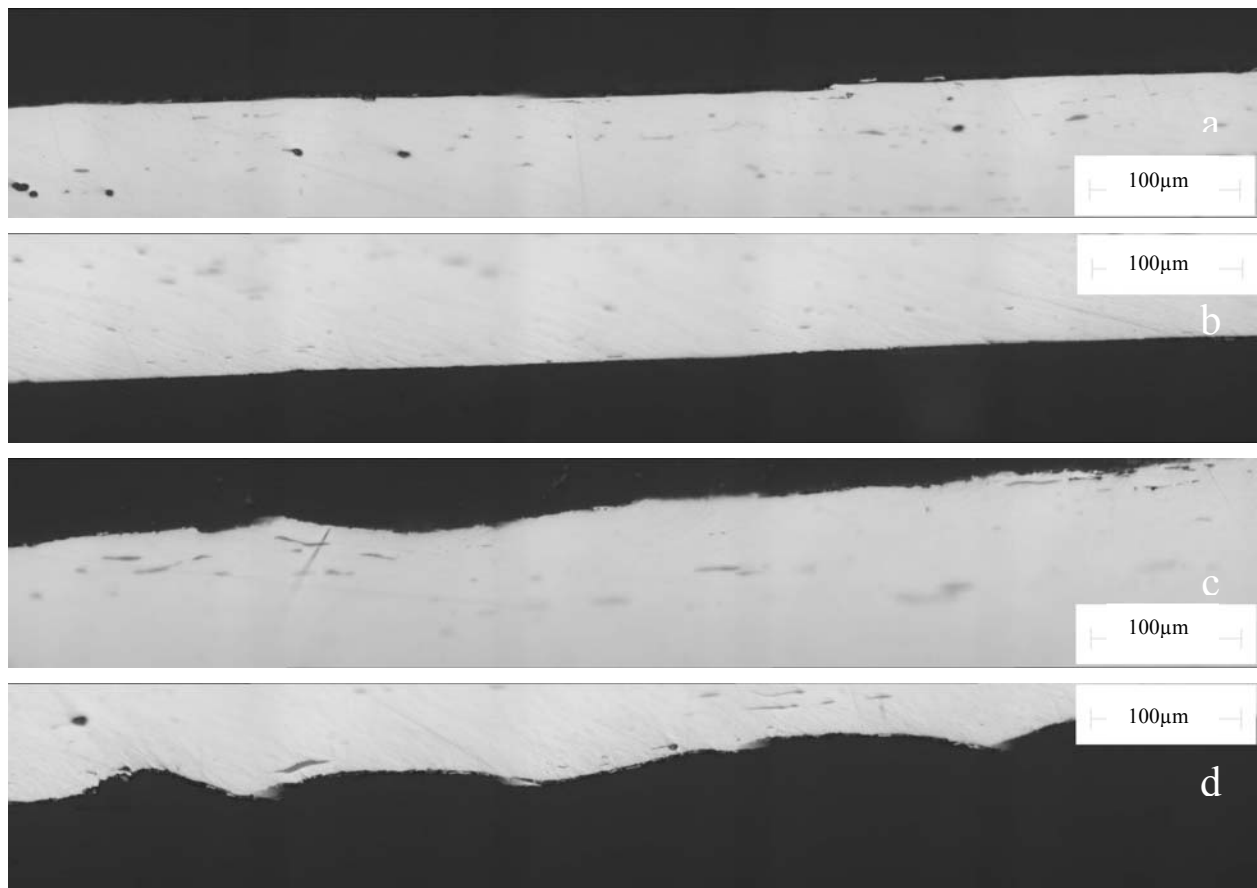
Figure 4.53.AISI 1141AC a,b) non shot-peened top and bottom c,d) shot-peened top and bottom
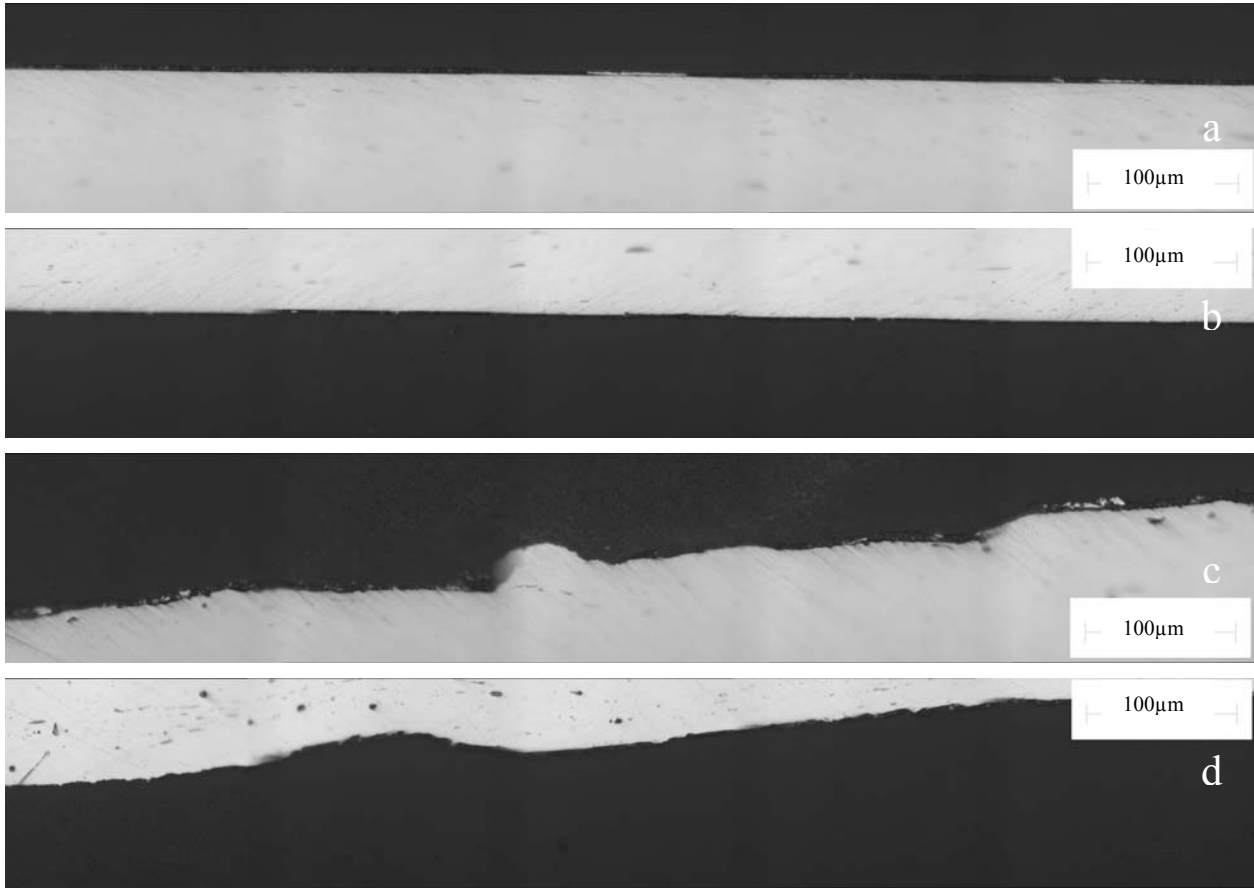
Figure 4.54.AISI 1151QT a,b) non shot-peened top and bottom c,d) shot-peened top and bottom
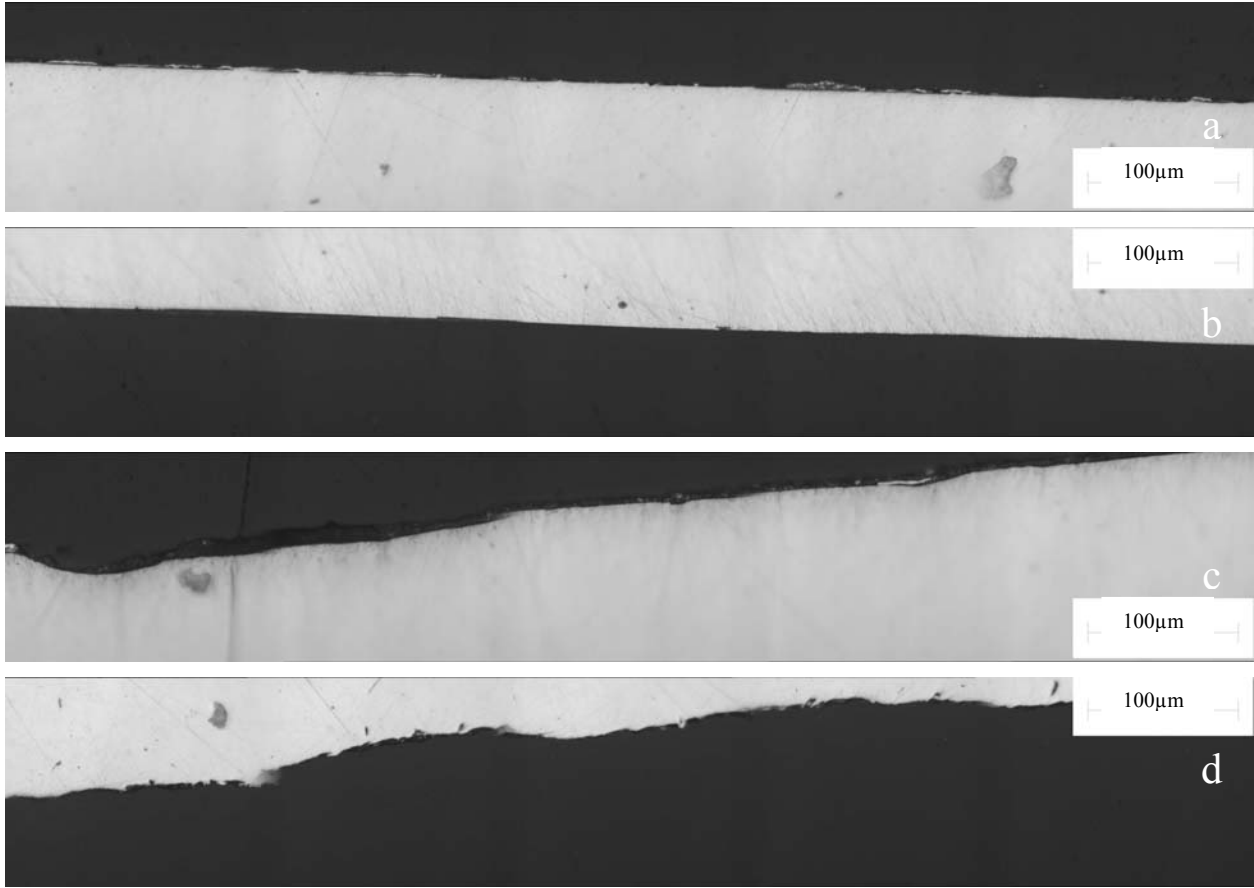
Figure 4.55.PM a,b) non shot-peened top and bottom c,d) shot-peened top and bottom
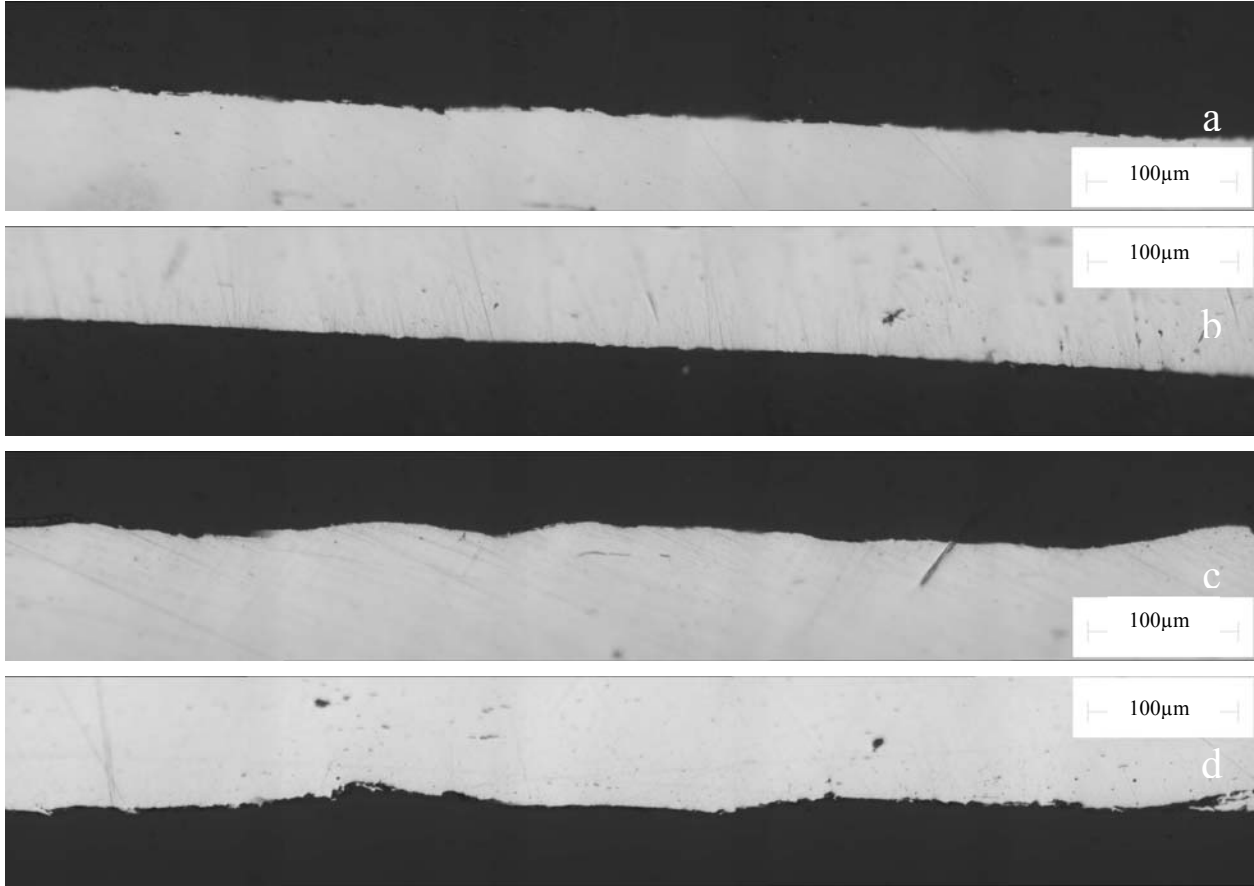
Figure 4.56.C70S6AC a,b) non shot-peened top and bottom c,d) shot-peened top and bottom

Chapter 5

Discussion

5.1. Air Cooled Medium Carbon Steel (AISI 1141AC)

5.1.1. AISI 1141AC fatigue strength

Table 5.1.AISI 1141AC fatigue strengths

Material	Cycle Number	Non Shot-Peened (MPa)	Shot-Peened (MPa)	Fatigue Strength Ave. Change (%)
AISI 1141AC	10^6	323.2±7.3	342.7±14.9	6.0%
	10^7	324.3±5.1	331.6±2.6	2.3%

At 10^6 and 10^7 cycles, AISI 1141AC fatigue strengths after shot-peening increased 6.0% and 2.3% respectively which are small improvements when the standard deviations are considered.

5.1.2. AISI 1141AC L-S microhardness profiles (grip vs. gage)

Figure 5.1 shows the grip and gage hardness curves of the non shot-peened and shot-peened AISI 1141AC in the L-S direction.

The hardness values in the grip and gage sections of the non shot-peened (normalized) AISI 1141AC were 285.4±9.4 and 283.6±9.5 HV0.5 respectively are shown in Figure 5.1 indicating that neither cyclic softening nor hardening occurred after 5.0×10^5 cycles at σ_a=349.9 MPa in the non shot-peened condition. These values were similar to the center hardness (293.4±14.9 HV0.1-0.5) in the grip section of the shot-peened specimen before cycling.

The gage hardness in the center of the shot-peened specimen was 302.2±15.1 HV0.1-0.5 after 9.2×10^5 cycles at σ_a=349.7 MPa. When the hardness in the grip and gage are compared, it becomes apparent that shot-peening resulted in only a very small increase of hardness.
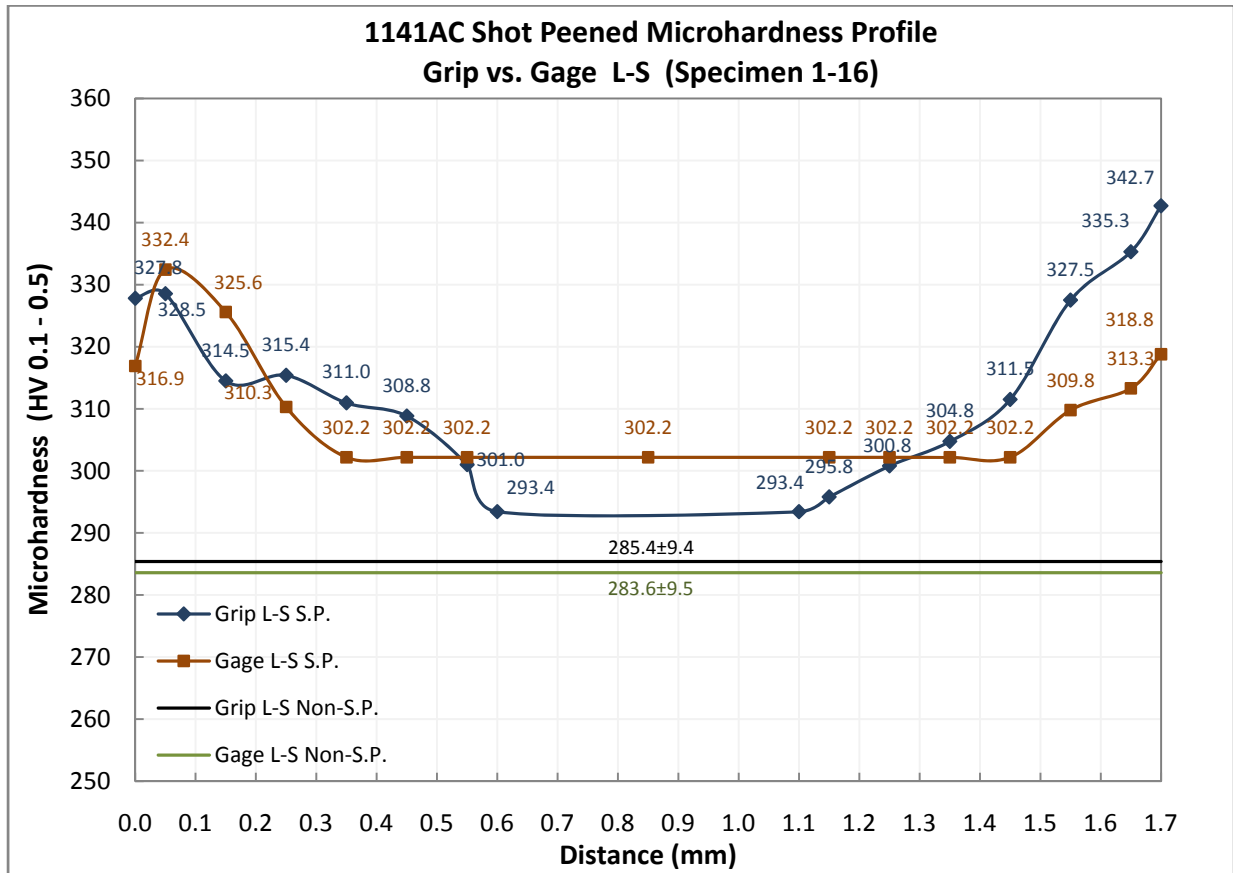
Figure 5.1.AISI 1141AC L-S microhardness profile non shot-peened vs. shot-peened

Higher surface hardness values were apparent in the shot-peened regions of the grip than those in the gage after 9.2×10^5 cycles at σ_a=349.7 MPa. Cyclic softening (from 342.7 to 318.8, right side and 327.8 to 316.9, left side) occurred that was accompanied by a decrease in the depth of surface hardness from 0.6 to 0.25mm on the left side and from 1.15 to 1.45mm on the right side. The surface hardness decreased 3.0% left side and 7.0% right side. The amount of softening in the shot-peened region was 1.50% on the left side and 13.2% on the right side.

5.2. Quenched-Tempered Medium Carbon Steel (AISI 1151QT)

5.2.1. AISI 1151QT fatigue strength

Table 5.2 shows fatigue strengths for the non shot-peened and shot-peened AISI 1151QT. The high cycle fatigue strengths decreased 11.0 and 12.0% respectively at 10^6 and 10^7 cycles on shot-peening.

78

Table 5.2.AISI 1151QT fatigue strengths

Material	Cycle Number	Non Shot-Peened (MPa)	Shot-Peened (MPa)	Fatigue Strength Ave. Change (%)
AISI 1151QT	10^6	418.3±18.6	372.3±31.3	-11.0%
	10^7	427.3±7.6	375.9±32.7	-12.0%

The decrease of fatigue strengths after shot-peening could be due to the higher plastic strain amplitudes which are always measured for the shot-peened quenched-tempered medium carbon steels [15] with similar stress amplitudes and comparable number of cycles than for non shot-peened ones under tension-compression loading. Besides, the onset of cyclic softening is shifted to smaller numbers of cycles after shot-peening in quenched-tempered medium carbon steel [15].

5.2.2. AISI 1151QT L-S microhardness profiles (grip vs. gage)
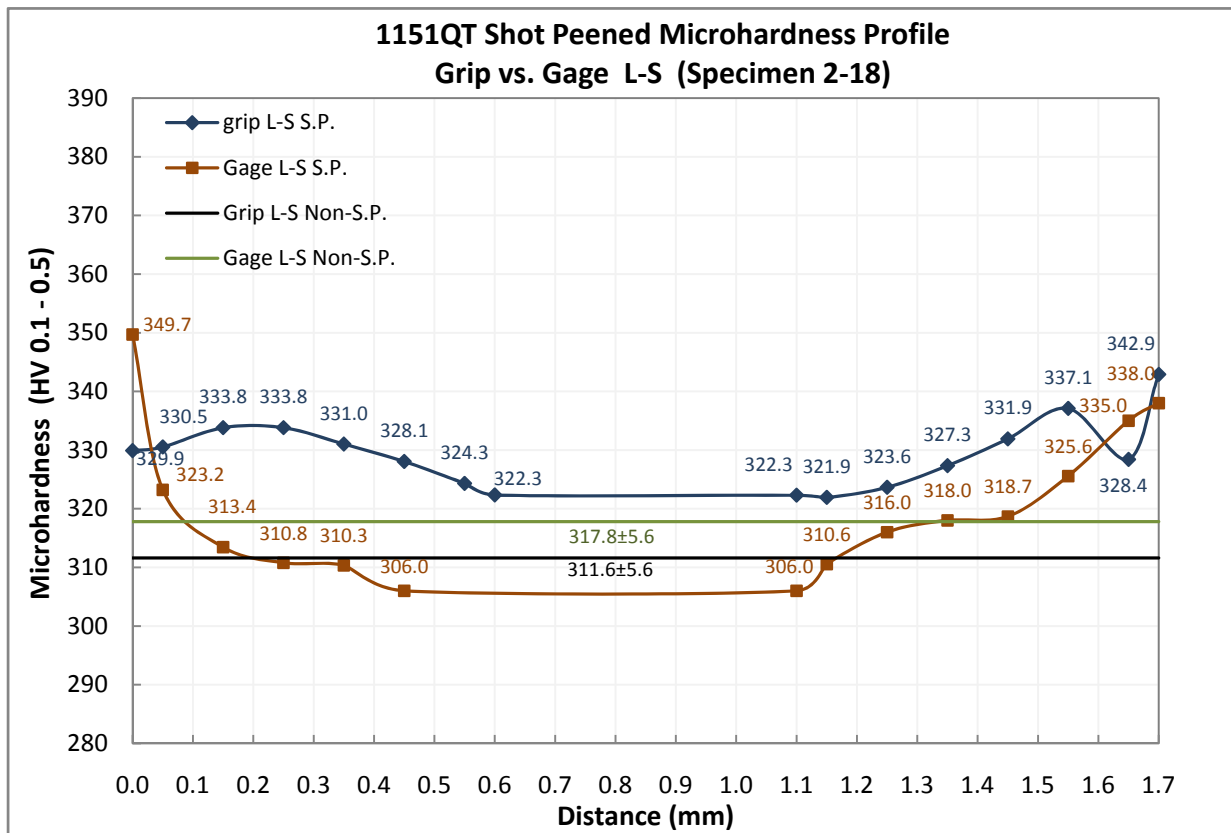
Figure 5.2 shows the grip and gage hardness curves in the non shot-peened and shot-peened AISI 1151QT in L-S direction.
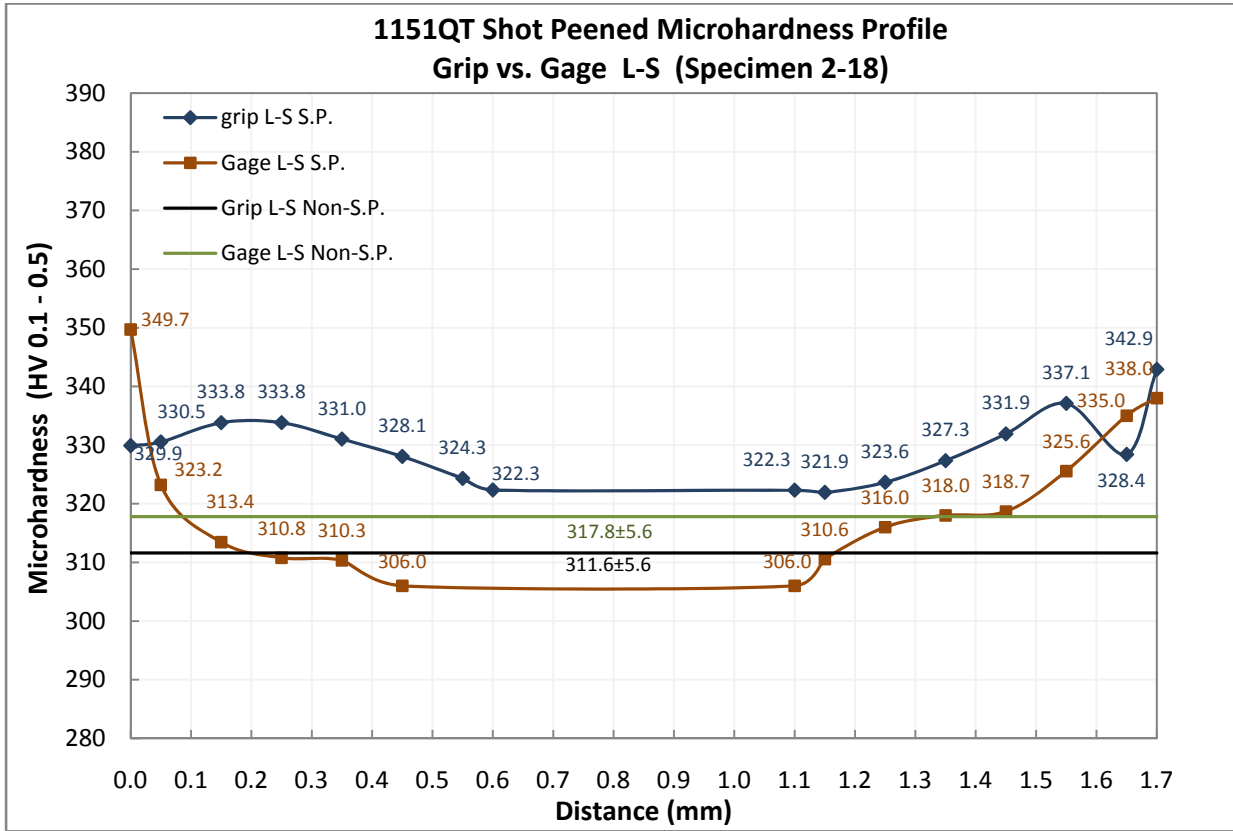
Figure 5.2.AISI 1151QT L-S microhardness profile non shot-peened vs. shot-peened

The hardness in the grip section of the non shot-peened AISI 1151QT was 311.6±5.6 HV0.5 and in the gage section the hardness was 317.8±5.6 HV0.5. These similar hardness values indicate that no cyclic softening or hardening occurred in the quenched-tempered (non shot-peened) conditions after 6.5×10^5 cycles at σ_a=440.8MPa. These values were similar to the center hardness (306.0±11.6 HV0.1-0.5) in the grip section of the shot-peened specimen before cycling.

The grip and gage hardness values in the center for the shot-peened specimens were 322.3±11.2 and 306.0±11.6 HV0.1-0.5 respectively. This decrease in hardness shows that cyclic softening occurred after 2.9×10^4 cycles at σ_a=461.1MPa in the shot-peened condition.

The L-S microhardness profile of the grip and gage sections for the shot-peened specimen showed higher surface hardness values in the shot-peened regions in the grip section than in the gage after 2.9×10^4 cycles at σ_a=461.1MPa. A decrease in the depth of surface hardness from 0.6mm to 0.45mm on the left side occurred and the amount of softening in the shot-peened region was 33.8% on the left side and 14.1% on the right side.

Eifler et. al.[15] showed that for quenched-tempered AISI 4140 steel, cyclic softening occurred sooner in shot peened specimens than non shot-peened ones. In addition, higher plastic strain amplitudes occurred in shot-peened samples. This showed that relaxation of compressive residual stresses in the shot-peened specimens during cycling was higher than the non shot-peened ones [15].

5.3. Powder Metallurgy (PM)

5.3.1. PM fatigue strength

Table 5.3 shows fatigue strengths for the non shot-peened and shot-peened PM specimens.

Table 5.3. PM fatigue strengths

Material	Cycle Number	Non Shot-Peened (MPa)	Shot-Peened (MPa)	Fatigue Strength Ave. Change (%)
PM	10^6	310.0±13.8	353.5±19.4	14.0%
	10^7	311.0±19.5	343.2±22.4	10.4%

After shot-peening, the fatigue strengths increased to 353.5±19.4MPa at 10^6 cycles and 343.2±22.4 at 10^7 cycles, indicating 14.0% and 10.4% fatigue limit improvements respectively on shot-peening.

5.3.2. PM L-S microhardness profiles (grip vs. gage)

Figure 5.3 shows microhardness profile in the non shot-peened and shot-peened PM in L-S direction. The hardness values in the grip and gage sections of the non shot-peened PM were 303.5±27.3 and 300.3±21.8 HV0.5. These similar hardness values indicate that no cyclic softening nor hardening occurred in the non shot-peened condition after 8.1×10^5 cycles at σ_a=304.3MPa. These values were different to the center hardness (333.2±35.5 HV0.1-0.5) in the grip section of the shot-peened specimen before cycling.
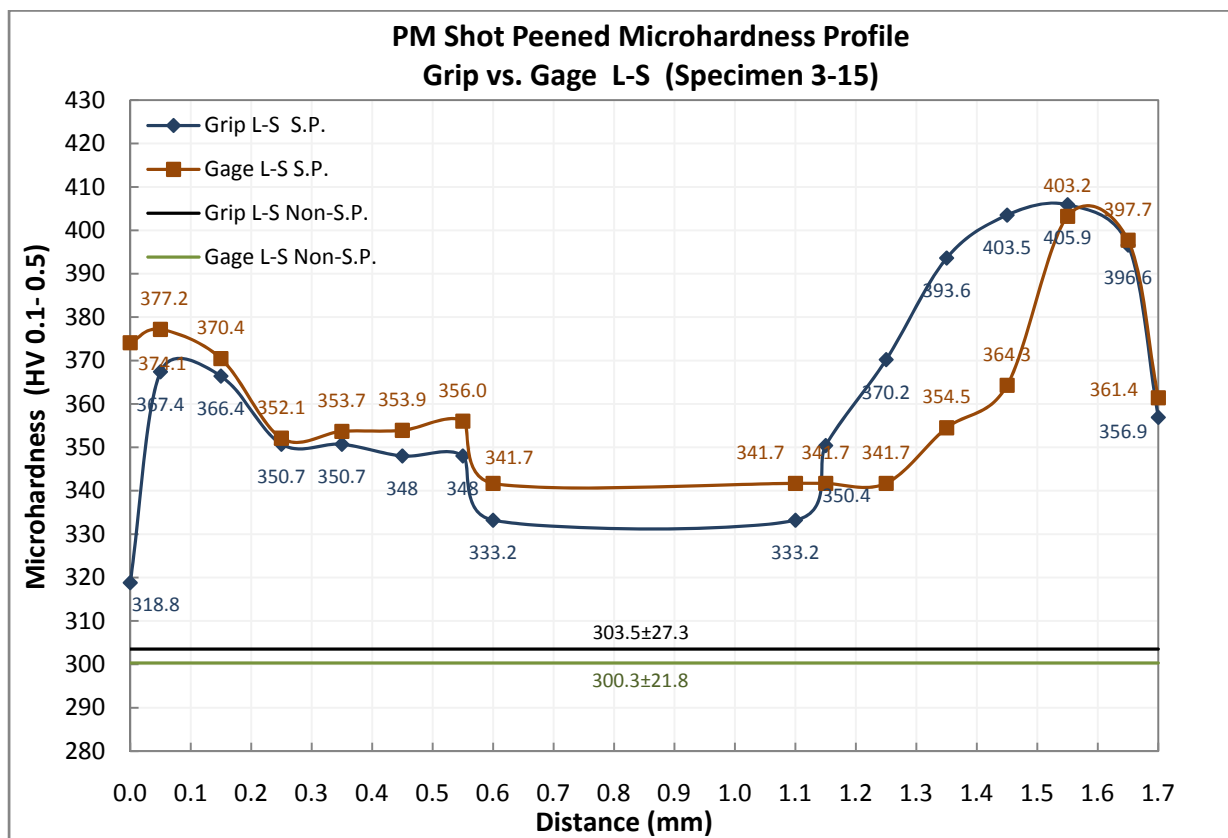
Figure 5.3.PM L-S microhardness profile non shot-peened vs. shot-peened

The hardness of the shot-peened sample was 333.2±35.5 in the grip center and 341.7±27.9 HV0.1-0.5 in the gage center. Considering the standard deviations, no difference is seen in the center, indicating that significant cyclic softening or hardening had not occurred in this region after 1.8×10^6 cycles at σ_a=368.5MPa.

In the shot peened regions cyclic softening or hardening was not apparent, however, on the right side there is an indication that some softening occurred between 1.15 to 1.5mm. A decrease in the depth of surface hardness from 1.1mm to 1.25mm on the right side is seen and the amount of softening in the shot-peened region on the right side was 31%.

5.4. Air Cooled High Carbon Crackable Steel (C70S6AC)

5.4.1. C70S6AC fatigue strength

Table 5.4 shows fatigue strengths for the non shot-peened and shot-peened PM specimens.

Table 5.4.C70S6AC fatigue strengths

Material	Cycle Number	Non Shot-Peened (MPa)	Shot-Peened (MPa)	Fatigue Strength Ave. Change (%)
C70S6AC	10^6 10^7	349.8±5.2 348.8±5.5	342.6±8.4 341.3±7.4	-2.1% -2.2%

The change of fatigue limits for C70S6AC was negligible, -2.1 and -2.2% at 10^6 and 10^7 cycles indicating that the effect of shot peening, if any, was extremely small.

5.4.1. C70S6AC L-S microhardness profiles (grip vs. gage)

Figure 5.4 shows the L-S direction microhardness profile in the grip and gage sections of the selected non shot-peened and shot-peened C70S6 specimens. The hardness values in the grip and gage sections of the non shot-peened were 301.5±11.0 HV0.5 and 305.3±14.3 HV0.5 after 7.4×10^5 cycles at σ_a=355.0MPa. The hardness values are similar and no difference is apparent, indicating that neither cyclic softening nor hardening occurred. These values were similar to the center hardness (313.9±15.5 HV0.1-0.5) in the grip section of the shot-peened specimen before cycling.
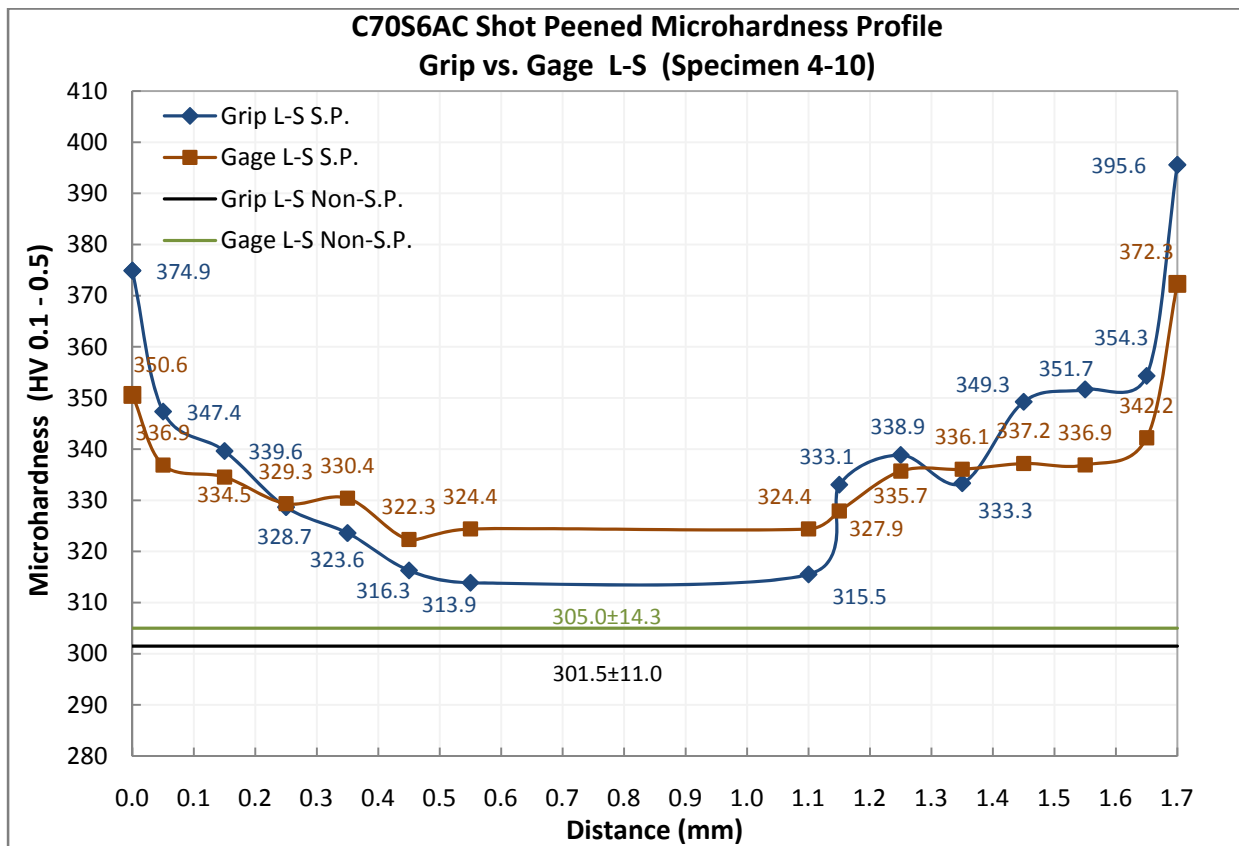
Figure 5.4.C70S6AC L-S microhardness profile non shot-peened vs. shot-peened

The values of hardness in the grip and gage sections in non shot-peened condition were similar to the center hardness (293.4±14.9 HV0.1-0.5) in the grip section of the shot-peened specimen before cycling. The grip and gage hardness values in the center of shot-peened C70S6 were 313.9±15.5 and 324.4±12.3 HV0.1-0.5 respectively. Considering the standard deviations, only a very small increase of hardness was apparent in the center indicating that a very small amount of cyclic hardening occured after 10^7 cycles at σ_a=347.4MPa. Cyclic softening occurred at the surface of shot-peened C70S6 after 10^7 cycles at σ_a=347.4MPa leading to a hardness decrease (from 395.6 to 372.3, right side and from 374.9 to 350.6, left side). The hardened surface decreased in the depth from 0.55 to 0.25mm on the left and from 1.1 to 1.55mm on the right side. The surface hardness decreased 7.0% and the net amount of softening in the shot-peened region of C70S6 steel was 12.8% on the right side.

5.5. Surface Roughness

Surface roughness was measured using a Talysurf. The surface roughness of 0.26±0.03μm was similar for all in the non shot-peened condition, likewise after shot-peening all the specimens had a similar surface roughness of 3.60±0.44μm [9].

5.6. Compressive Residual Stresses
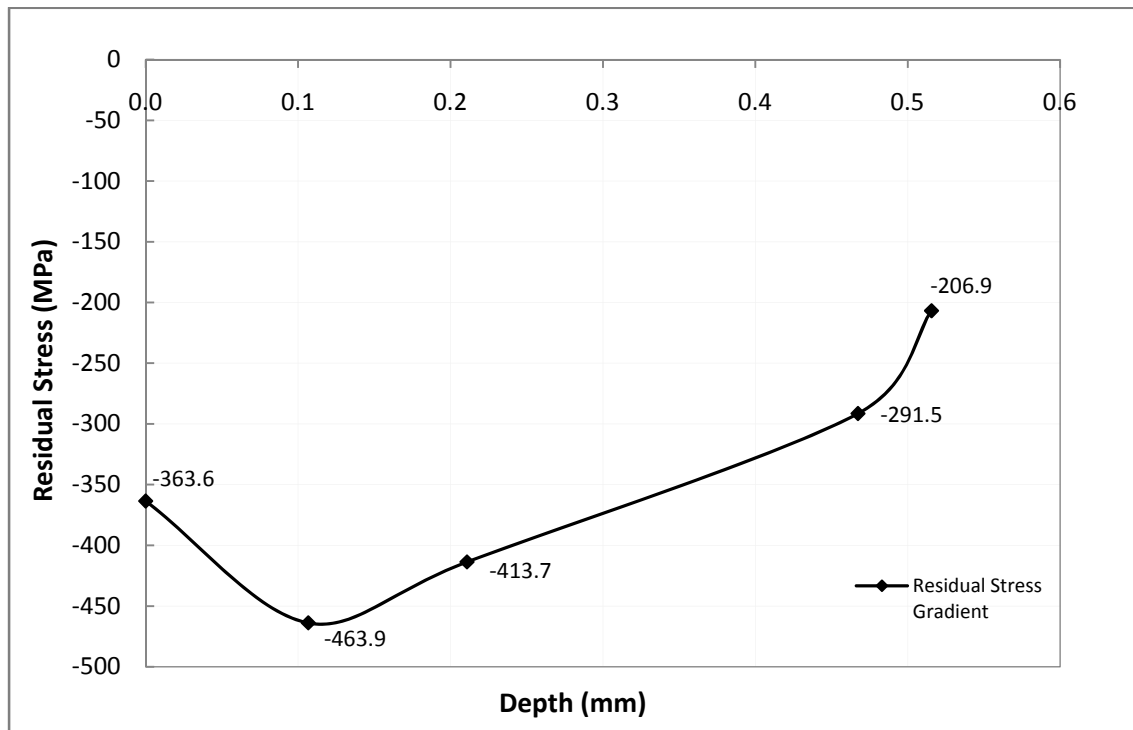
Figure 5.5.Compressive residual stress profile after shot-peening

Figure 5.5 represents the similar residual stress profiles for all the shot-peened specimens. The maximum stress of -463.9MPa at a depth of 0.1mm decreased to -206.9MPa at the depth of 0.5mm [9].

A comparison between the microhardness profiles in the non shot-peened and shot-peened conditions before cycling shows a relatively high increase of hardness at the surface of all the steels indicating that significant work hardening took place on shot peening. In AISI 1141AC and AISI1151QT the surface hardness values increased from 285.4±9.4 HV0.5 to 327.8 (surface1) and 342.7 HV0.1-0.5 (surface2) and from 311.6±5.6 HV0.5 to 329.9 (surface1) and 342.9 HV0.1-0.5 (surface2) respectively. The surface hardness values increased from 303.5±27.3

HV0.5 to 318.8 (surface1) and 356.9 HV0.1-0.5 (surface2) in PM steels and from 301.5±11.0 HV0.5 to 374.9 (surface1) and 395.6 HV0.1-0.5 (surface2) in C70S6AC.

Comparing the non shot-peened and the shot-peened steels showed a range of effects from the relatively high beneficial effect of shot peening on the push-pull fatigue limit of PM (10.4 to 14.0%) to the relatively negative effect on AISI 1151QT (-12.0%). The effect of shot peening on AISI1141AC and C70S6AC steels were extremely small, (2.3 to 6.0% and -2.2% respectively).

In this study, the improvement (2.3 to 6.0%) in the fatigue strength of the air cooled steel (AISI 1141AC) was small when compared to the 14.0% improvement in bending fatigue strength of quenched shot-peened AISI 1045 (medium carbon steel) observed by [8]. This increase, (2.3 to 6.0%), was also smaller than the 20.5% and 21.9% improvement in rotating-bending fatigue strengths that was observed after shot-peening of smooth air cooled medium carbon steels by [6]. This difference is due to different type of fatigue testing, as explained later.

In the present work, the push-pull fatigue strength in the quenched-tempered medium carbon steel (AISI 1151) decreased 12.0% after shot-peening which is different from other similar researches. The bending fatigue limit of shot-peened quenched-tempered medium carbon steel (AISI 1045) increased 22.0% for smooth specimens [8]. This improvement is restricted to small loading amplitudes, i.e. 0.5 to $0.65\sigma_{ys}$, leading to the high number of cycles to fracture i.e. 10^6 to 10^7 cycles [8].

 Guechichi and Castex [10] showed respectively 9.0%, 12.0% and 22.0% enhancement in rotary bending, tension-compression and torsion fatigue limits of low-alloy quenched-tempered medium carbon steels (35NiCrMo16 and 32CrMoVa13) after shot-peening. Torres and Voorwald [13] showed a 9.0 to 12.0% improvement in the rotating-bending fatigue limit in smooth quenched-tempered medium carbon steel (AISI 4340) using four different intensities of shot-peening.

In this study, the fatigue strengths of air cooled high carbon steel (C70S6) decreased -2.2% which is regarded as insignificant. Farrahi et al. [3] performed shot-peening on high carbon spring steel (AFNOR 60SC7) using four different types of shots for the shot-peening process. They showed a 14.0 to 24.0% increase in the torsion fatigue limit after shot-peening.

The results of this study show that the influence of shot-peening on the fatigue limits are not pronounced. Fatigue stress gradients generated by the tension-compression loading conditions are shallower than in bending and rotating-bending. Therefore the gradient of compressive residual stresses is still higher than the loading stresses preventing initiation of cracks on the surface. This leads to crack initiation in the sub-surface layers where the loading stresses exceed the local fatigue strength, reducing the negative effect of surface roughness on the fatigue behaviour of the shot-peened specimens. Fatigue cracks initiate in the subsurface layers where the applied tensile stress counters the compressive residual stresses created by shot peening [10, 30].

Metallographic examination has shown that fatigue cracking in shot-peened specimens shifted to the interior, so that the detrimental effects of the roughened surfaces by shot-peening became less important [16]. Hoffmann et.al [8] showed that cracks initiate 0.5mm below the surface in smooth quenched medium carbon steels (AISI 1045). A model by Guechichi and Castex [10] determined the position of the crack source for shot-peened quenched-tempered low alloy steel at a depth of 0.3mm below the surface, which was similar to the thickness of the shot-peened layer.

Wang et.al [14] performed three-point bending fatigue test on 20Cr, 30CrMo, 40Cr, GC4, 45 steels and Al-alloy LC9 after shot-peening. They showed that fatigue cracks were always located at the surface for non shot-peened cases, whereas these cracks were located beneath the compressive residual stress zone in all the shot-peened specimens except medium carbon steel (AISI 1045 steel) in which crack sources were located inside the hardened layer within compressive residual stress zone.

Compressive residual stresses and work hardening are the beneficial effects of shot peening whereas surface roughness is an accompanying detrimental effect [3,7]. In the present case, the surface roughness profile increased from 0.26 ± 0.03 to $3.6\pm0.44\mu m$ after shot-peening [9].

The beneficial effects of induced compressive residual stresses and work hardening are countered by surface roughness. Guechichi and Castex [10] introduced a model which demonstrated that work hardening was the more important effect. Pariente and Guagliano [11] studied shot-peened 42CrMo4 steel (low-alloy steel) specimens in pre-crack conditions. They

concluded that retardation of fatigue crack propagation after shot-peening was associated more with the surface work hardening than with the residual stress field caused by shot peening.

Another study by A.M.Eleiche [6] et.al on the high cycle fatigue behaviour of high-strength martensitic steels, indicated that the induced compressive residual stresses were not the only reason for the high cycle fatigue strength improvement in smooth specimens, but rather most of the shot-peening strengthening effect on high cycle fatigue behaviour could be attributed to the change of surface texture introduced by the rotation of surface crystals.

Chapter 6

Conclusions and Recommendations

6.1. Conclusions

The following conclusions are based on the results of fatigue testing smooth specimens that have been shot peened.

1. Considering the push-pull fatigue limit (10^6 cycles, R=-1) of the air cooled medium carbon steel (AISI 1141), shot-peening was found to have a small beneficial effect of 6.0%.

2. Shot-peening had a small negative influence on the fatigue limit of the quenched-tempered medium carbon steel (AISI 1151) after 10^6 cycles. The push-pull fatigue limit decreased 11.0%.

3. The effect of shot-peening on the powder metallurgy (PM 0.5%C) steel was relatively high. The push-pull fatigue limit increased 14.0% after 10^6 cycles.

4. Shot-peening had a very small effect on the air cooled 0.72% carbon steel (C70S6). The push-pull fatigue limit decreased 2.1% after 10^6 cycles.

5. It was shown that the effect of surface roughness was not a significant factor in controlling the tension-compression fatigue lives of all the steels tested.

6. For all the steels investigated, the surface hardness after shot-peening was found to be different on each side of the specimen.

7. The surface hardness of the shot-peened air cooled medium carbon AISI 1141 steel decreased 3.0% left side and 7.0% right side after 9.2×10^5 cycles. The depth of surface hardness decreased from 0.60mm to 0.25mm on both sides.

8. For the shot-peened quenched-tempered AISI 1151 steel, the depth of surface hardness decreased from 0.60mm to 0.45mm on the left side and showed no change on the right side after 2.9×10^4 cycles.

9. For the shot-peened PM steel, the surface hardness showed no change on the left side, however, decreased from 0.60mm to 0.25mm on the right side after 1.8×10^6 cycles.

10. The surface hardness of the air cooled crackable C70S6 steel decreased 6.0% left and 7.0% right side after 10.1×10^7 cycles. The depth of surface hardness decreased from 0.55mm to 0.25mm on the left side and from 0.6mm to 0.45mm on the right.

11. Considering the grip sections, shot-peening increased the surface hardness as expected. However, the amount of surface hardening varied with the type of steel. For the AISI 1141AC steel, shot-peening increased the average surface hardness by 17.5%. For the AISI 1151QT, shot-peening increased the average surface hardness by 8.0%. For the PM and C70S6AC steels, shot-peening increased the average surface hardnesses by 11.3% and 27.8% respectively.

6.2. Recommendations

In the present work, the effect of shot-peening on the high cycle fatigue behaviour of four different medium carbon heat treated steels was studied. The following recommendations are suggested for the future work.

1. Compressive residual stresses should be measured before, during and after cycling at a given stress amplitude to investigate the relaxation rate of residual stresses for each steel in its normalized and heat treated condition. When the stress relaxation history is determined, the

dominant effect of shot-peening on fatigue life, either compressive residual stress or work hardening, in the different steels can be resolved.

2. Once the residual stresses have been determined, the theoretical model developed by Guechichi and Castex [10] should be applied to the results of this study to predict the high cycle fatigue behaviour of shot-peened steels - the main variables (steel type, heat treatment and stress amplitude) of this model have already been recorded.

3. To locate the fatigue crack initiation sites, the fracture surfaces in non shot-peened and shot-peened cracked specimens must be examined microscopically. This investigation would be particularly important for the AISI 1151QT and C70S6AC steels (in which shot-peening decreased their fatigue limits) to determine whether the fatigue cracks initiated at or below the surface.

Appendices

Appendix A

A.1. Mechanical Properties of Steels

Table A1.Mechanical properties†

Material	Yield Strength (MPa)	Tensile Strength (MPa)	Elongation (%)	Reduction of Area (%)
AISI 1141	575.7	855.0	17.0	39.0
AISI 1151	930.8	999.8	12.0	31.0
PM	565.4	889.5	15.0	30.0
AISI 1070	575.7	1006.7	13.0	27.0

†Galt Testing Laboratories report

Appendix B

B.1. Fatigue Testing Data for AISI 1141AC

Table B1.The fatigue test data for AISI 1141AC non shot-peened

No.	Average Thickness (mm)	Net Width (mm)	Area (mm²)	Load (KN)	σ₀ (MPa)	σₐ (MPa)	Cycles to Failure (Nf)	Remark
1-1	1.78	12.00	21.36	7.51		414.878	192600	Crack
1-2	1.76	12.04	21.19	6.40	213.904	356.388	467000	Crack*
1-3	1.72	11.98	20.61	6.11		349.895	587800	Crack
1-4	1.74	12.02	20.92	5.91	199.797	333.439	1889100	Crack*
1-5	1.75	9.03	15.80	4.21	141.513	314.367	2406100	Crack*
1-6	1.74	8.97	15.61	4.21	142.325	318.289	7108000	Crack*
1-7	1.74	8.72	15.17	4.11		319.640	10073900	No crack
1-8	1.76	8.93	15.72	4.31		323.590	12346700	No crack
1-9	1.72	9.05	15.57	4.35		329.757	10190700	No crack

Table B2.The fatigue test data for AISI 1141AC shot-peened

No.	Average Thickness (mm)	Net Width (mm)	Area (mm²)	Load (KN)	σ₀ (MPa)	σₐ (MPa)	Cycles to Failure (Nf)	Remark
1-10	1.780	12.100	21.5380	6.110		334.748	11876700	No crack
1-11	1.790	12.080	21.6232	6.180		337.249	1069800	Crack
1-12	1.820	12.180	22.1676	6.310		335.887	557700	Crack
1-13	1.820	12.050	21.9310	6.150		330.902	10000000	No crack
1-14	1.800	12.100	21.7800	6.130		332.112	13942300	No crack
1-15	1.760	12.060	21.2256	5.910		328.556	10981000	No crack
1-16	1.760	12.040	21.1904	6.280		349.705	920400	Crack
1-17	1.780	12.000	21.3600	6.510		359.635	8788600*	No crack
1-18	1.760	12.080	21.2608	6.640		368.528	2903100	Crack
1-19	1.760	12.180	21.4368	8.910		490.456	51800	Crack

B.2. Fatigue Testing Data for AISI 1151QT

Table B3.The fatigue test data for AISI 1151QT non shot-peened

No.	Average Thickness (mm)	Net Width (mm)	Area (mm^2)	Load (KN)	σ_0 (MPa)	σ_a (MPa)	Cycles to Failure (N_f)	Remark
2-1	1.74	8.98	15.6252	6.100		460.67	366900	Crack
2-2	1.73	8.99	15.5527	5.810		440.81	653600	Crack
2-3	1.74	9.01	15.6774	5.320		400.42	1148100	Crack*
2-4	1.76	9.12	16.0512	5.520		405.80	3022700	Crack*
2-5	1.74	9.00	15.660	5.210		392.58	6573800	Crack*
2-6	1.74	9.08	15.7992	5.650		421.98	11838400	No crack
2-7	1.72	8.99	15.4628	5.670		432.69	10878000	No crack
2-8	1.74	9.00	15.660	5.810		437.79	1119000	Crack*
2-9	1.72	8.81	15.1532	5.610		436.86	3710900	Crack*

Table B4.The fatigue test data for AISI 1151QT shot-peened

No.	Average Thickness (mm)	Net Width (mm)	Area (mm^2)	Load (KN)	σ_0 (MPa)	σ_a (MPa)	Cycles to Failure (N_f)	Remark
2-10	1.82	16.74	21.9492	6.590		354.28	240400	Crack
2-11	1.82	16.82	21.9856	6.210		353.30	12429900	No crack
2-12	1.86	16.78	22.4688	8.210		431.17	13294100	No crack
2-13	1.80	16.78	21.7080	6.450		350.61	6403400	Crack*
2-14	1.78	16.88	21.5380	7.310		400.49	10463200	No crack
2-15	1.82	16.80	21.8400	6.520		352.27	10204300	No crack
2-16	1.82	16.80	21.8764	6.560		353.84	10221200	No crack
2-17	1.80	16.84	21.7800	6.730		364.62	10063500	No crack
2-18	1.84	16.80	22.2640	8.710		461.10	29100	Crack
2-19	1.80	16.80	21.7080	7.999		434.81	164400	Crack

B.3. Fatigue Testing Data for PM

Table B5.The fatigue test data for PM non shot-peened

No.	Average Thickness (mm)	Net Width (mm)	Area (mm²)	Load (KN)	σ_0 (MPa)	σ_a (MPa)	Cycles to Failure (N_f)	Remark
3-1	1.740	11.980	20.8450	5.100		288.699	10775500	No crack
3-2	1.780	11.980	21.3240	5.500	181.758	304.346	811700	Crack *
3-3	1.760	11.980	21.0848	5.400	180.481	302.208	3038000	Crack*
3-4	1.720	12.000	20.6400	5.310	181.601	303.576	1557600	Crack*
3-5	1.740	11.980	20.8452	5.400		305.682	10007900	No crack
3-6	1.760	12.000	21.1200	5.550	185.495	310.085	1491200	Crack*
3-7	1.740	11.980	20.8452	5.750	194.388	325.495	1874700	Crack*
3-8	1.760	8.990	15.8224	4.210		313.973	10952800	No crack
3-9	1.740	8.990	15.6426	4.450		335.685	10935700	No crack

Table B6.The fatigue test data for PM shot-peened

No.	Average Thickness (mm)	Net Width (mm)	Area (mm²)	Load (KN)	σ_0 (MPa)	σ_a (MPa)	Cycles to Failure (N_f)	Remark
3-10	16.900	1.840	22.1904	6.150		327.033	5335000	Crack
3-11	16.740	1.840	22.0800	6.820		364.475	426400	Crack
3-12	16.820	1.840	22.1904	6.570		349.367	3536900	Crack
3-13	16.760	1.820	21.9492	6.920	223.659	372.023	914500	Crack*
3-14	16.780	1.860	22.3572	6.890	217.900	364.178	1365200	Crack*
3-15	16.760	1.860	22.3200	6.970		368.486	1804900	Crack
3-16	16.780	1.840	22.0800	6.850		366.078	10310300	No crack
3-17	16.820	1.820	21.9856	6.900		370.333	7210800	Crack
3-18	16.820	1.800	21.7260	6.300		342.171	10313400	No crack
3-19	16.860	1.820	21.9856	5.988		321.385	10000000	No crack

B.4. Fatigue Testing Data for C70S6AC

Table B7.The fatigue test data for C70S6AC non shot-peened

No.	Average Thickness (mm)	Net Width (mm)	Area (mm^2)	Load (KN)	σ_0 (MPa)	σ_a (MPa)	Cycles to Failure (N_f)	Remark
4-1	1.72	9.05	15.566	5.210	178.181	394.951	627000	Crack*
4-2	1.75	9.05	15.8375	5.410		403.081	474300	Crack
4-3	1.73	9.00	15.570	4.510		341.798	10618300	No crack
4-4	1.75	8.98	15.715	4.710		353.662	2773200	Crack*
4-5	1.73	9.02	15.5595	4.690		355.00	739800	Crack
4-6	1.75	8.93	15.6275	4.600		347.34	10503500	No crack
4-7	1.76	8.94	15.7344	4.690		351.726	11371500	No crack
4-8	1.75	8.99	15.5008	5.610		427.06	680390	Crack
4-9	1.73	8.96	15.5008	4.655		354.36	10335000	No crack

Table B8.The fatigue test data for C70S6AC shot-peened

| No.	Average Thickness (mm)	Net Width (mm)	Area (mm^2)	Load (KN)	σ_0 (MPa)	σ_a (MPa)	Cycles to Failure (N_f)	Remark
4-10	1.78	12.04	21.4312	6.310		347.428	10140400	No crack
4-11	1.92	11.98	23.0016	6.910		354.488	130000	Crack
4-12	1.82	12.06	21.9492	6.220		334.390	10029300	No crack
4-13	1.82	12.05	21.9310	6.330		340.586	315100	Crack
4-14	1.88	12.00	22.5600	6.450	201.815	337.367	38900	Crack*
4-15	1.84	12.02	22.1168	6.310	201.726	336.658	39700	Crack*
4-16	1.90	11.96	22.7240	6.480	200.619	336.490	70200#	No crack
4-17	1.82	11.98	21.8036	6.210		336.080	6089100	Crack
4-18	1.80	12.04	21.6720	6.160		335.401	19062000	No crack
4-19	1.82	12.02	21.8764	6.450		347.909	13434900	No crack

B.5. AISI 1141AC S-N curve
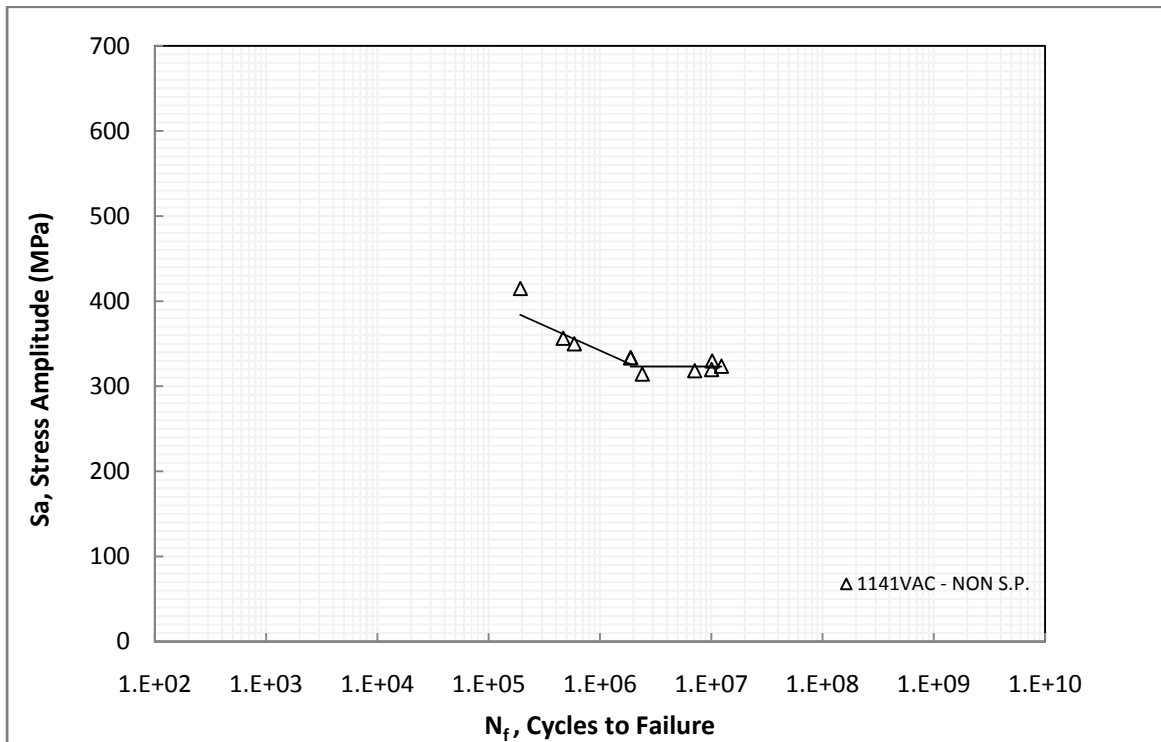
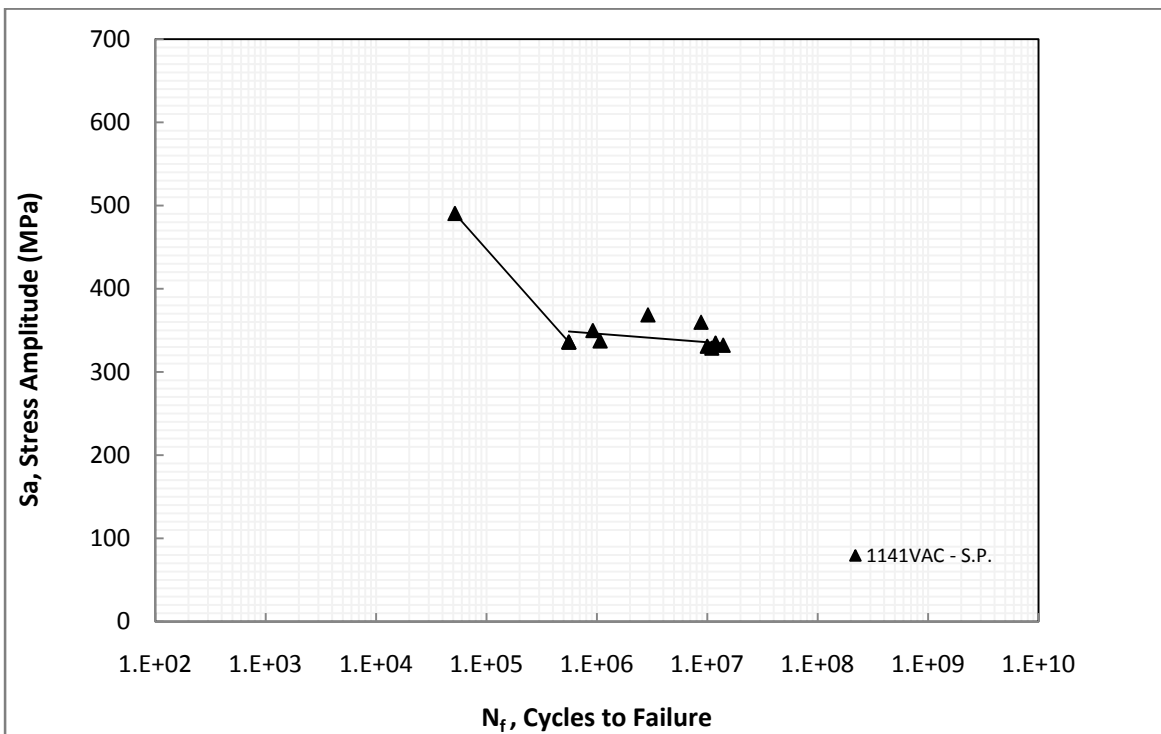**Figure B1.S-N curve for AISI 1141AC non shot-peened**

Figure B2.S-N curve for AISI 1141AC shot-peened
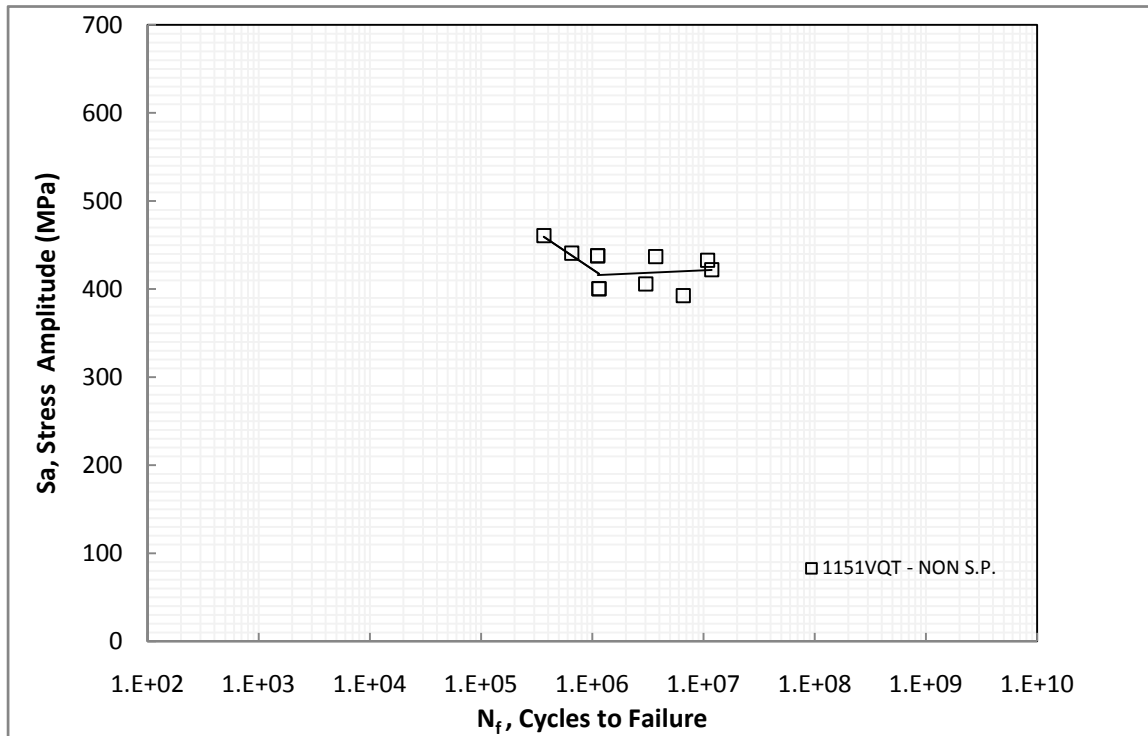
B.6. AISI 1151QT S-N curve

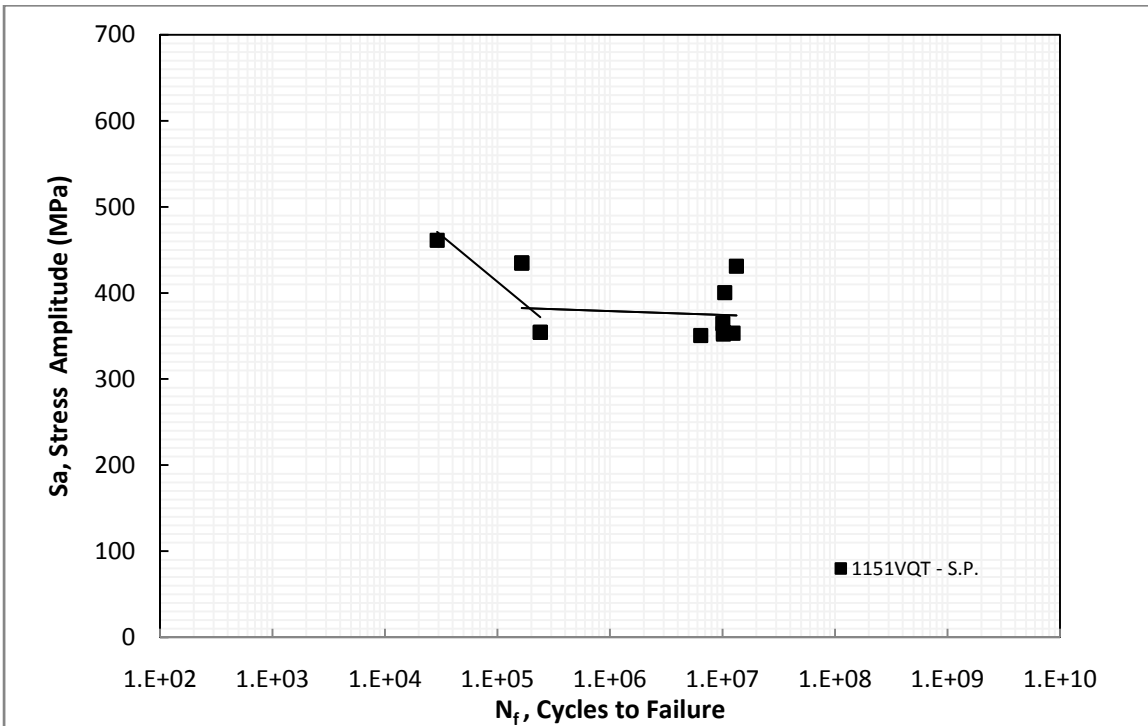**Figure B3.S-N curve for AISI 1151QT non shot-peened**

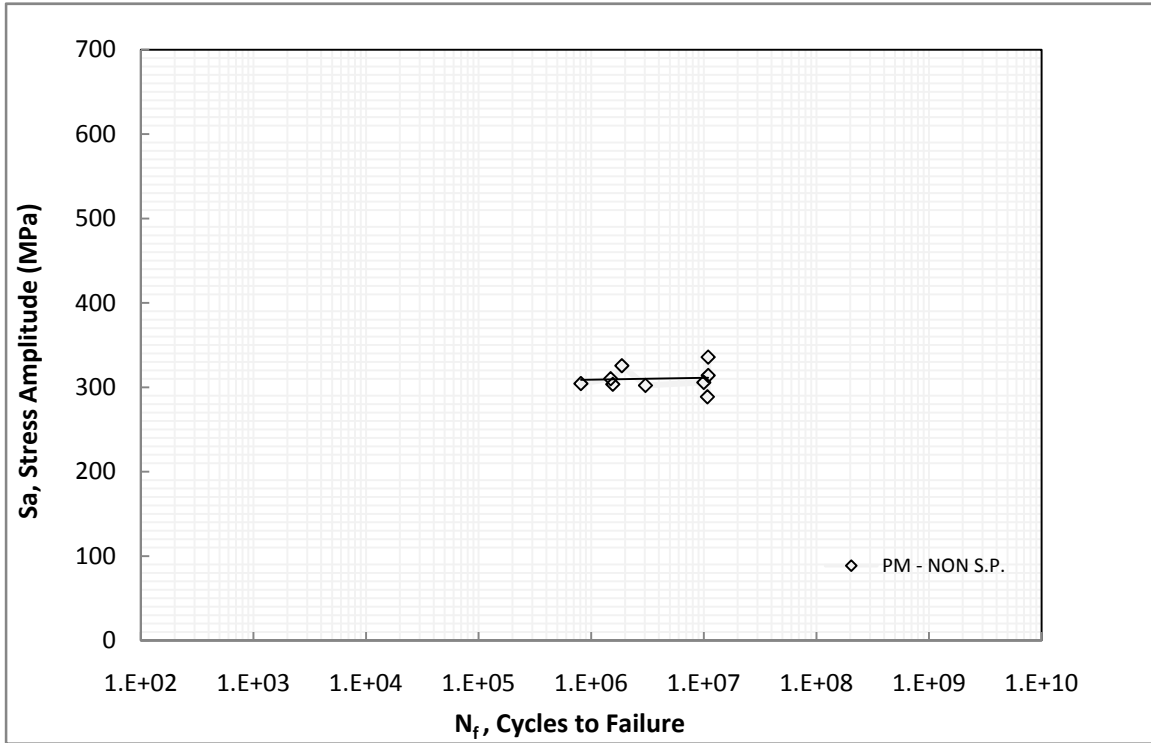**Figure B4.S-N curve for AISI 1151QT shot-peened**

B.7.PM S-N curve

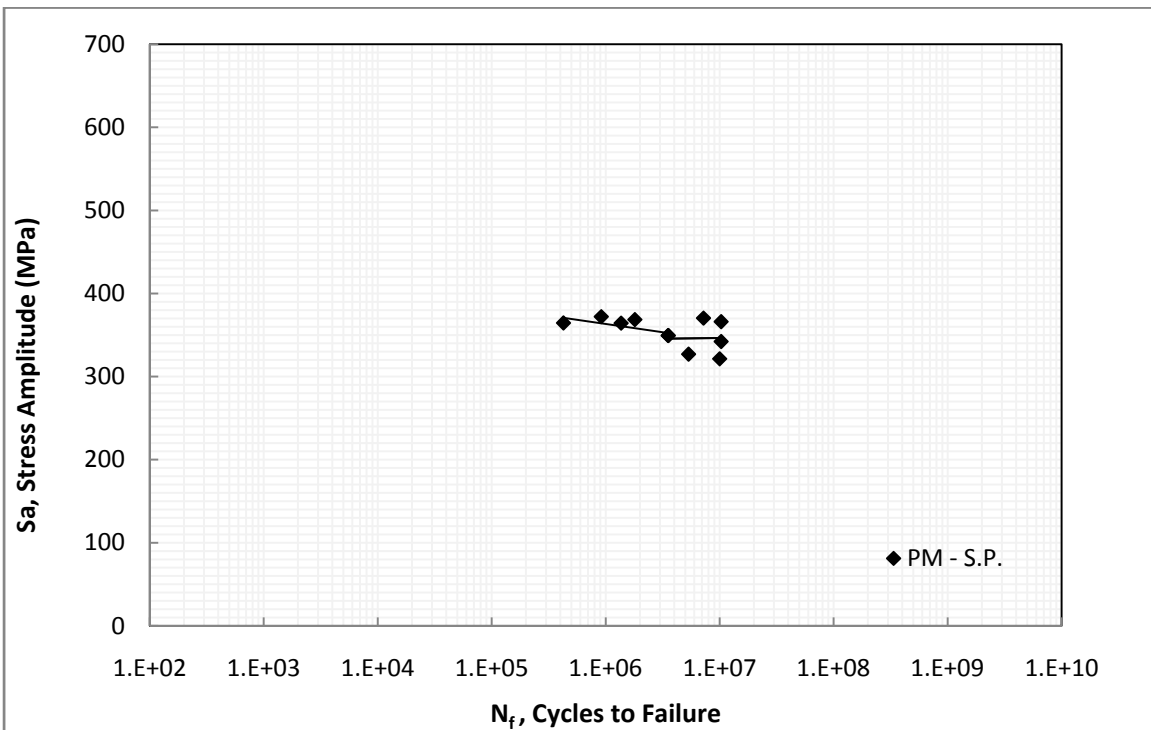**Figure B5.S-N curve for PM non shot-peened**

Figure B6.S-N curve for PM non shot-peened
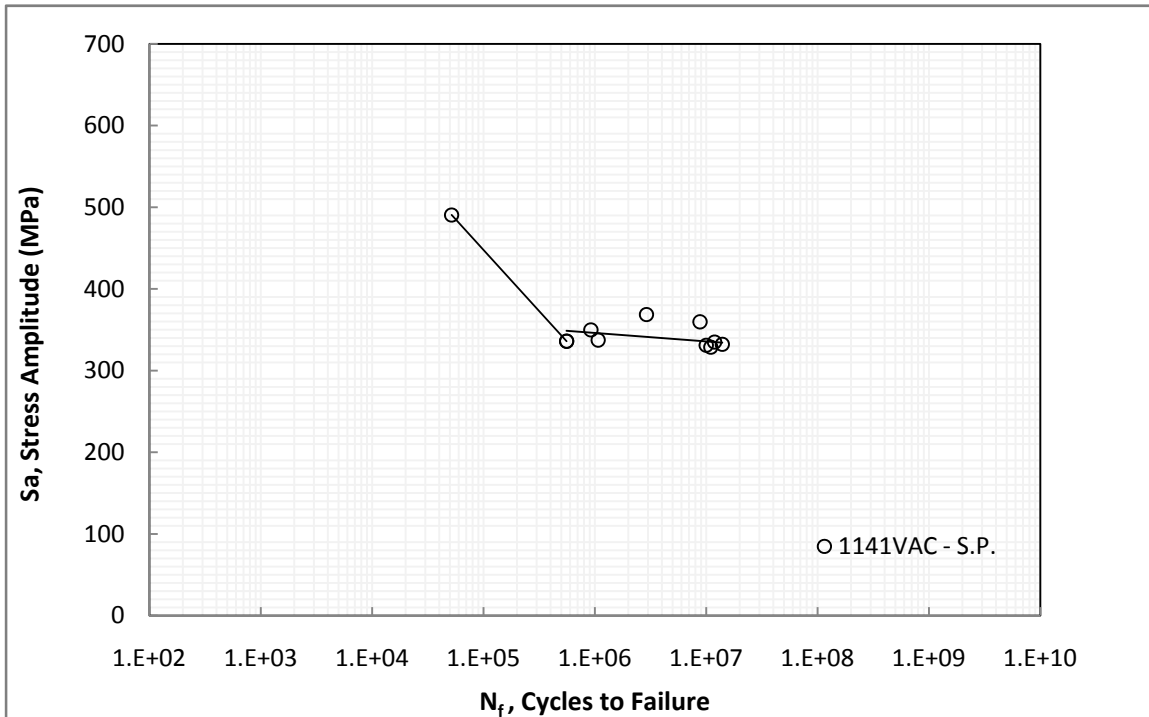
B.8. C70S6AC S-N curve

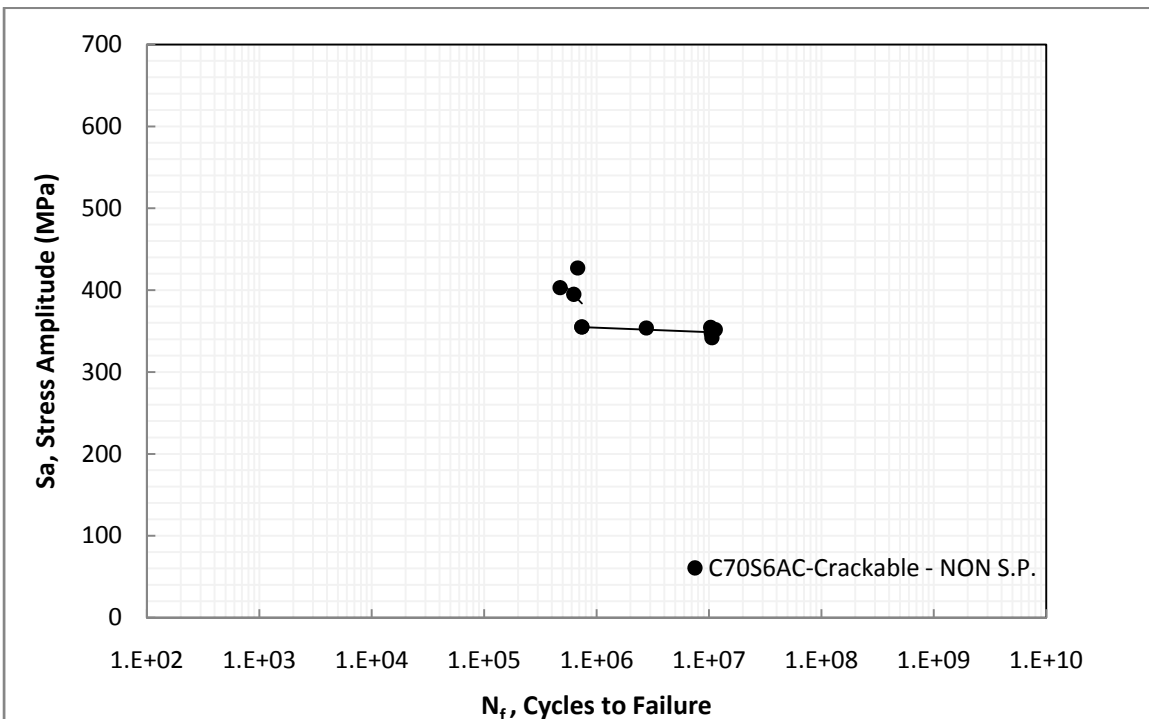**Figure B7.S-N curve for C70S6AC non shot-peened**

Figure B8.S-N curve for C70S6AC shot-peened

Appendix C

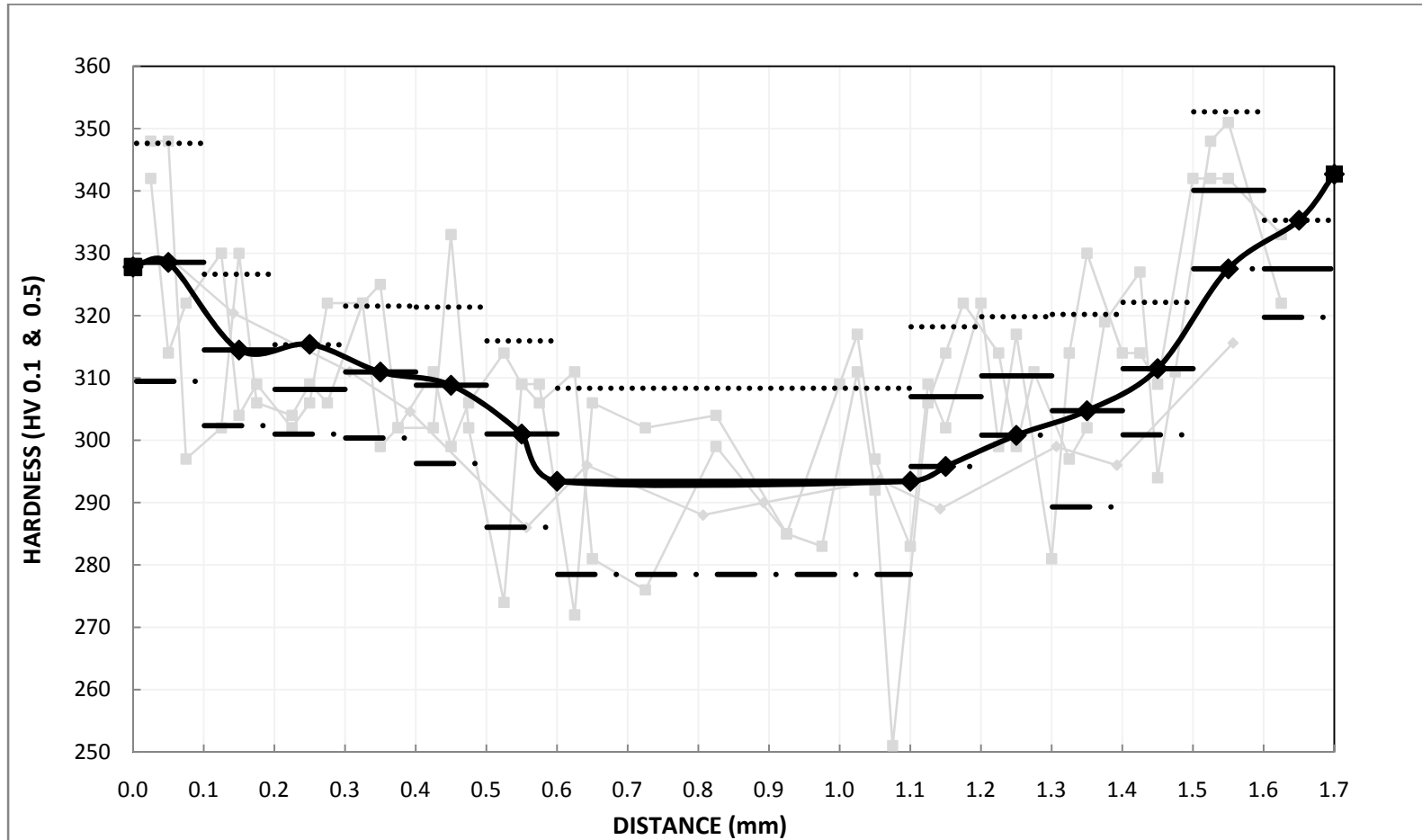## C.1. Original Hardness Curves for AISI 1141AC

Figure C1.AISI 1141AC Shot-peened Microhardness Profile Grip L-S (Specimen 1-16)
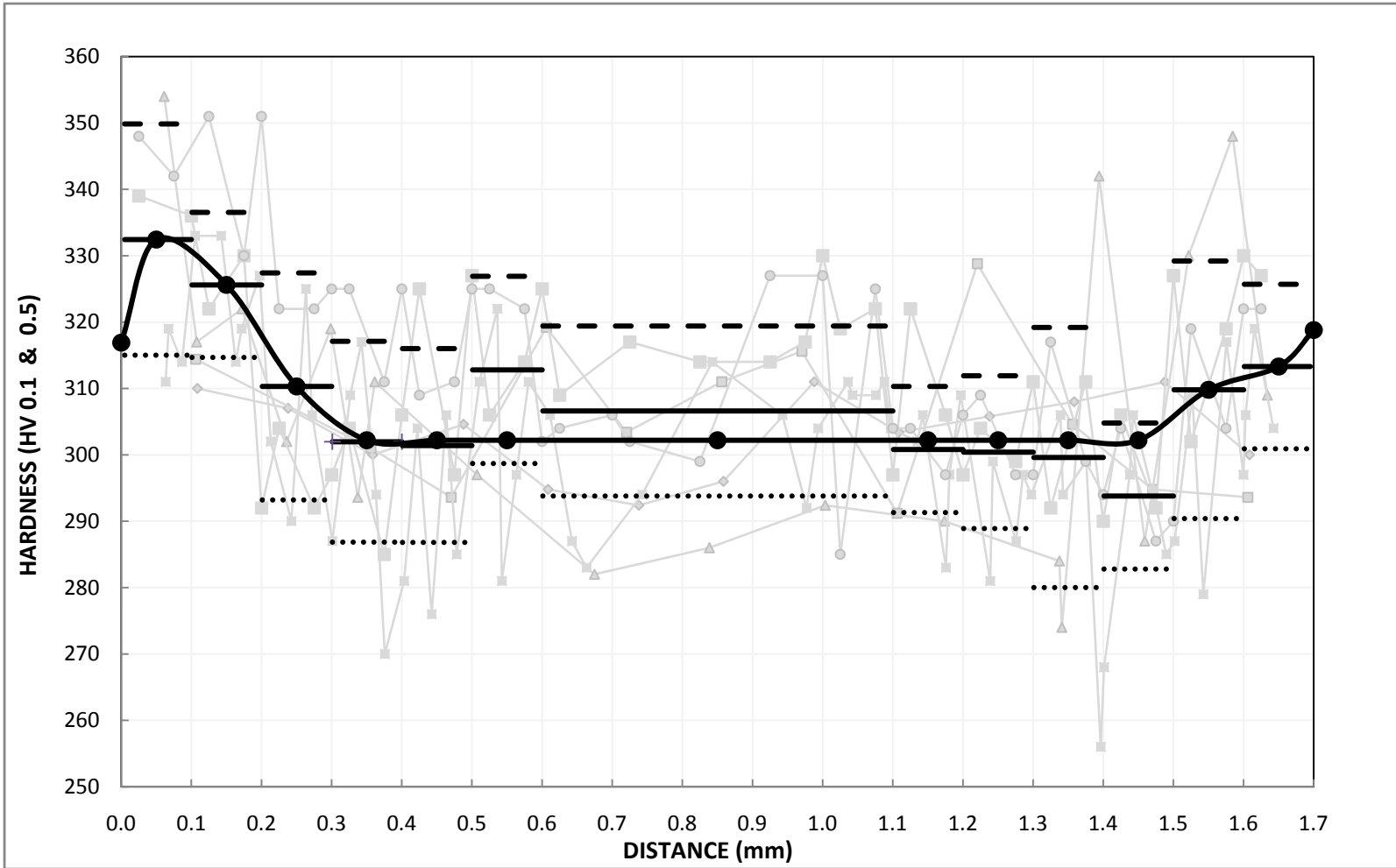
Figure C2.AISI 1141AC Shot-peened Microhardness Profile Gage L-S (Specimen 1-16)

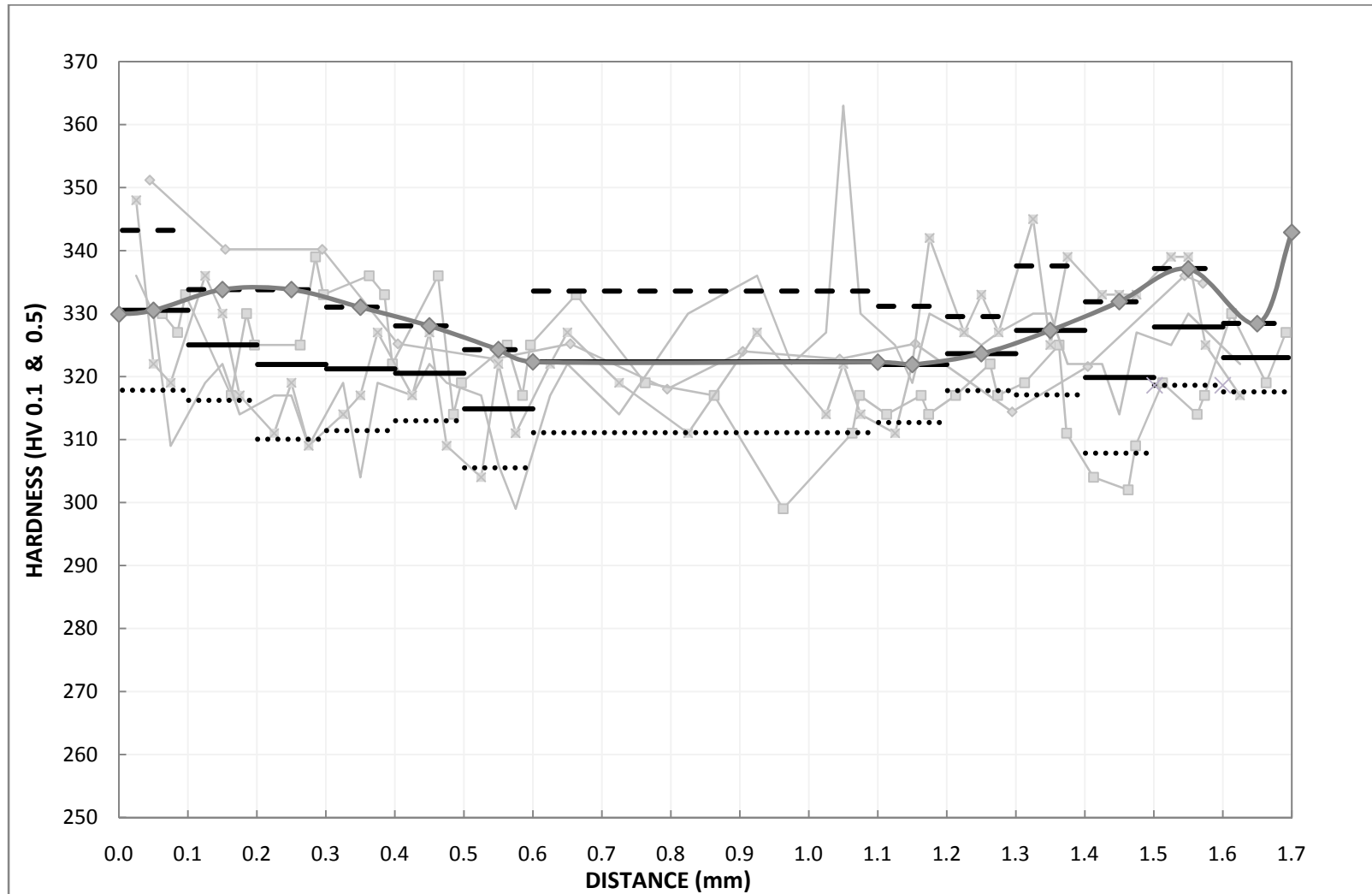## C.2. Original Hardness Curves for AISI 1151QT

Figure C3.AISI 1151QT Shot-peened Microhardness Profile Grip L-S (Specimen 2-18)

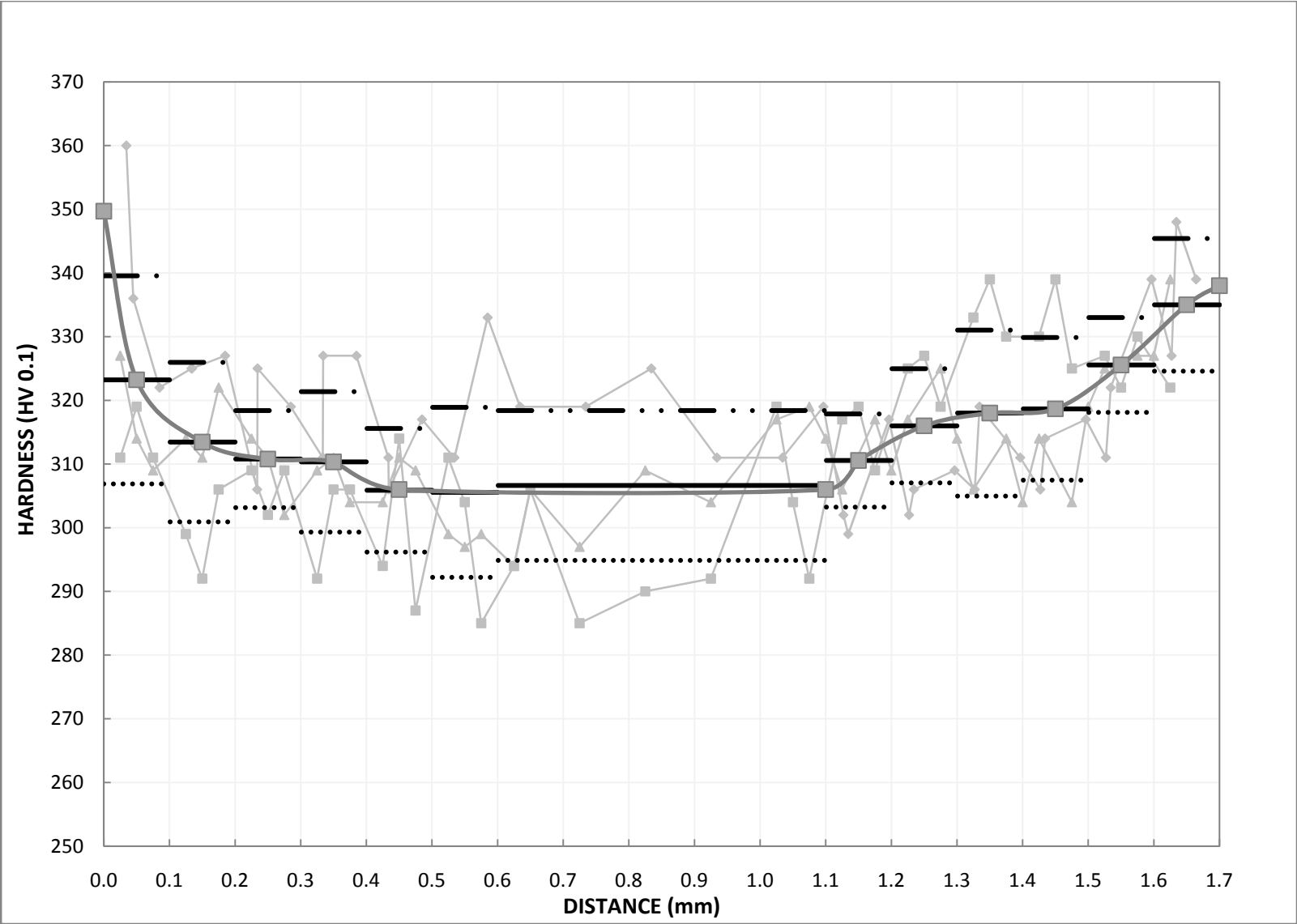**Figure C4.AISI 1151QT Shot-peened Microhardness Profile Gage L-S (Specimen 2-18)**

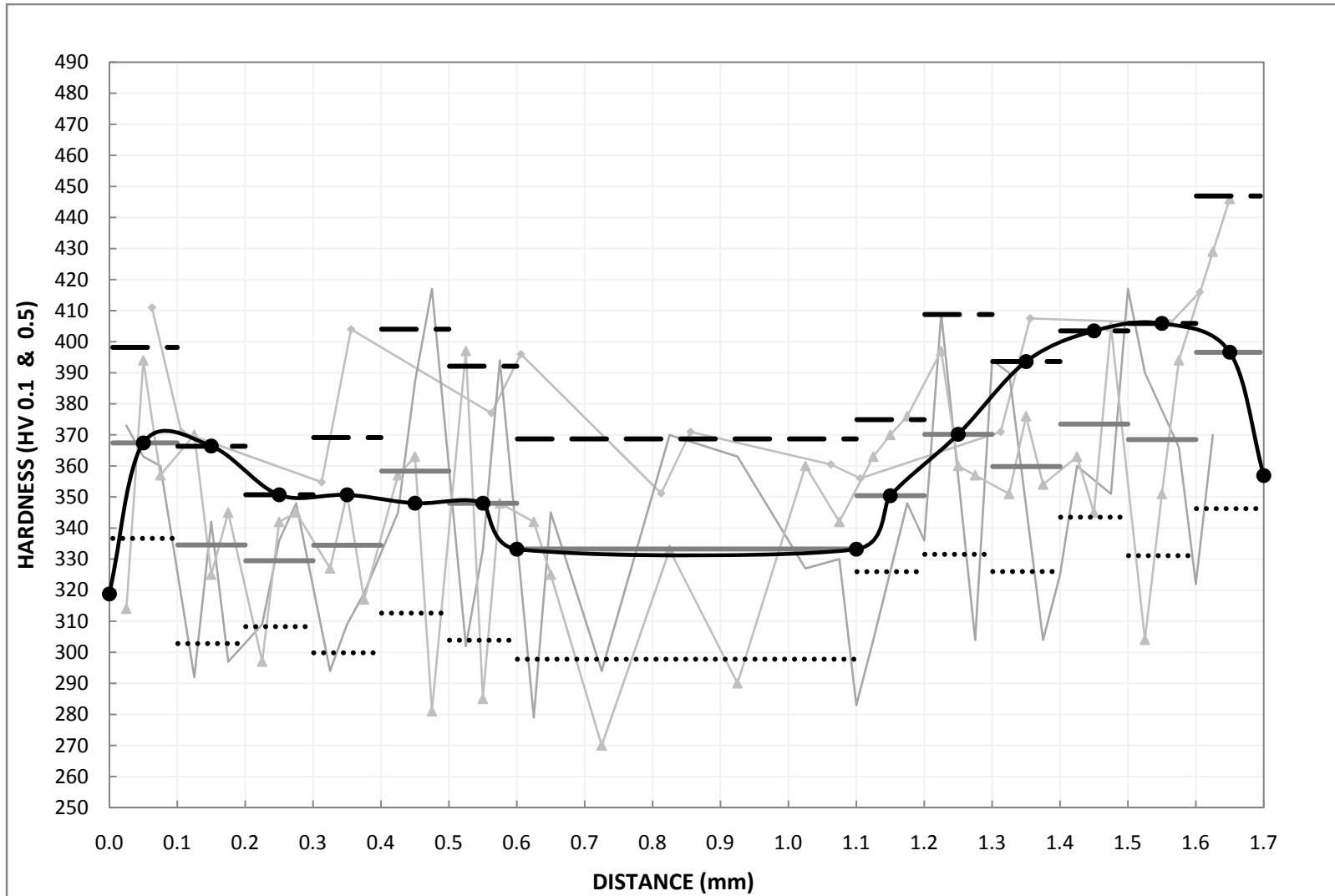# C.3. Original Hardness Curves for PM

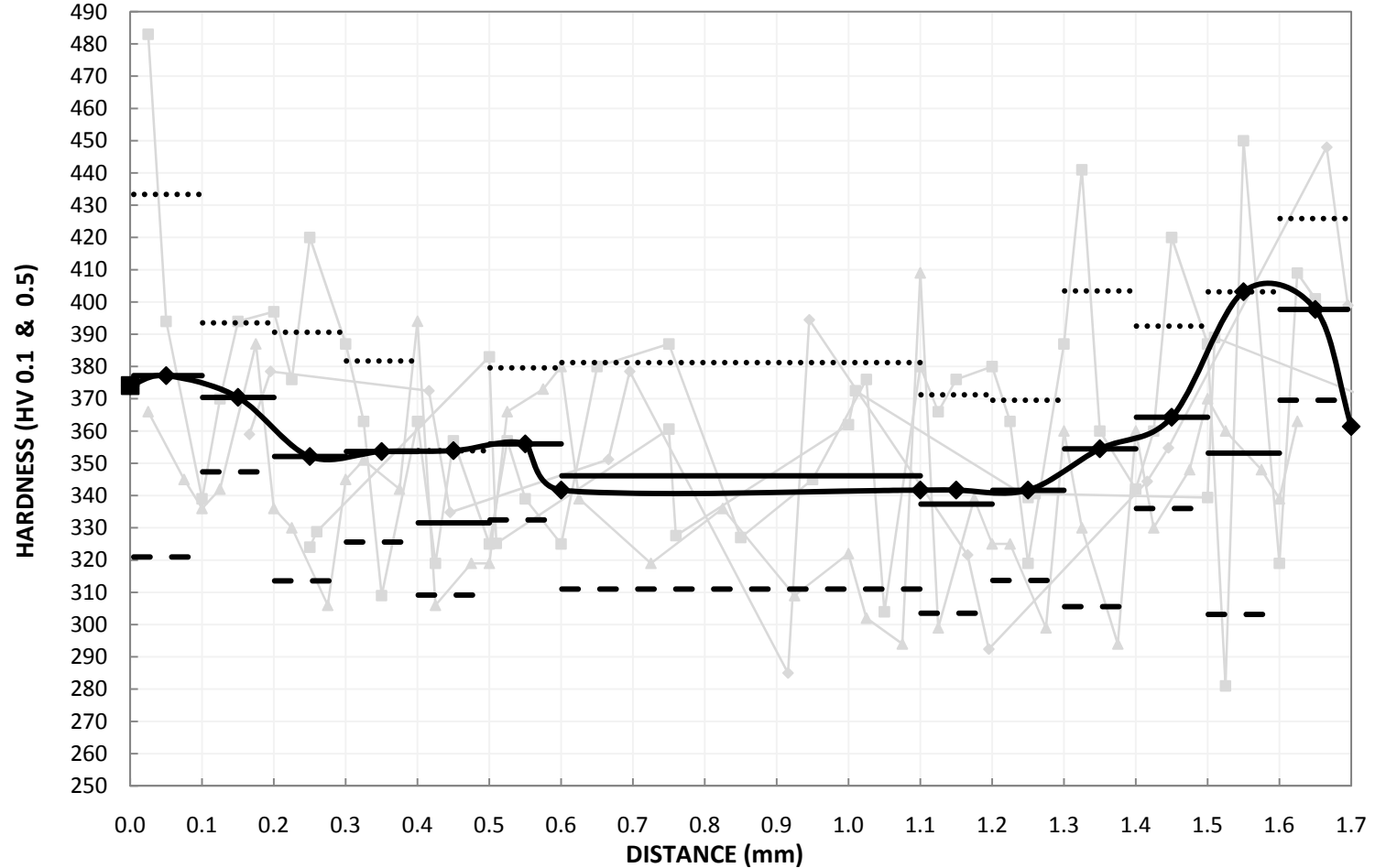**Figure C5.PM Shot-peened Microhardness Profile Grip L-S (Specimen 3-15)**

Figure C6.PM Shot-peened Microhardness Profile Gage L-S (Specimen 3-15)
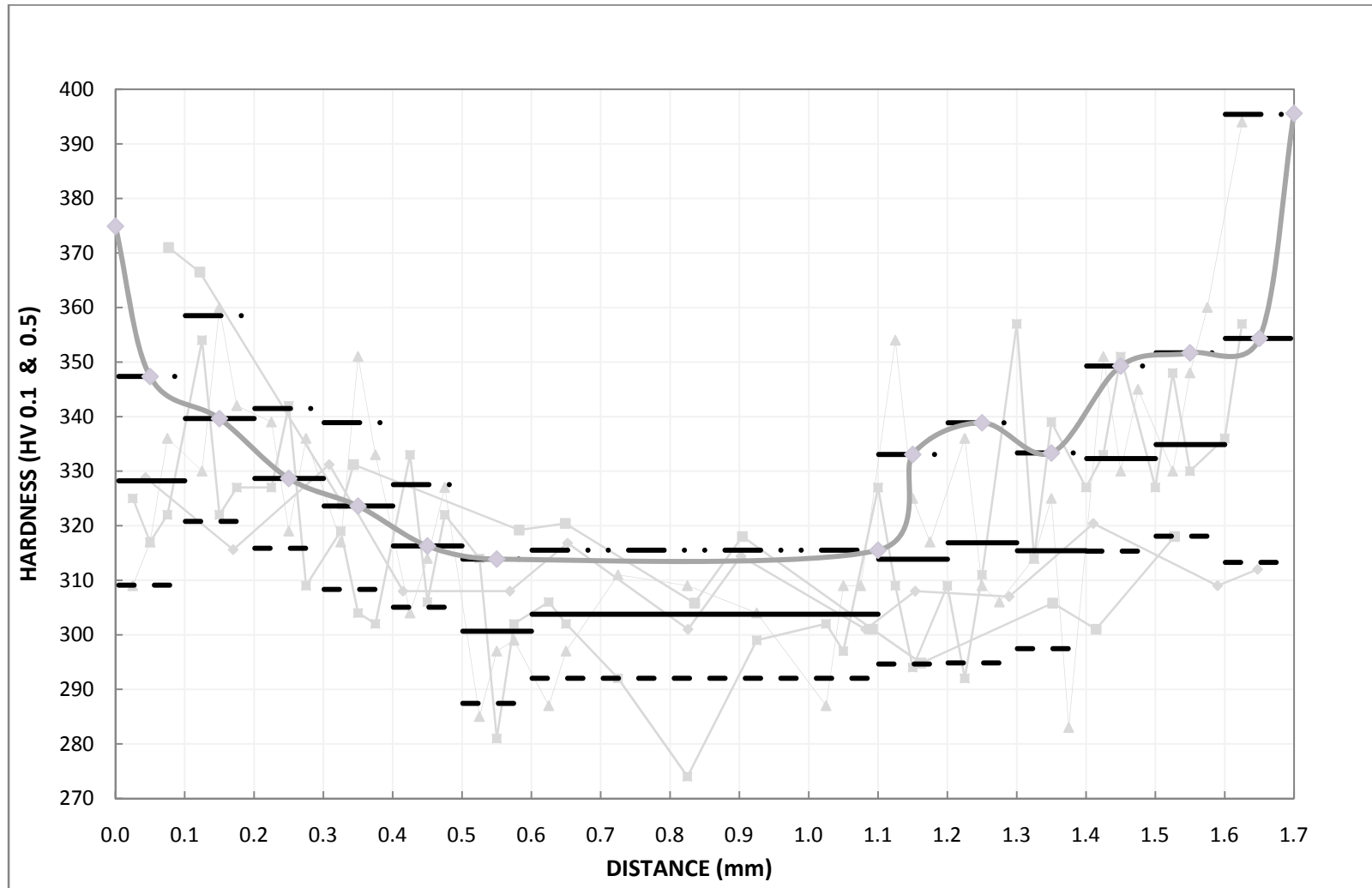
C.4. Original Hardness Curves for C70S6AC

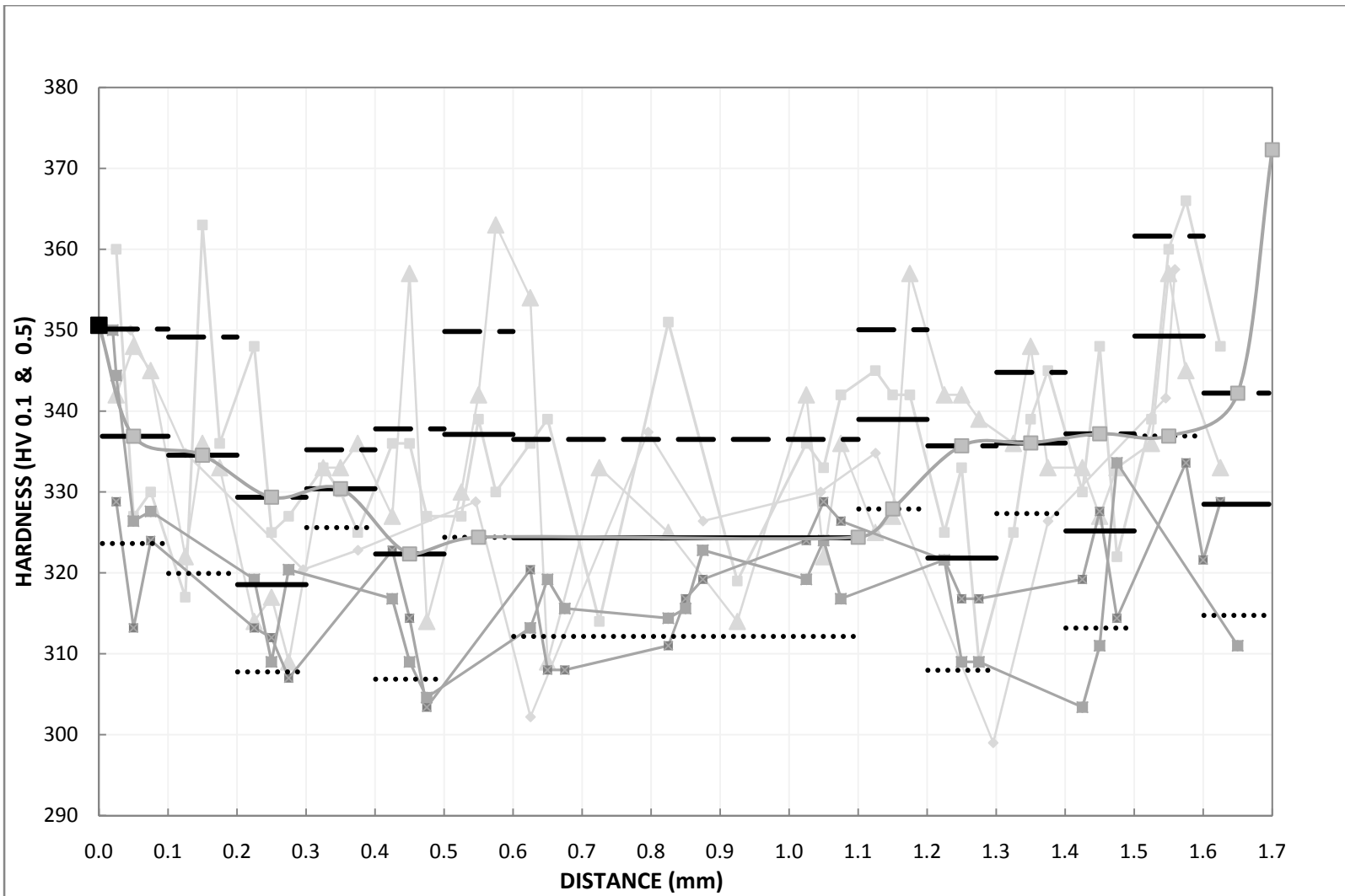**Figure C7.C70S6AC Shot-peened Microhardness Profile Grip L-S (Specimen 4-10)**

Figure C8.C70S6AC Shot-peened Microhardness Profile Gage L-S (Specimen 4-10)

References

[1]   R.M.Pelloux, "Case Studies of Fatigue Failures in Aeronautical Structures", Fatigue 93, Montreal, Canada, 1993, 1727-1737.

[2]   G.Glinka, "Fatigue & Fracture Mechanics Analysis & Design", Mechanical Engineering Department, University of Waterloo, Waterloo, Ontario, Canada, 2008, 109-115.

[3]   G.H.Farrahi, J.L.Lebrun and D.Courtain, "Effect of Shot Peening on Residual Stress and Fatigue Life of a Spring Steel", Fatigue & Fracture of Engineering Materials and Structures, Vol.18, 1995, 211-220.

[4]   ASM Handbook, Surface Engineering Vol.5, American Society of Materials International, ASM Publication, Materials Park, OH, USA, 1994.

[5]   X.P.Jiang, C.S.Man, M.J.Shepard, T.Zhai, "Effects of Shot Peening and Reshot Peening on Four-Point Bend Fatigue Behaviour of Ti–6Al–4V", Materials Science and Engineering, Vol.468–470, 2007, 137–143.

[6]   A.M.Eleiche, M.M.Megahed, N.M.Abd-Allah, "The Shot Peening Effect on the HCF Behaviour of High Strength Martensitic Steels", Journal of Material Processing Technology, Vol.113, 2001, 502-508.

[7]   R.Fathallah, A.Laamouri, H.Sidhom, C.Braham,"High Cycle Fatigue Behavior Prediction of Shot Peened Parts", International Journal of Fatigue, Vol.26, 2004, 1053–1067.

[8]   J.E.Hoffmann, D.Lohe and E.Macherauch, "Influence of Shot Peening on the Bending Fatigue Behaviour of Notched Specimens of CK 45", International Conferences on Shot Peening (ICSP-3), Garmisch-Partenkirchen, Germany, 1987, 631-638.

[9]   A.Plumtree, "Shot peening Effects on Fatigue Life", 12th International Conference on Fracture, Ottawa, Canada, 2009.

[10]   H.Guechichi, L.Castex, "Fatigue Limits Prediction of Surface Treated Materials", Journal of Materials Processing Technology, Vol.172, 2006, 381–387.

[11]   I.F.Pariente, M.Guagliano, "The Role of Residual Stresses and Surface Work Hardening on Fatigue Δk_{th} of a Nitrided and Shot Peened Low-Alloy Steel", Surface & Coatings Technology, Vol.202, 2008, 3072–3080.

[12]   W.Cao, "Cyclic Softening of Steels and Residual Stress Relaxation of Shot-Blasting in Fatigue", PhD thesis, ENSAM, Paris, France, 1989.

[13]   M.A.S Torres, H.J.C Voorwald, "An Evaluation of Shot Peening, Residual Stress and Stress Relaxation on the Fatigue Life of AISI 4340 Steel", International Journal of Fatigue, Vol.24, 2002, 877-886.

[14]   S.Wang, Y.Li, M.Yao, R.Wang, "Fatigue Limit of Shot Peened Metal", Journal of Material Processing Technology, Vol.73, 1998, 57-63.

[15]   D.Eifler, D.Löhe, B.Scholtes, "Residual Stresses and Fatigue of Metallic Materials", Residual Stresses - Measurement, Calculation and Evaluation, DGM Informationsgesellschaft Verlag, Oberursel, 1991, 157-166.

[16]   Y.Gao, X.Li, Q.Yang and M.Yao, "Influence of Surface Integrity on Fatigue Strength of 40CrNi2Si2MoVA Steel", Material Letters, Vol.61, 2007, 466-469.

[17]   W.Z.Zhuang, G.R.Halford, "Investigation of Residual Stress Relaxation under Cyclic Load", International Journal of Fatigue, Vol.23, 2001, 31–37.

110

[18]   Y.K.Gao, X.B.Li, Q.X.Yang, M.Yao, "Influence of Surface Integrity on Fatigue Strength Of 40CRNi2Si2MoVA Steel", Material Letters, Vol.61, 2007, 466-469.

[19]   M.Giagliano, L.Vergani, "An Approach for Prediction of Fatigue Strength of Shot-Peened Components", Engineering Fracture Mechanics, Vol.71, 2004, 501-512.

[20]   J.Lindemann, C.Buque, F.Appel, "Effect of Shot-Peening on Fatigue Performance of a Lamellar Titanium Aluminide Alloy", Acta Materialia, Vol.54, 2006, 1155-1164.

[21]   ASM Handbook, Properties and Selection: Irons, Steels and High Performance Alloys Vol.1, American Society of Materials International, ASM Publication, Materials Park, OH, USA, 1990.

[22]   G.E.Totten, M.A.H.Howes, "Steel Heat Treatment Handbook", Marcel Dekker Inc., NY, USA, 1997.

[23]   ASM Handbook, Heat Treating Vol.4, American Society of Materials International, Materials Park, OH, USA, 1991.

[24]   J.R.Dale, "Connecting Rod Evaluation", Metal Powder Industries Federation, Princeton, NJ, USA, 2005.

[25]   Z.Gu, S.Yang, S.Ku, Y.Zhao, X.Dai, "Fracture Splitting Technology of Automobile Engine Connecting Rod", International Journal of Advanced Manufacturing Technology, Vol.25, 2005, 883–887.

[26]   H.J.Kwon, "Fatigue and Fracture Analysis of Engineering Materials", Mechanical Engineering Department, University of Waterloo, Waterloo, Ontario, Canada, 2010.

[27]   N.E.Dowling, Mechanical Behaviour of Materials, Pearson Prentice Hall, Pearson, Education, Inc, NJ, USA, 2007.

[28]   E.R.Rios, A.Walley, M.T.Millan and G.Hammersley, "Fatigue Crack Initiation and Propagation on Shot-Peened Surfaces in A316 Stainless Steel, International Journal of Fatigue, Vol.17, 1995, 493-499.

[29]   Y.Ochi, K.Masaki, T.Matsumura, T.Sekino, "Effect of Shot-Peening Treatment on High Cycle Fatigue Property of Ductile Cast Iron", International Journal of Fatigue, Vol.23, 2001, 441–448.

[30]   R.W.Landgraf, R.A.Chernenkoff, "Residual Stress Effects on Fatigue of Surface Processed Steels", Analytical and experimental Methods for Residual Stress Effects in Fatigue, ASTM STP 1004, R.L.Champoux, J.H.Underwood and A.Kapp, ASTM, Philadelphia, USA,1988.

[31]   D. Lorincz," Study Confirms Forged Crackable Steel Connecting Rods Cost Less and Perform Better than Forged Powder Metal Rods", Press Releases July 2004, Automotive Communications, AISI, Detroit, MI.

[32]   R.W.Hertzberg, "Deformation and Fracture Mechanics of Engineering Materials", Fourth Edition, John Wiley and Sons, 1996.